universität wien

MASTERARBEIT / MASTER'S THESIS

Titel der Masterarbeit / Title of the Master's Thesis

Biophysical Characterization of the Interaction between α-actinin-2 and the Proteins with the ZASP-like Motif

verfasst von / submitted by

Ana Oršolić, univ. bacc. biol.

angestrebter akademischer Grad / in partial fulfilment of the requirements for the degree of

Master of Science (MSc)

Wien, 2021 / Vienna, 2021

Studienkennzahl lt. Studienblatt / degree programme code as it appears on the student record sheet:	UA 066 834
Studienrichtung lt. Studienblatt / degree programme as it appears on the student record sheet:	Masterstudium Molekulare Biologie
Betreut von / Supervisor:	Univ.-Prof. Dipl.-Ing. Dr. Kristina Djinović-Carugo

Acknowledgements

Firstly, I would like to thank my supervisor, Univ.-Prof. Dipl.-Ing. Dr. Kristina Djinović-Carugo, for giving me the opportunity to work in a wonderful lab on a new and exciting project and allowing me to pursue my ideas and deepen my knowledge in biochemistry and structural biology.

Next, I want to express my deepest respect and gratitude to Dipl.-Ing. Dr. Dalibor Milić who was my biggest support and mentor during my project. He was there to show me exciting new methods, give valuable input, constructive criticism, advice and teach me that even a small discovery takes time and proves valuable.

I would like to thank Dr. Joan Lopez Arolas and Antonio Sponga for the help and advice on isothermal titration calorimetry measurements, Mag. Julius Kostan, PhD, for stepping in whenever needed, Ing. Claudia Schreiner for constant support and all other colleagues in the group for making each day in the lab a memory for lifetime.

Finally, I want to thank my mother for being my constant support in the darkest times and for sacrificing so much to get me where I am now.

Abstract

The Z-disk protein network is a complicated assembly of more than 40 proteins which with their coordinate functions give rise to contraction and movement. α-actinin-2 plays a central role in organizing the Z-disk, antiparallelly crosslinking actin filaments. Numerous binding partners of α-actinin-2 are involved in the organization of the Z-disk, many of them belonging to the ALP and Enigma subfamilies of proteins. Three of them, ALP, CLP36 and ZASP, stand out with their characteristic 26-amino-acid-long region, called the ZASP-like motif (ZM). It has been shown that the motif plays a crucial role in different myopathies, but its role in the Z-disk and α-actinin-2 binding remains largely unknown.

In this study, isothermal titration calorimetry (ITC) measurements revealed a clear binding between the rod domain of α-actinin and the flexible internal region of ALP, CLP36 and ZASP, where the ZM is located. ALP and CLP36 revealed a binding governed by enthalpic contributions, whereas the more flexible, disordered ZASP showed a major entropic contribution. Crosslinking confirmed that α-actinin-2 dimer binds two molecules of ALP, CLP36 or ZASP and engineered disulfide-bridged complexes are shown to stabilize the initial complex. Crystallization revealed numerous positive hits, but the presence of the complex could not be confirmed by silver staining, nor by solving the structure since it showed only the presence of the rod domain.

Altogether, these findings provide new insight on the interaction between α-actinin-2 and proteins containing the ZM, giving rise to more understanding of the motif and its function in binding to the spectrin repeats of α-actinin-2. Furthermore, structural studies done on the ZM provide a strong ground for further optimization and analysis to finally reveal the structural background of the interaction between α-actinin-2 and the ZM of ALP, CLP36 and ZASP.

Zusammenfassung

Das Z-Scheiben-Proteinnetzwerk ist eine komplizierte Anordnung von mehr als 40 Proteinen, die mit ihren koordinierten Funktionen zu Kontraktion und Bewegung führen. α-Aktinin-2 spielt eine zentrale Rolle bei der Organisation der antiparallel vernetzten Aktinfilamente der Z-Scheibe. Zahlreiche Bindungspartner von α-Aktinin-2 sind an der Organisation der Z-Scheibe beteiligt, von denen viele zur ALP- und Enigma-Unterfamilie von Proteinen gehören. Drei von ihnen, ALP, CLP36 und ZASP, zeichnen sich durch ihre charakteristische 26-Aminosäuren-lange Domäne aus, die als das ZASP-ähnliche Motiv (ZM) bezeichnet wird. Es wurde gezeigt, dass das Motiv bei verschiedenen Myopathien eine entscheidende Rolle spielt, aber seine Rolle bei der Bindung von Z-Scheiben und α-Aktinin-2 ist jedoch weitgehend unbekannt.

In dieser Studie zeigten Messungen der isothermen Titrationskalorimetrie (ITC) eine klare Bindung zwischen der Stabdomäne von α-Aktinin und der flexiblen inneren Region von ALP, CLP36 und ZASP, in der sich das ZM befindet. ALP und CLP36 zeigten eine Bindung, die durch enthalpische Beiträge gesteuert wird, während das flexiblere, ungeordnete ZASP einen wesentlichen entropischen Beitrag zeigte. Die Vernetzung bestätigte, dass das α-Aktinin-2-Dimer zwei Moleküle von ALP, CLP36 oder ZASP bindet, und es wurde gezeigt, dass konstruierte disulfidverbrückte Komplexe den Ausgangskomplex stabilisieren. Die Kristallisation ergab zahlreiche positive Treffer, aber das Vorhandensein des Komplexes konnte weder durch Silberfärbung noch durch Lösen der Struktur bestätigt werden, da nur das Vorhandensein der Stabdomäne gezeigt wurde.

Insgesamt liefern diese Ergebnisse neue Erkenntnisse über die Verbindung zwischen α-Aktinin-2 und Proteinen, die das ZM enthalten, was zu einem besseren Verständnis des Motivs und seiner Funktion bei der Bindung an die Spektrin-Wiederholungen von α-Aktinin-2 führt. Darüber hinaus bieten Strukturstudien zum ZM eine solide Grundlage für weitere Optimierungen und Analysen, um schließlich den strukturellen Hintergrund der Verbindung zwischen α-Aktinin-2 und dem ZM von ALP, CLP36 und ZASP aufzudecken.

Table of Contents

Sarcomere Structure and Function

Striated muscle tissue is one of the most organized tissues in human body and its main function is to convert chemical energy into physical work by contracting and thus creating force. As there are two types of striated muscle tissue, cardiac and skeletal, the created force is used for posture and movement when it comes to skeletal muscles, and for blood flow throughout the body in cardiac muscle tissue. The muscle tissue is composed out of bundles which are further divided into muscle fibers. These bundles of muscle fibers are wrapped with a cell membrane, sarcolemma. Muscle fibers are long and composed out of many nuclei, being characteristic for skeletal muscle, whereas the cardiac muscle tissue is made out of cells, myocytes. Both of them are formed in a process called myogenesis and are built out of special contractile fibers, called myofibrils. Under the microscope, these myofibrils appear as alternating dark and light lines – sarcomeres (Figure 1A), which are the main contractile units of the striated muscle tissue (Frontera and Ochala, 2015; Gautel and Djinović-Carugo, 2016; Luther, 2009; Shadrin et al., 2016).

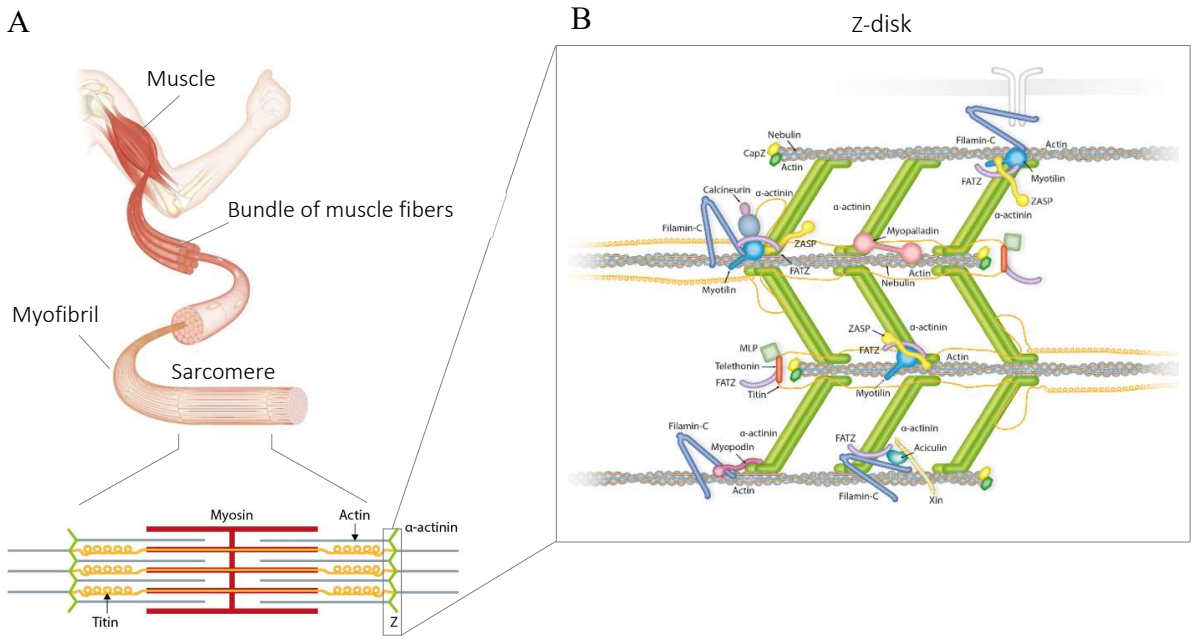

Figure 1 - Schematic representation of the structural organization of the striated muscle tissue

(A) Muscles are formed out of a bundle of muscle fibers where each of them is built out of myofibrils. These myofibrils are made out of the main contractile unit of the muscle tissue, the sarcomere which is placed between two Z-disks. (B) Z-disk is a complex structure formed out of actin crosslinked with antiparallel α-actinin-2 molecules, with numerous important proteins being present in the protein network. Courtesy of the Djinović-Carugo group.

The two main proteins building the sarcomere are actin and myosin which are responsible for muscle contraction (Powers et al., 2021). The sarcomere located between two Z-lines, also called Z-disks (Figure 1B). Between them, there are multiple regions, isotropic (I-band), anisotropic (A-band), H-zone and M-line (Squire, 1997) which give the muscle the striated appearance. In the Z-disk, actin filaments are crosslinked with antiparallel α-actinin-2 molecules. The Z-disk is a structurally and functionally complex network of proteins, each of them with very different and specific functions. This complicated network resembles a basketweave, or a small-square lattice (Goldstein et al., 1990; Luther et al., 2002; Perz-Edwards and Reedy, 2011) and is with its robust structure important for sarcomere assembly, maintenance and function (Luther, 2009).

Proteins of the Z-disk Network

The view on the Z-disk function has dramatically changed over the years. First, it was thought to be responsible primarily for mechanical stability, but over the years, multiple novel proteins have been detected which led to additional functions being assigned to the Z-disk. Among others, this would include the importance for mechanosensation and mechanotransduction (Ottenheijm et al., 2010), protein turnover and autophagy (Jokl and Blanco, 2016) and intracellular signaling (Pyle and Solaro, 2004).

Actin is the major component of the sarcomere, alongside with myosin, therefore the Z-disk network is also built around actin and the most important proteins are the actin binding proteins, which regulate the polymerization and depolymerization of actin filaments, as well as the higher organization of the whole Z-disk network (Winder and Ayscough, 2005). One side of the actin filament is capped by CapZ (Casella et al., 1987) to prevent fast growing and expanding (Cooper and Schafer, 2000). Nebulin/nebulette wraps its filament around the actin filament (Jin and Wang, 1991), stabilizes it and determines its length (Chu et al., 2016). Another giant polymer protein, titin, is responsible for the passive muscle elasticity (Wang et al., 1979; Young et al., 1998) and multiple other actin binding proteins like filamin (Wang et al., 1975), myotilin (Salmikangas et al., 1999), palladin (Parast and Otey, 2000), myopalladin (Bang et al., 2001), fascin (Yamashiro et al., 1998) and many more, play a massive role in the structural organization of the Z-disk. In the Z-disk, actin filaments are crosslinked with antiparallel homodimers of α-actinin-2 (Takahashi and Hattori, 1989) which also have an important function in the Z-disk, as well as numerous binding proteins supporting the organization of this complex network.

Structure and Function of α-actinin-2

α-actinin-2 is an actin binding protein in muscles (Masaki et al., 1967; Takahashi and Hattori, 1989) that belongs to the spectrin superfamily of proteins and, alongside with the three paralogs (*ACTN1-4*) fulfills the actin crosslinking function in muscle and non-muscle cells (Sjöblom et al., 2008). Both non-muscle isoforms of α-actinin, 1 and 4, are calcium sensitive, meaning that the actin binding to the protein is regulated by calcium binding to the calmodulin-like domain (CAMD) (Foley and Young, 2014). They mediate membrane attachment at junctions along microfilament bundles (Mills et al., 2001). Muscle isoforms 2 and 3 are calcium insensitive, and their binding properties are regulated in a different manner (Ribeiro et al., 2014). α-actinin-2 is expressed in all skeletal muscle, whereas the expression of α-actinin-3 is limited only to a subset of type 2 fibers (North and Beggs, 1996).

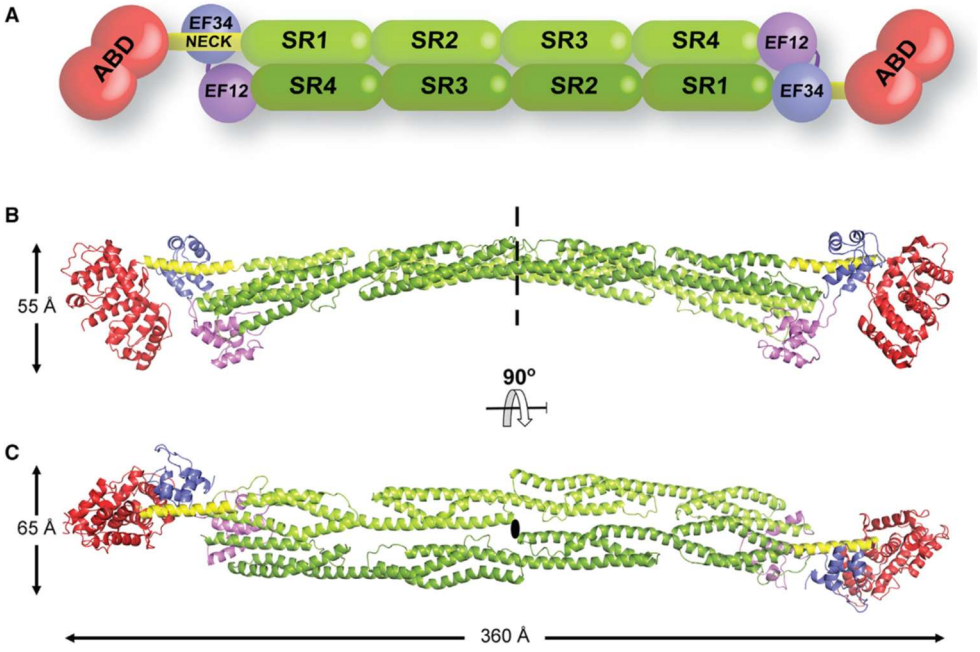

Figure 2 - Structure of α-actinin-2

(A) Schematic representation of the domain composition of α-actinin-2 dimer – actin binding domain (red), neck (yellow), spectrin-like repeats 1-4 (green), EF1-2 (violet), EF3-4 (blue). (B) α-actinin-2 dimeric structure with indicated dimensions. (C) Same as in (B), rotated 90º (Modified after Ribeiro et al., 2014).

α-actinin-2 is cylindrically shaped 360 Å long and 65 Å (Figure 2B and 2C) wide heterodimer. One protomer is composed out of a N-terminal actin-binding-domain (ABD), an α-helical linker (neck) that connects the actin-binding-domain with the rod domain composed out of four spectrin-like repeats (SR1-4) and a C-terminal calmodulin-like domain (CAMD) made out of two pairs of EF hands (EF1-2 and EF3-4) (Figure 2A) (Ribeiro et al., 2014). The ABD of α-actinin-2 has two calponin homology (CH) domains which are in closed conformation when actin is not present (Franzot et al., 2005; Galkin et al., 2010). The α-helical

neck that connects the ABD with the rod domain is also connected to the EF3-4 hands and can be mutated in such manner that it produces a constitutively open variant (NEECK mutant) (Ribeiro et al., 2014). Crystal structure of the rod domain of α-actinin-2 showed that the spectrin repeat 1 shows least similarity with other spectrin repeats (Ylänne et al., 2001). EF hands are in general helix-loop-helix structural domains and two of them, EF1-2 and EF3-4, connected by a short linker, form the C-terminal CAMD of α-actinin-2.

Mutations in α-actinin-2 are known to cause various diseases like familial hypertrophic cardiomyopathy (Chiu Christine et al., 2010), nemaline body myopathy (Nowak et al., 1999), dilated cardiomyopathy (Mohapatra et al., 2003), multiple structured core disease (Lornage et al., 2019) and it may have at least an indirect pathogenic role in diseases like schizophrenia, epilepsy and lupus (Oikonomou et al., 2011). Due to the variety of diseases caused by different mutations in the α-actinin-2 gene, it is important to understand the function behind the structure of the protein, as well as interactions with various binding partners.

Besides interacting with actin via the ABD, α-actinin-2 has numerous binding partners in the Z-disk like nebulin (Nave et al., 1990), titin (Young and Gautel, 2000), myotilin (Salmikangas et al., 1999), FATZ (Faulkner et al., 2000), ZASP (Faulkner et al., 1999), ALP (Xia et al., 1997) and CLP36 (Pomiès et al., 1999).

ALP and Enigma Subfamilies of PDZ and LIM Domain Containing Proteins

Proteins belonging to the PDZ-LIM family all have multiple functional domains and all share one PDZ domain combined with at least one LIM domain. The PDZ domain is a 80-100 amino acids long interaction motif with a highly conserved GLGF sequence (Ponting and Phillips, 1995). Due to being such an abundant interaction motif, the PDZ domain is involved in a wide variety of cellular processes like signaling complex organization, formation and function of signal transduction complexes, anchoring proteins to the membranes, regulation of different signaling pathways involved in cell death, mechanosensory signaling or enzymatic activity (Harris and Lim, 2001; Jani and Schöck, 2007; Lee and Zheng, 2010; Maday et al., 2008; Maisonneuve et al., 2014). One interesting example of a PDZ domain protein involved in signaling pathways is InaD, composed almost entirely out of five PDZ domains which bind various other proteins, for example NorpA. The PDZ domain of InaD binds NorpA at is C-terminus, comparable to the binding of α-actinin-2 with ALP/Enigma proteins, but with one main difference: formation of a disulfide bond in the interaction site is needed for high affinity interaction and complex stabilization (Kimple et al., 2001).

The LIM domain is a conserved zinc finger motif with a cysteine-rich consensus sequence $CX_2CX_{16-23}HX_2CX_2CX_2CX_{16-2}CX_2(C/H/D)$ (Gill, 1995) composed out of two zinc finger domains which are separated by a two amino acid long hydrophobic linker. LIM domains mediate protein-protein interactions that are crucial for diverse cellular processes like neuronal path finding, cytoskeletal organization, tissue-specific gene expression (Jani and Schöck, 2007; Kadrmas and Beckerle, 2004; Schaffar et al., 2008; Zheng et al., 2010).

Based on structural similarity, PDZ-LIM proteins have been divided into four subfamilies: Actinin-associated LIM protein (ALP), Enigma, LIM kinases (LMK1 and LMK2) and LMO7 subfamily (Velthuis et al., 2007). Four proteins have been classified into the ALP subfamily: ALP (PDLIM3), CLP36 (CLIM1, Elfin, PDLIM1), Ril (PDLIM4) and Mystique (SLIM, PDLIM2) (Figure 3A). Each of the protein members has one N-terminal PDZ domain and one C-terminal LIM domain. ALP was identified first (Xia et al., 1997), followed shortly by CLP36 (Wang et al., 1995). Ril is the smallest member of the subfamily, first identified in rat fibroblast (M et al., 1995), it is known to interact with α-actinin-2 (Vallenius et al., 2004) and PTP-BL (van den Berk et al., 2007). The most recently identified member of the ALP subfamily is Mistique (Loughran et al., 2005; Torrado et al., 2004) which also interacts with α-actinin-2 (Torrado et al., 2004). One special characteristic of the ALP subfamily is the presence of a 34 amino acid long motif named ALP-like motif (AM) (Figure 3A). This motif contains a putative consensus protein kinase C phosphorylation site and two α-helices (Velthuis et al., 2007) but more studies are needed to explain the function of this motif.

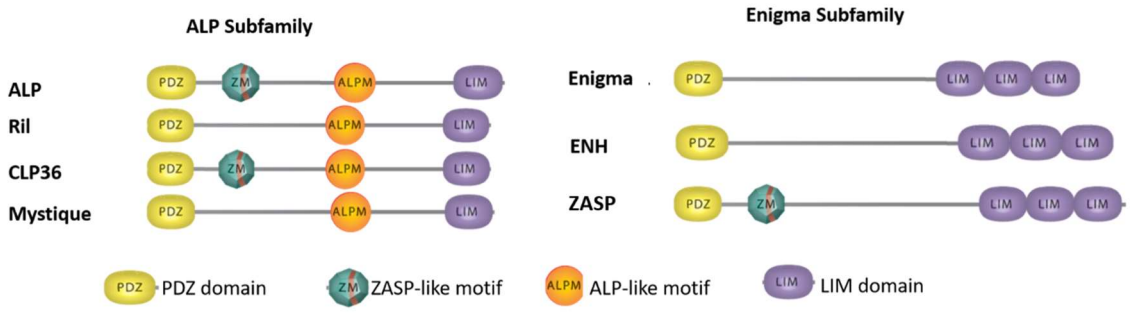

Figure 3 - ALP/Enigma Proteins in Vertebrates

(A) ALP subfamily in vertebrates characterized with four genes (ALP, RIL, CLP36 and Mystique) that encode ALP subfamily proteins and multiple splice isoforms. (B) Three genes (Enigma, ENH and Cypher/ZASP) encoding proteins from the Enigma subfamily in vertebrates. ZASP-like motif is conserved between ALP, CLP36 and ZASP, whereas the ALP-like motif is specific for the proteins from the ALP subfamily. Domain organization of the canonical isoforms is only shown.

The Enigma subfamily has three members (Figure 3B): Enigma, ENH and Cypher (mouse)/ZASP (human), with one N-terminal PDZ domain and three C-terminal LIM domains. Enigma plays a role in mitogenic activity, glucose metabolism and insulin-related actin

organization (Barrès et al., 2006; Durick et al., 1998; Wu and Gill, 1994). ENH was shown to interact with PKC (Kuroda et al., 1996) and with α-actinin-2 (Nakagawa et al., 2000). Cypher was isolated from mice (Zhou et al., 1999) and its human ortholog ZASP was independently identified in skeletal muscle (Faulkner et al., 1999), both of them localizing with α-actinin-2. Experimental analysis of the proteins from ALP and Enigma subfamily revealed a characteristic motif that is present only in ALP, CLP36 and ZASP, called the ZASP-like motif (ZM) (Klaavuniemi et al., 2004; Klaavuniemi and Ylänne, 2006; Velthuis et al., 2007) which is suggested to interact with the spectrin repeats of α-actinin-2 (Klaavuniemi et al., 2004).

Actinin-associated LIM protein (ALP)

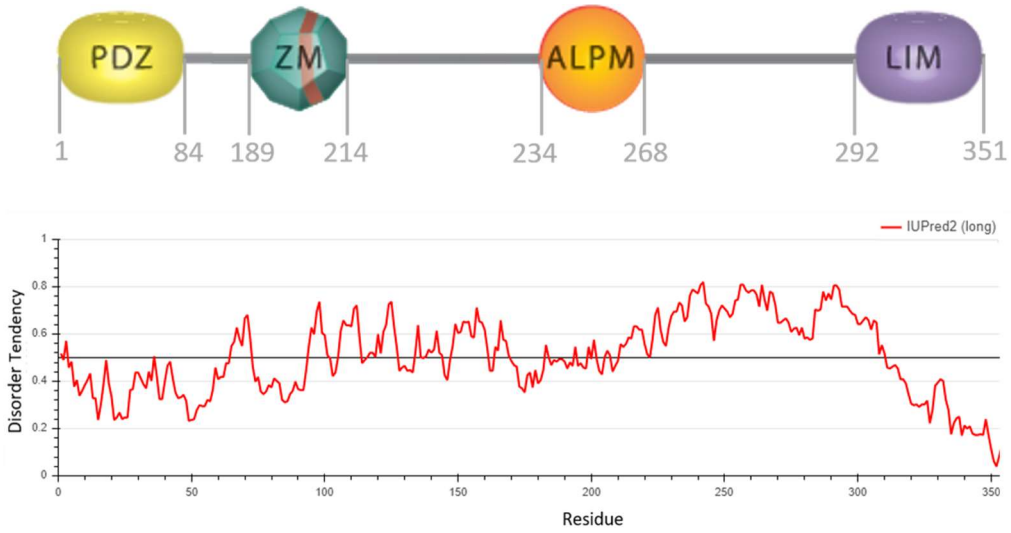

Figure 4 - Schematic Representation of ALP and its Disorder Tendency

ALP is a 364-residues long protein of the Z-disk consisting out of one N-terminal PDZ domain and one C-terminal LIM domain which both show low disorder tendency in comparison with the internal region that consists out of the ZM and ALP-like motif. Disorder tendency calculated on the iupred2a server (Mészáros et al., 2018)

ALP was identified as a 364 residues long, 39 kDa protein in rat skeletal muscle, with a shorter isoform in heart (Xia et al., 1997). It is highly expressed in skeletal muscle tissue (isoform 1), and in lower levels in the cardiac tissue (isoform 2). Like some other members from the ALP and Enigma subfamilies, it forms isoforms via alternative splicing and there are at least two isoforms known in humans. The N-terminal PDZ domain, together with the C-terminal LIM domain show low disorder tendency whereas the internal region that contains the ZM and ALP-like motif shows higher disorder tendendcy (Figure 4). It is known that ALP plays a role in heart development since ALP-deficient mice develop right ventricular cardiomyopathy (Pashmforoush et al., 2001), but when it comes to muscle structure, ALP-deficient mice show no abnormalities suggesting that some other protein takes the role in the absence of ALP (Jo et al., 2001). Due to the presence of the ALP-like motif, it is suggested that ALP plays also a role

as a signaling molecule, but that still hasn't been confirmed. The only known interaction partner of ALP is α-actinin-2, with which it interacts via its PDZ domain, as well as the ZM motif (Klaavuniemi et al., 2009, 2004), but despite that, the function of this protein is largely unknown.

36 kDa C-Terminal LIM Domain Protein (CLP36)

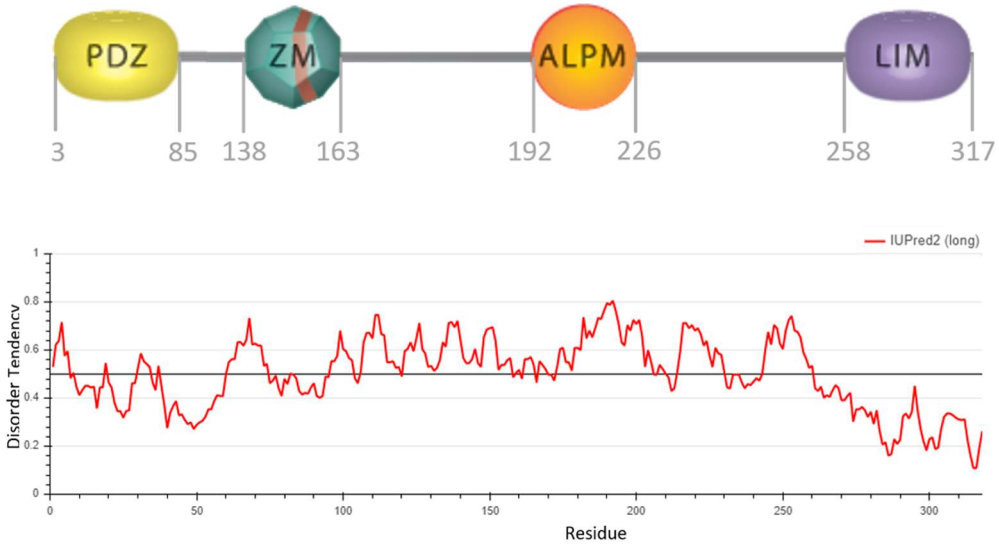

Figure 5 - Schematic Representation of CLP36 and its Disorder Tendency

CLP36 is 329-residue long Z disk protein which shows a moderate disorder tendency in general, except for the fairly ordered C-terminal LIM domain. CLP36 has as well an N-terminal PDZ domain and internal ZM and ALP-like motif. Disorder tendency calculated using the iuprot2a server (Mészáros et al., 2018).

CLP36 was first identified in rat hepatocytes (Wang et al., 1995) where it showed high similarity to Ril. Later it was found in human, highly expressed in skeletal and cardiac muscle tissue, moderately expressed in spleen, small intestine, placenta, colon and lung as well as weakly expressed in the liver, kidney, pancreas, prostate and thymus (Kotaka et al., 1999). It is 329-residues long, 36 kDa protein comprised out of a C-terminal LIM domain which is fairly ordered (Figure 5), as well as an N-terminal PDZ domain and a ZM and ALP-like motif in the internal region which show overall moderate disorder tendency. α-actinin-1 was described as the first binding partner of CLP36 showing association with actin filaments and stress fibers in activated platelets and endothelial cells (Bauer et al., 2000). In parallel it was showed that CLP36 also interacts with α-actinin-4 in non-muscle cells, specifically in colonic epithelium (Vallenius et al., 2004). It has been reported that CLP36 localized to stress fibers in fibroblasts, osteoblasts and choriocarcinoma cell lines (Hasegawa et al., 2010; Maeda et al., 2009; Tamura et al., 2007). It doesn't bind to actin directly, but associates with it (Bauer et al., 2000; Miyazaki et al., 2012; Tamura et al., 2007), via α-actinin-1, α-actinin-2, α-actinin-4 and palladin (Klaavuniemi et al., 2004; Maeda et al., 2009; Vallenius et al., 2000) which suggest that it uses

actin-binding proteins as mediators for localization to stress fibers (Miyazaki et al., 2012). It plays a crucial role in multiple diseases, including in supravalvular aortic stenosis and Williams syndrome (Okagawa et al., 1993).

Z-Disk-Associated, Alternatively Spliced, PDZ Motif-Containing Protein (ZASP)

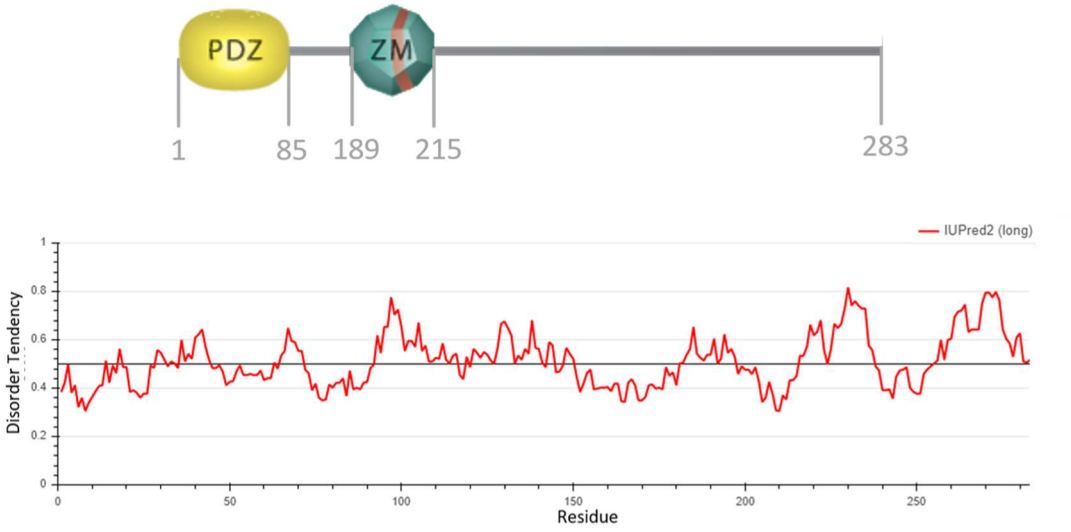

Figure 6 - Schematic Representation of ZASP isoform 6 and its Disorder Tendency

ZASP isoform 6 is a 283 residues long protein missing the C-terminal LIM domains. It shows moderate disorder tendency, especially in the internal region. It has a N-terminal PDZ domain and internal ZM motif. Disorder tendency calculated using the iuprot2a server (Mészáros et al., 2018).

ZASP was independently identified in human (Faulkner et al., 1999) and in mice where it holds the name Cypher (Zhou et al., 1999). It is formed via alternative splicing where exons 1–3 encode the PDZ domain, exons 4 and 6 the ZM motif and exons 12–16 the LIM domains (Klaavuniemi and Ylänne, 2006). The number of exons varies from species to species, in humans there are 16 exons. Up to date, there are 8 known isoforms of ZASP in humans, all of them containing a PDZ domain. Some of the isoforms don't possess any LIM domains, or the ZM motif. The only isoform not expressed in skeletal muscle is isoform 3, whereas the cardiac tissue doesn't show any expression of isoforms 3, 4 and 7 (Martinelli et al., 2014). ZASP has multiple functions as well as diverse binding partners. It binds the mechanosensing protein Ankrd2 and the tumor suppressor protein p53, both of them having a role in signal transduction, gene expression regulation and muscle differentiation (Martinelli et al., 2014). It is shown that ZASP binds FATZ and myotilin (von Nandelstadh et al., 2009), as well as telethonin forming a complex with the sodium channel Na(v)1.5 (Xi et al., 2012), nebulette (Holmes and Moncman, 2008), phosphoglucomutase 1 (Arimura et al., 2009, 2004) and PKC (Yamashita et al., 2014). Alongside its important role in signaling capacity, ZASP plays a crucial role in myofibril assembly (González-Morales et al., 2019), it interacts with actin (Liao et al., 2020;

Watts et al., 2017) and α-actinin-2 (Klaavuniemi and Ylänne, 2006; Zhou et al., 1999) stabilizing the final functional unit.

ZASP/Cypher null mutations in mice cause disorganized and fragmented Z-discs which turned out to be lethal (Arimura et al., 2004). There are numerous myopathies connected to ZASP – dilated cardiomyopathy (Zheng et al., 2009), left ventricular non-compaction (Vatta Matteo et al., 2003), hypertrophic myopathy (Theis et al., 2007), and inclusion body myositis (Britson et al., 2018). Additionally, there is zaspopathy - autosomal dominant form of progressive muscular dystrophy, a collection of myofibrillar myopathies (Griggs et al., 2007) where mutations in ZASP cause the highest percentage of cases. Interestingly, most of the disease associated mutations in ZASP are located in exons that code the ZM motif – exons 4 and 6 (Griggs et al., 2007; Selcen and Engel, 2005; Vatta Matteo et al., 2003).

Importance of the ZM Motif in Interactions with α-actinin-2

A highly interesting feature between the members of ALP and Enigma subfamily of proteins is the presence of a conserved 26 amino acid residues long motif, named the ZM motif, shared between ALP, CLP36 and ZASP. This motif is conserved evolutionary (van der Meer et al., 2006), as well as between the ALP, CLP36, ZASP and their isoforms (Figure 7). Most of the disease associated mutations are specific for exons encoding this motif, showing its significance. Nevertheless, the function of the motif is not precisely known.

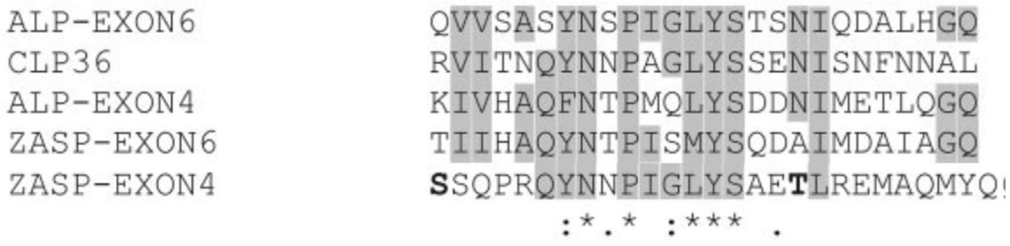

Figure 7 - ZM Motif is Highly Conserved

Alignment of the ZM motif consensus sequence in human ALP, CLP36, and ZASP. No other matches in vertebrates can be found with this motif. (Modified after Klaavuniemi et al., 2004)

On the other hand, function and structure of the PDZ domain are very well known, especially when it comes to the interaction with α-actinin-2. The PDZ domain of ZASP has been solved by NMR (Au et al., 2004), showing that the PDZ domain is a typical class I PDZ domain which interacts with α-actinin-2 EF hands which lost its calcium binding abilities. This interaction has been measured by following fluorescence signal of the unique PDZ tryptophan upon interaction with α-actinin-2, yielding the dissociation constant (K_D) 35.8 μM (Au et al., 2004) which would not correspond to studies done on the interaction between ALP and CLP36,

respectively, with α-actinin-2. An extensive study has been done on the interactions between said proteins, examining the interaction between the PDZ domain of the ALP/Enigma proteins, as well as possible interactions with the ZM motif. Those studies were done using SPR, stating K_D 8.6 μM for the interaction between the PDZ domain of ALP and the EF hands of α-actinin-2, that is K_D 15 μM for the interaction between the PDZ domain of CLP36 (Klaavuniemi et al., 2004).

The ZM motif of ZASP has been suggested to interact with α-actinin-2 (Klaavuniemi and Ylänne, 2006), but that has been disputed in the literature (Liao et al., 2016). Studies on the ZM motif of ALP and CLP36 have been more conclusive, stating an interaction with the rod domain with K_D 6.8 μM (ALP) and 1.3 μM (CLP36) (Klaavuniemi et al., 2004). The authors went a step further and mapped the interaction with ALP to the spectrin repeats 2 and 3 (6.8 μM), but when they designed a peptide that would correspond to the ZM motif, it didn't bind to SR2-3, but only to the rod domain (Klaavuniemi et al., 2009). Even though it has been shown that α-actinin-2 interacts with these proteins, it still remains largely unknown what is the role of ZM motif in the interaction with α-actinin-2 (Figure 8) – does it interact with α-actinin-2 and if so, with what affinity?

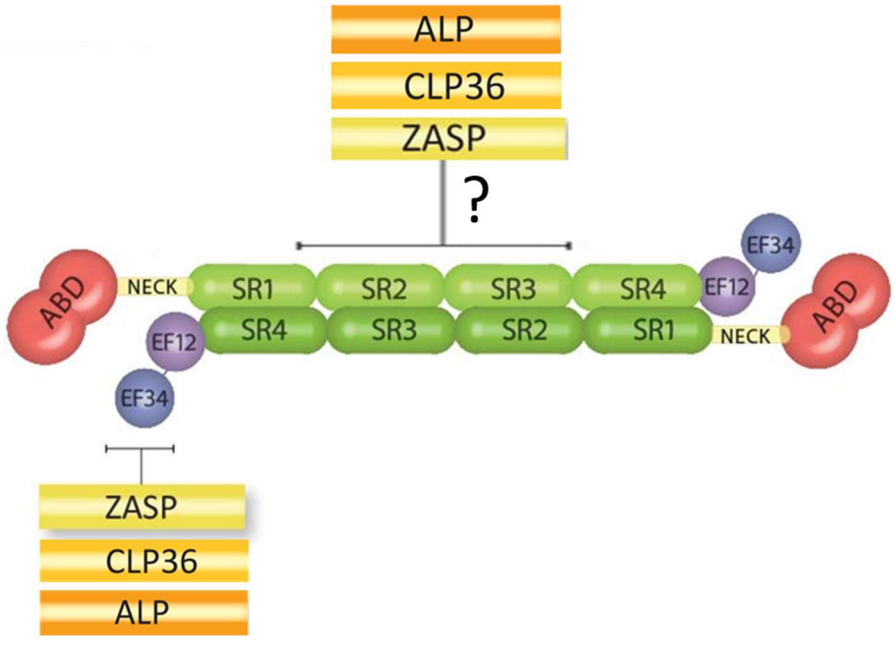

Figure 8 - α-actinin-2 : ALP/CLP36/ZASP Interactome

Interactions between the PDZ domain of ALP/Enigma proteins and the EF hands of α-actinin-2 are well known and characterized in contrast to interaction between the ZM motif and the rod domain.

Aim of the Study

In light of the aforementioned findings, it seems that ZM motif plays a crucial role in binding with α-actinin-2. It is shown, via SPR, that an internal region of ALP and CLP36 interacts with the rod domain of α-actinin-2 and it is suggested that the ZM motif of ZASP is sufficient for the interaction with α-actinin-2. Due to high variability of binding affinities between studies and the disputing literature, in this work I employed a combined set of biochemical, structural and biophysical methods to answer the main question: What are the structural details of the interaction between the ZM motif and α-actinin-2? Here, SEC-MALLS and crosslinking were employed to characterize the interaction, focusing on the stoichiometry and binding regions in order to fully understand out how ALP, CLP36 and ZASP interact with α-actinin-2. Furthermore, ITC was used to determine the dissociation constant and determine the contribution of changes in enthalpy and entropy to the final free energy of binding which could reveal potential differences in binding between ALP, CLP36 and ZASP. Finally, SAXS and X-ray crystallography were tried in order to structurally characterize the interaction between the ZM motif and the spectrin repeats of α-actinin-2 to deepen the understanding of the ZM motif function.

Materials and Methods

Protein Expression

A pET3d plasmid encoding the α-actinin-2 wild-type or the D893C mutant construct, respectively, was transformed into chemically competent *E. coli* Rosetta 2 (DE3) pLysS cells using the heat shock method and grown on agar plates containing 100 μg mL^{-1} ampicillin and 34 μg mL^{-1} chloramphenicol. One colony from the plate was used to grow a preculture at 37 ºC in LB media supplemented with the antibiotics overnight. The overnight culture was used to inoculate the ZYP-5052 auto-induction media supplemented with the corresponding antibiotics. The media was divided into 2-L flasks, with no more than 500 mL of bacterial solution per flask, and grown at 30 ºC overnight. The cells were harvested at 4 ºC and 5000 rpm for 20 minutes in a HITACHI centrifuge with a R9A2 rotor.

A pET3d plasmid encoding the α-actinin-2 NEECK mutant or the rod domain of α-actinin-2 were, respectively, transformed into competent *E. coli* BL21 (DE3) cells using the heat shock method and grown on agar plates containing 100 μg mL^{-1} ampicillin, for the rod domain, or 100 μg mL^{-1} ampicillin and 34 μg mL^{-1} chloramphenicol for the NEECK mutant. Precultures for both constructs were grown from one colony at 37 ºC in LB media supplemented with the corresponding antibiotics overnight. This culture was used to inoculate the LB media supplemented with the antibiotics, divided into 2-L flasks and grown at 37 ºC until OD_{600} reached 0.8 and finally induced with 1 mM IPTG and incubated for 4 hours at 37 ºC. The cells were harvested at 4 ºC and 5000 rpm for 20 minutes in a HITACHI centrifuge with a R9A2 rotor.

All ALP and CLP36 constructs encoded in a pET24d plasmid were kindly provided by Jari Ylänne (University of Jyväskylä, Finland) (Klaavuniemi et al., 2004), except for the ALP^{1-284} R16C and $CLP36^{1-284}$ R17C variants that were prepared by mutating the wild-type constructs by Dalibor Milić. They were, respectively, transformed into competent *E. coli* BL21 (DE3) cells using the heat shock method and grown on agar plates containing 50 μg mL^{-1} kanamycin. One colony from the plate was used to prepare an overnight culture at 37 ºC in LB media supplemented with kanamycin. That culture was used to inoculate the ZYP-5052 auto-induction media with 100 μg mL^{-1} kanamycin, which was divided into 2-L flasks with no more than 500 mL of bacterial solution per flask, and grown at 37 ºC until OD_{600} reached 1.0. The

temperature was then lowered to 20 ºC and the cells were incubated overnight. The cells were harvested at 4 ºC and 5000 rpm for 20 minutes in a HITACHI centrifuge with a R9A2 rotor.

All ZASP constructs, except the PDZ domain of ZASP, were encoded in a pACE_3NH plasmid and respectively transformed into competent *E. coli* phage resistant BL21 (DE3) cells. They were expressed in the same manner as ALP and CLP36 constructs, with the difference of being incubated overnight before harvesting at 37 ºC for the full-length ZASP isoform 6 and at 18 °C for ZASP ΔC.

The PDZ domain of ZASP was encoded in a pETM14-LIC plasmid, transformed into competent *E. coli* Rosetta 2 (DE3) pLysS cells and grown overnight on a LB-agar plate with 50 μg mL^{-1} kanamycin and 34 μg mL^{-1} chloramphenicol. Colonies from the LB-agar plate were used to prepare an overnight culture at 37 ºC in LB medium supplemented with kanamycin and chloramphenicol. The overnight culture was used to inoculate the ZYP-5052 auto-induction medium with 100 μg mL^{-1} kanamycin and 34 μg mL^{-1} chloramphenicol. The cells were grown while shaking at 37 ºC for 6 hours and then at 20 °C overnight. The cell pellets with the PDZ domain of ZASP were kindly provided by Valeria Stefania.

Protein Purification

Cells containing α-actinin-2 (wild type or D893C mutant) were resuspended in 50 mM Tris-HCl pH 7.5, 150 mM NaCl, 5% (v/v) glycerol, 0.5% (v/v) Triton X-100 supplemented with protease inhibitor cocktail, homogenized and passed through the cell disrupter (1.35 kbar) to release the protein. The solution was centrifuged at 4 ºC and 18 000 rpm for 30 minutes in the HITACHI centrifuge using the R20A2 rotor. Resulting supernatant was applied onto a HisTrap FF Crude column (Cytiva) equilibrated with buffer A (50 mM Tris-HCl pH 7.5, 150 mM NaCl, 20 mM imidazole, 2 mM β-mercaptoethanol) and eluted with 5 CV step gradient of 50% buffer B (50 mM Tris-HCl pH 7.5, 150 mM NaCl, 500 mM imidazole, 2 mM β-mercaptoethanol). The His-tag was then cleaved overnight with TEV protease (mass ratio 1:20) in TEV cleavage buffer (50 mM Tris-HCl pH 7.5, 0.5 M EDTA, 1 mM DTT). After running a reverse HisTrap purification and collecting the flow-through with the cleaved protein, the flow-through was diluted 3–5 times with anion-exchange buffer A (50 mM Tris-HCl pH 7.5, 0.5 mM EDTA, 0.1 mM PMSF, 2 mM β-mercaptoethanol) and loaded onto a Resource Q column (Cytiva) equilibrated with anion-exchange buffer A and eluted with a linear gradient in anion-exchange buffer B (50 mM Tris-HCl pH 7.5, 1 M NaCl, 0.5 mM EDTA, 0.1 mM PMSF, 2 mM β-mercaptoethanol). Finally, the peak containing the protein was pooled, concentrated and loaded onto a HiLoad 26/600 Superdex 200 pg (Cytiva) column and eluted with an isocratic

gradient of size exclusion buffer (20 mM Tris-HCl pH 7.5, 150 mM NaCl, 0.5 mM EDTA, 0.1 mM PMSF, 2 mM β-mercaptoethanol).

α-actinin-2 NEECK mutant cells were resuspended in the lysis buffer (50 mM Tris-HCl pH 7.5, 150 mM NaCl, 2 mM β-mercaptoethanol, protease inhibitor cocktail), homogenized and passed through the cell disruptor at 1.35 kbar. 0.1 mM PMSF was added afterwards and the solution was centrifuged at 4 ºC and 18 000 rpm for 30 minutes in the HITACHI centrifuge using the R20A2 rotor. Resulting supernatant was loaded onto a StrepTrep HP column (Cytiva) equilibrated with 50 mM Tris-HCl pH 7.5, 150 mM NaCl and eluted in a step gradient with 15 CV 50 mM Tris-HCl pH 7.5, 150 mM NaCl, 2.5 mM D-desthiobiotin. The eluted product was loaded onto a pre-equilibrated HiLoad 26/600 Superdex 200 pg (Cytiva) column and eluted with an isocratic gradient of size exclusion buffer (20 mM Tris-HCl pH 7.5, 150 mM NaCl).

Cells containing the rod domain of α-actinin-2 were resuspended in 50 mM Tris-HCl pH 8.0, 150 mM NaCl, 2 mM β-mercaptoethanol, 10 mM imidazole, DNase I, protease inhibitor cocktail, homogenized and disrupted at 1.35 kbar in a cell disruptor. 0.1 mM PMSF was added and the mixture containing the protein was centrifuged at 4 ºC and 18 000 rpm for 30 minutes in the HITACHI centrifuge using the R20A2 rotor. The supernatant was loaded onto a HisTrap FF Crude (Cytiva) column equilibrated with buffer A (50 mM Tris-HCl pH 8.0, 150 mM NaCl, 2 mM β-mercaptoethanol, 10 mM imidazole) and eluted with 10 CV of 100% buffer B (50 mM Tris-HCl, 150 mM NaCl, 2 mM β-mercaptoethanol, 400 mM imidazole). Eluted protein was immediately diluted 3 times with buffer A before the cleavage of the His-tag overnight with TEV protease (mass ratio 1:20) in TEV cleavage buffer (50 mM Tris-HCl pH 8.0, 100 mM NaCl). After running a reverse HisTrap purification, the flow-through with the cleaved protein was collected and loaded onto a HiLoad 26/600 Superdex 75 pg (Cytiva) column and eluted with an isocratic gradient of size exclusion buffer (20 mM Tris-HCl pH 7.5, 150 mM NaCl).

All ALP and CLP36 protein constructs were purified following the same protocol. The cells were resuspended in 50 mM Tris-HCl pH 8.0, 200 mM NaCl, 20 mM imidazole, 5% (v/v) glycerol, 0.5% (v/v) Triton X-100, 0.2 mM TCEP, homogenized and disrupted via sonication at 50% amplitude, 3 times 3 minutes (1 s pulse, 1 s pause) on ice. Disrupted cells were then centrifuged at 4 ºC and 18 000 rpm for 30 minutes in the HITACHI centrifuge using the R20A2 rotor. Supernatant was loaded onto a HisTrap FF Crude column (Cytiva) equilibrated with 20 mM Tris-HCl pH 8.0, 200 mM NaCl, 20 mM imidazole, 5% glycerol (v/v), 0.2 mM TCEP and eluted with 5 CV a two-step gradient of 6% and 100% buffer B (20 mM Tris-HCl pH 8.0, 20 mM NaCl, 400 mM imidazole, 5% glycerol (v/v), 0.2 mM TCEP). The His-tag was left on

constructs used for the formation of the disulfide-bridged complex, as well as for those used in cross-linking where they were subjected to western blot. In all other cases, the tag was cleaved overnight with TEV cleavage protease (mass ratio 1:20) in 10 mM Tris-HCl, 100 mM NaCl, 2% (v/v) glycerol and 0.2 mM TCEP. After running a reverse HisTrap, the flow-through containing the cleaved protein was collected, diluted 10 times with anion-exchange buffer A (20 mM Tris-HCl, 2% (v/v) glycerol, 0.2 mM TCEP) and loaded onto a Resource Q column (Cytiva) equilibrated with the same buffer. Protein was eluted in a linear gradient of 20% anion-exchange buffer B (20 mM Tris-HCl pH 8.0, 2 M NaCl, 5% glycerol (v/v), 0.2 mM TCEP) in 15 CV. The peak containing the protein was collected, 20 mM DTT was added to reduce all possible cysteine bonds and loaded onto a a HiLoad 26/600 Superdex 75 pg (Cytiva) column and eluted with an isocratic gradient of size exclusion buffer (50 mM Tris-HCl pH 8.0, 150 mM NaCl, 1 mM DTT).

Cells containing the PDZ domain of ZASP were resuspended in 50 mM Tris-HCl pH 7.5, 150 mM NaCl, 5% (v/v) glycerol, 0.5% (v/v) Triton X-100 supplemented with protease inhibitor cocktail, homogenized and passed through the cell disrupter (1.35 kbar) before being centrifuged at 4 ºC and 18 000 rpm for 30 minutes in the HITACHI centrifuge using the R20A2 rotor. The supernatant was loaded onto a GSTrap HP column (Cytiva) equilibrated with 20 mM HEPES pH 7.2, 150 mM NaCl, 5% glycerol (v/v) and eluted in 10 CV of 20 mM HEPES pH 7.2, 150 mM NaCl, 5% (v/v) glycerol, 10 mM reduced glutathione. The GST-tag was cleaved off overnight with TEV cleavage protease (mass ratio 1:10) in 20 mM HEPES, 150 mM NaCl, 5% (v/v) glycerol, 1 mM DTT, 0.5 mM EDTA. The tag was separated from the protein on a HiLoad 26/600 Superdex 75 pg (Cytiva) column in 20 mM HEPES pH 7.2, 150 mM NaCl, 5% (v/v) glycerol.

Full-length ZASP isoform 6 R16C mutant was kindly purified by Claudia Schreiner. The cells were resuspended in 1× PBS (137 mM NaCl, 2.7 mM KCl, 10 mM Na_2HPO_4, 1.8 mM KH_2PO_4) pH 7.5, 4 M GuHCl, 0.2% (v/v) Tween 20, 1 mM DTT with addition of a protease inhibitor cocktail. The cells were disrupted via sonication at 50% amplitude, 3 times 3 minutes (1 s pulse, 1 s pause) on ice. Disrupted cells were then centrifuged at 4 ºC and 18 000 rpm for 30 minutes in the HITACHI centrifuge using the R20A2 rotor. The supernatant was loaded onto a HisTrap FF Crude column (Cytiva) that was equilibrated with buffer A (1× PBS pH 7.5, 4 M GuHCl, 300 mM NaCl, 5% (v/v) glycerol, 20 mM imidazole, 1 mM DTT) and eluted with a linear gradient (in 20 CV) to 100% buffer B (1× PBS pH 7.5, 4 M GuHCl, 300 NaCl, 5% (v/v) glycerol, 500 mM imidazole, 1 mM DTT). After the elution was collected, 20 mM DTT was

added to avoid formation of disulfide bridges and the sample was loaded onto a pre-equilibrated HiLoad 26/600 Superdex 200 pg (Cytiva) column and eluted in 1× PBS pH 7.5, 3 M GuHCl, 300 mM NaCl, 5% (v/v) glycerol, 1 mM DTT. Since the protein was expressed in inclusion bodies, after it was separated using size exclusion chromatography, it was subjected to a serial dialysis in buffer 50 mM NaOAc pH 5.0, 100 mM NaCl, 1M DTT with a decreasing urea concentration (3 M, 2 M, 1 M, 0 M) to allow refolding. The final dialysis step was with the refolding buffer (50 mM Na_2HPO_4/NaH_2PO_4 pH 6.1, 100 mM NaCl, 1 mM DTT).

ZASP ΔC variant was kindly purified by Cristina Lazar. The cells were resuspended in 50 mM Tris-HCl pH 7.5, 500 mM NaCl, 20 mM imidazole, 5% (v/v) glycerol, 0.2% (v/v) Tween 20 supplemented with protease inhibitor cocktail, DNase I and 0.2 mM PMSF. The cells were homogenized and disrupted via sonication 50% amplitude, 2 times 2 minutes (1 s pulse, 1 s pause). Cell debris was spun down at 4 ºC and 18 000 rpm for 30 minutes in the HITACHI centrifuge using the R20A2 rotor. The supernatant was loaded onto a HisTrap FF Crude column (Cytiva) equilibrated with 20 mM Tris-HCl, 500 mM NaCl, 20 mM imidazole, 5% (v/v) glycerol and eluted with 6 CV of 20 mM Tris-HCl pH 7.5, 150 mM NaCl, 500 mM imidazole, 5% (v/v) glycerol. The elution was collected and diluted 10 times with cation-exchange buffer A (10 mM Tris-HCl, 0.5 mM EDTA, 0.1 mM PMSF) and loaded onto a Resource S column (Cytiva) pre-equilibrated with the same buffer. The protein was eluted with linear gradient up to 20% cation-exchange buffer B (20 mM Tris-HCl pH 7.5, 1 M NaCl, 0.5 mM EDTA, 0.1 mM PMSF) in 60 CV. The fractions containing the protein were pooled and loaded onto a HiLoad 26/600 Superdex 75 pg (Cytiva) column and eluted in an isocratic gradient in 20 mM Tris-HCl pH 7.5, 150 mM NaCl, 0.5 mM EDTA, 0.1 mM PMSF.

Preparation of Disulfide-Bridged Complexes

Cysteine mutant constructs of ALP, CLP36, ZASP and α-actinin-2 were dialyzed overnight in 50 mM Tris-HCl pH 7.5, 100 mM NaCl, 1 mM DTT. They were centrifuged at 186000 rcf for 70 minutes at 4 ºC (Beckmann Ultracentrifuge) and mixed in a 2:1 molar ratio [*n*(ligand): *n*(α-actinin-2)]. 3 mM oxidized glutathione was added and the protein mixture was incubated overnight at 4 ºC on ice. The solution was then diluted 6 times with 10 mM Tris-HCl pH 7.5, 100 mM NaCl, 10 mM imidazole and loaded onto a HisTrap FF Crude (Cytiva) column pre-equilibrated with the same buffer. The protein complex was eluted within 10 CV in 100% 20 mM Tris-HCl, 100 mM NaCl, 400 mM imidazole. The eluted complex was then loaded onto a HiLoad 26/600 Superdex 75 pg (Cytiva) column and eluted in an isocratic gradient in 50 mM Tris-HCl, 100 mM NaCl.

ALP peptide 3

The ALP peptide 3 (sequence PLEMELPGVKIVHAQFNTPMQL) corresponding to the one tested in literature which binds to the rod domain of α-actinin-2 (Klaavuniemi et al., 2004) was synthetized by GenScript. It was provided as white lyophilized powder with ≥95% purity. It was not soluble in pure water, but in DMSO, therefore the used buffer for dissolving was 1× PBS, 1 mM β-mercaptoethanol, 2% (v/v) DMSO. The concentration of the peptide was determined by diluting the peptide 10× and measuring the absorbance at 205 nm on a NanoPhotometer (IMPLEN).

Dynamic Light Scattering (DLS)

Dynamic light scattering was used to assess protein polydispersity. DynaPro NanoStar DLS Detector from Wyatt Technology was used to perform the measurements on 15 µL sample in a reusable quartz cuvette. Each measurement was carried out as a set of 10 5-second-long sub-measurements. They were set up as well as analyzed using the Dynamics 7.9.0.5 software (Wyatt Technology).

Size Exclusion Chromatography – Multiple Angle Laser Light Scattering (SEC-MALLS)

SEC-MALLS was used to characterize the proteins. They were centrifuged at 20 000 g for 10 minutes at 4 ºC (Eppendorf 5417R) and their concentration was determined using NanoDrop 2000c (Thermo Scientific). Either a Superdex 200 Increase 10/300 GL or Superose 6 Increase 10/300 GL was equilibrated overnight in 50 mM Tris-HCl, 150 mM NaCl and 90 µL of the sample was loaded with the flow rate of 0.5 mL/min. Agilent Technologies 1260 Infinity II system equipped with miniDAWN detector (Wyatt Technology) and a refractive index detector Shodex RI-501 was used to perform the measurements. Analysis was done on the ASTRA 7.3.2 software (Wyatt Technology).

Thermal Shift Assay

Thermal shift assay was used to assess the stability of ALP and CLP36 under varying buffers and pH. Master mix was prepared with 420 µL of the protein (1 mg/mL for ALP, 2 mg/mL for CLP36), 2.1 µL of 5000× Spyro Orange dye (Thermo Fisher Scientific) and filled up with water to 525 µL. 5 µL of the mix was added to each well of the home-made pH/Buffer Screen 1 (Mlynek et al., 2020), sealed with Microseal "B" PCR Plate Sealing Film (Bio-Rad) and centrifuged for 2 minutes (Eppendorf 5810-R). The assay was run heating up from 15 ºC to 95 ºC, with 1 ºC increase per minute (CFX96 Real-Time System, C1000 Touch)

Isothermal Titration Calorimetry (ITC)

Proteins were dialyzed overnight in 1× PBS pH 7.5, 1 mM β-mercaptoethanol and centrifuged at 20 000 g for 10 minutes at 20 ºC (Eppendorf 5417R). The concentration of the proteins was determined using the NanoDrop 2000c (Thermo Scientific). Ligands (ALP, CLP36, ZASP) were titrated into a cell containing the protein (α-actinin-2 constructs) with at least 10 times lower concentration. All measurements were performed on Malvern Panalytical MicroCal Peaq ITC at 25 ºC with the stirring speed of 500 rpm, reference power 5 (20 µW), 60 second delay with 180 seconds recovery time and 20 injections in total. The binding between the rod domain of α-actinin-2 and the ALP peptide was performed in the same manner, with the difference being 2% (v/v) DMSO present in the buffer. Analysis was performed using MicroCal Analysis Software (Malvern Panalytical).

Statistical Data Analysis

The binding parameters obtained from ITC measurements were analyzed using an independent *t*-test in Microsoft Office Excel with a R Studio add-in.

Crosslinking

Proteins used for crosslinking were first dialyzed overnight in 1× PBS, pH 7.5, 1 mM β-mercaptoethanol to remove Tris-HCl buffer which interferes with cross-linkers. Used cross-linkers were EDC:sulfo-NHS in a 1:2.5 molar ratio and DMTMM. Ligands (ALP, CLP, ZASP) were mixed in an increasing concentration (10–50 µM) with 5 µM protein (α-actinin-2 constructs) and incubated for 30 minutes before 2 mM cross-linker was added. The mixture was then incubated for 2 hours at room temperature while shaking at 600 rpm for the reaction to be then finally stopped by adding 5× SDS-PAGE loading dye. 15 µL of the samples was loaded onto a Tris-Glycine gel (6% or 8%) and run at 200 V for 43 minutes. The appropriate bands were cut out and sent for mass spectrometry analysis.

Crosslinking of the disulfide-bridged complexes was performed in non-reducing conditions. The protein complexes were as well dialyzed overnight in 1× PBS pH 7.5, and DMTMM as well as EDC:sulfo-NHS were used as cross-linkers. 5 µM proteins were mixed with an increasing concentration of cross-linkers (0–5 mM) and incubated for 30 minutes at room temperature. The reaction was stopped by adding 5× SDS-PAGE loading dye. One portion of the protein complex samples containing cross-linkers was removed and mixed with 0.5 M β-mercaptoethanol to reduce the disulfide bridge and check for the newly formed cross-

links. 10 µL of the samples was loaded onto a 6% Tris-Glycine gel and run at 200 V for 43 minutes.

Western Blot

Gel was transferred onto a mini membrane using Trans-Blot Turbo Transfer System (Bio-Rad). The membrane was after the transfer incubated in TBS (10 mM Tris-HCl pH 7.5, 150 mM NaCl) with 5% milk powder for 1 h at room temperature. It was afterwards washed twice for 10 minutes in TBST (10 mM Tris-HCl, 150 mM NaCl, 0.05% (v/v) Tween-20) and twice for 10 minutes in TBS. A 1:1000 dilution of 6x-His Tag Monoclonal Antibody HIS.H8 (Invitrogen) and 1:200 dilution of secondary Rb pAb to Ms IgG antibody (Abcam) was prepared in TBS with 5% milk powder and the membrane was incubated in it for 1 h at room temperature. The membrane was again washed twice with TBST for 10 minutes and twice with TBS for 10 minutes. One Sigmafast BCIP/NBT (Sigma Aldrich) alkaline phosphatase tablet was dissolved in 10 mL deionized water and the membrane was incubated in it until bands were visible. The reaction was quenched by washing the membrane 3 times with deionized water.

Crystallization

For initial screening, purified rod domain of α-actinin-2 was concentrated to 5 mg mL^{-1} as well as ALP_112-284 and CLP36_117-256. 1 mL of ALP_112-284 and CLP36_117-256 was, respectively, mixed with 1 mL of the rod domain and the mixture was concentrated in Vivaspin 6, 3.5 kDa MWCO until the final volume reached 1 mL, allowing both proteins in the mixture to be at the same concentration. The mixture was immediately used to set up sitting drops in MRC 3-well plates with Mosquito pipetting robot (TTP Labtech) in different protein (150 nL, 200 nL, 250 nL) to reservoir (200 nL) ratios. 6 commercial screens were used: Crystal Screen (Hampton Research), Index Screen (Hampton Research), PACT Premier (Molecular Dimensions), PEG Ion (Hampton Research), Wizard Classic 1&2 (Molecular Dimensions), MIDAS (Molecular Dimensions). The plates were set up at 4 ºC and at 22 ºC (Rock Maker 1000, Formulatrix). Crystal optimization was performed in manually designed screens, varying mostly in pH and PEG concentrations. They were pipetted manually in pre-greased 24-well plates, again in different protein (300 nL, 400 nL, 500 nL) to reservoir (400 nL) ratios as hanging drops. Optimization screens were used to set up the crystallization of the rod domain of α-actinin-2 with the ALP peptide, where the rod domain was concentrated to 5 mg mL^{-1} and the peptide was dissolved to the same concentration. Both were mixed together and the mixture was concentrated in Vivaspin 6, 3.5 kDa MWCO until the final volume reached 1 mL

Structure Determination

X-ray diffraction data were collected at 100 K at the European Synchrotron Radiation Facility (ESRF) on the fully automated beamline ID30A-1 (MASSIF-1; wavelength 0.966 Å) (using flash-frozen crystals soaked in reservoir solution containing 30% (v/v) glycerol (crystals from the initial screening) or the reservoir solution with higher polymer concentration (30% (w/v) PEG 3350 or 40 % (w/v) PEG 8000) for the optimized crystals. The diffraction data were reduced using XDS (Kabsch, 2010) and the structures solved by molecular replacement in *Phaser* (McCoy et al., 2007) using the α-actinin-2 rod monomer (PDB ID 1hci, polypeptide chain A) as a search model. The structural models were refined in REFMAC5 (Murshudov et al., 2011) and manually built in *Coot* (Emsley et al., 2010) as part of the CCP4 program suite (Winn et al., 2011).

Results

Protein Constructs

In order to biophysically characterize the interaction between α-actinin-2 and the proteins of the ALP/Enigma family, different α-actinin-2 constructs were used (Table 1). α-actinin-2 was used as the wild type full-length construct, as well as the D893C mutant, which was used to form the disulfide-bridged complexes. In α-actinin-2 NEECK mutant residues R268, I269 and L273 were replaced with negatively charged glutamates, which disrupt the contact between the neck and the EF3-4 hands keeping the protein in a constitutively open conformation. The rod domain of α-actinin-2 was used to probe for specific interactions, which do not include the PDZ domain of the ligands.

From the ALP/Enigma family of proteins, three proteins containing the special ZM motif were used – ALP, CLP36 and ZASP. The full-length ALP construct, lacking the LIM domain was used for characterizing the interaction, as well as $ALP^{112-284}$ construct lacking the PDZ domain which allowed to determine the interaction happening around or at the ZM motif. CLP36 was used in the same manner – one full-length construct lacking the LIM domain, as well as one lacking the LIM and the PDZ domain. The same constructs were used for cross-linking, with the difference being in their tag – it was not cleaved so that the proteins can be detected via western blot. Both ALP^{1-284} and $CLP36^{1-256}$ were mutated at residue R16 and R17, respectively, in order to obtain constructs that would form a disulfide-bridged complex with α-actinin-2 D893C mutant.

Due to low solubility of multiple constructs of ZASP isoform 6 (the isoform lacking the LIM domains), ZASP ΔC (amino-acid residues 1–179) was used for characterization of interactions with α-actinin-2. This construct is truncated at the C-terminal part and can be concentrated to higher concentrations needed for the binding studies. To examine the interactions between the PDZ domain and the EF hands of α-actinin-2, the PDZ domain of ZASP was as well used for binding studies. For preparation of the disulfide-bridged complex, the full-length ZASP isoform 6 construct was used, with a cysteine mutation inserted at position of residue R16.

Table 1 - Protein constructs used for biophysical characterization of the interaction between α-actinin-2 and the selected proteins of the ALP/Enigma family

	Name	Description/Mutations	Affinity tags	Plasmid/ Antibiotic resistance	Expression system/ Expression media	Molecular Mass* [kDa]
	ACTN2	Full-length wild type	Nt-His6	pET3d, ampicillin	*E.coli*, Rosetta 2 (DE3) pLysS strain, ZYP-5052	105.9 (103.9) 211.8† (207.8†)
	ACTN2 D893C	Full-length D893C mutant	Nt-His6	pET3d, ampicillin	*E.coli,* Rosetta 2 (DE3) pLysS strain, ZYP-5052	105.9 (103.9) 211.8† (207.8†)
	ACTN2 NEECK	Full-length R268E+I269E+L273E	Nt-Strep	pET3d, ampicillin	*E.coli*, BL21 (DE3) strain, LB media	58.1 (56.1) 116.2† (112.2†)
	rod ACTN2	rod domain of ACTN2	Nt-His6	pET3d, ampicillin	*E.coli*, BL21 (DE3) strain, LB media	116.1 (112.3)
	ALP$^{1-284}$	ALP isoform 1 without LIM domain	Nt-His6	pET24d, kanamycin	*E.coli*, BL21 (DE3) strain, ZYP-5052	33.7 (30.7)
	ALP$^{112-284}$	ALP isoform 1 without PDZ and LIM domain	Nt-His6	pET24d, kanamycin	*E.coli,* BL21 (DE3) strain, ZYP-5052	21.8 (18.8)
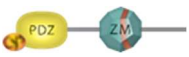	ALP$^{1-284}$ R16C	ALP isoform 1 without PDZ and LIM domain, with R16C mutation	Nt-His6	pET24d, kanamycin	*E.coli,* BL21 (DE3) strain, ZYP-5052	33.6
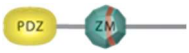	CLP36$^{1-256}$	CLP36 without LIM domain	Nt-His6	pET24d, kanamycin	*E.coli,* BL21 (DE3) strain, ZYP-5052	30.9 (27.9)
	CLP36$^{117-256}$	CLP36 without PDZ and LIM domain	Nt-His6	pET24d, kanamycin	*E.coli,* BL21 (DE3) strain, ZYP-5052	18.3 (15.3)
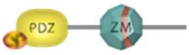	CLP36$^{1-284}$ R17C	CLP36 without PDZ and LIM domain, with R17C mutation	Nt-His6	pET24d, kanamycin	*E.coli,* BL21 (DE3) strain, ZYP-5052	30.9
	ZASP R16C	ZASP isoform 6 without LIM domains with R16C mutation	Nt-His6	pACE_3NH, kanamycin	*E.coli*, BL21 (DE3) phage strain, ZYP-5052	33.2
	ZASP ΔC	C-terminally truncated ZASP isoform 6 R16C mutant	Nt-His6	pACE_3NH, kanamycin	*E.coli*, BL21 (DE3) phage resistant strain, ZYP-5052	21.2
	ZASP PDZ	PDZ domain of ZASP	Nt-GST-His6	pETM14-LIC, kanamycin	*E.coli*, Rosetta2 (DE3) pLysS strain, LB media	37.0 (9.1)

* Molecular mass after tag removal by the protease cleavage is given in parentheses.
† Molecular mass of the dimer.

Characterization of the Protein Constructs

Protein constructs of ALP and CLP36 were all purified in the same manner and exhibited similar behavior. These protein constructs were expressed in *E. coli* BL21 (DE3) cells in ZYP-5052 media and the protein was isolated from the lysate using nickel-affinity chromatography. Following overnight cleavage with the TEV protease and separation of the cleaved protein in a second nickel-affinity step, the constructs were purified by anion-exchange chromatography. The tag was left for crosslinking experiments where the gels were subjected to western blot. Finally, ALP and CLP36 constructs were eluted from a size exclusion column resulting in a high yield. The constructs could be concentrated to high concentrations, more than 10 mg mL^{-1}, showed a high degree of purity on SDS-PAGE and displayed different degrees of polydispersity in DLS measurements (Figure 9).

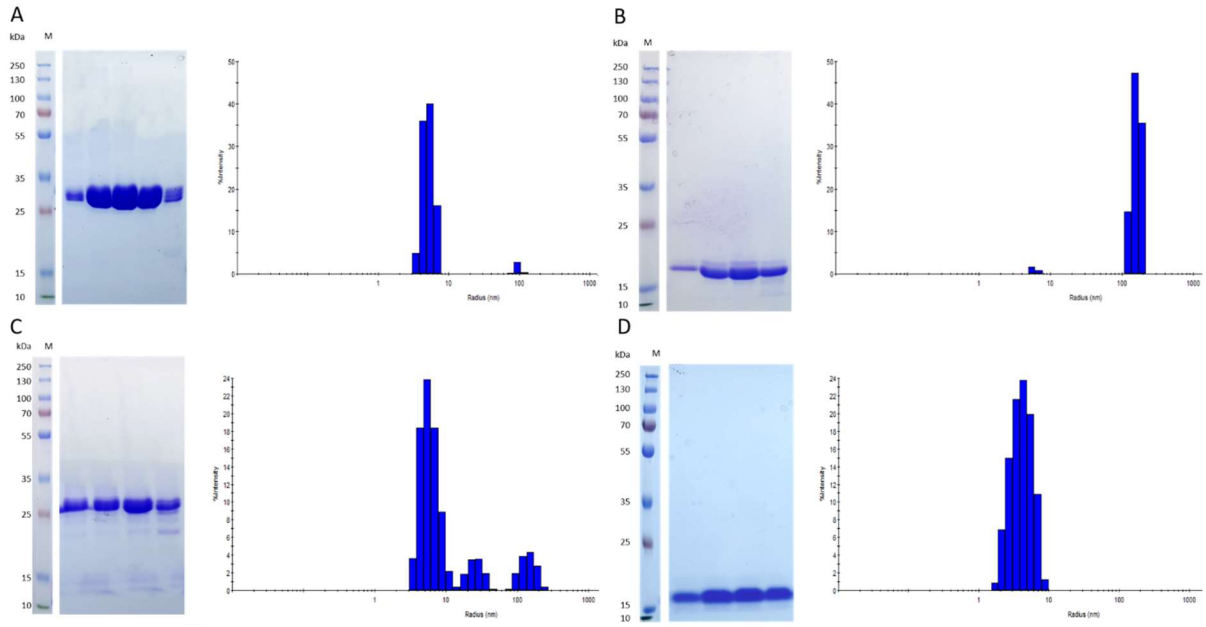

Figure 9 - Characterization of Purified ALP and CLP36 Protein Constructs

After purification, the SDS-PAGE gel shows a high degree of purity for purified proteins and the DLS measurements show that the samples are homogeneous for (A) ALP^{1-284}, a 30 kDa protein, construct showing 19.11 % polydispersity, and (B) $ALP^{112-284}$, a 18 kDa protein, showing 11.64 % polydispersity, whereas the CLP36 constructs show low level of homogeneity (C) $CLP36^{1-256}$, a 28 kDa protein, showing 30.17 % polydispersity and (D) $CLP36^{117-256}$, a 15 kDa protein, showing 34.95 % polydispersity, respectively.

ALP^{1-284} and $CLP36^{1-256}$ were furthermore subjected to a thermal shift assay to determine the ideal buffer and pH conditions for handling and storage of the proteins. Constructs lacking the PDZ domain were excluded from this assay, since the absence of the PDZ domain, as well as the lacking LIM domains, leaves the constructs with highly flexible internal region which is thought to be unstable and would presumably result in non-interpretable results.

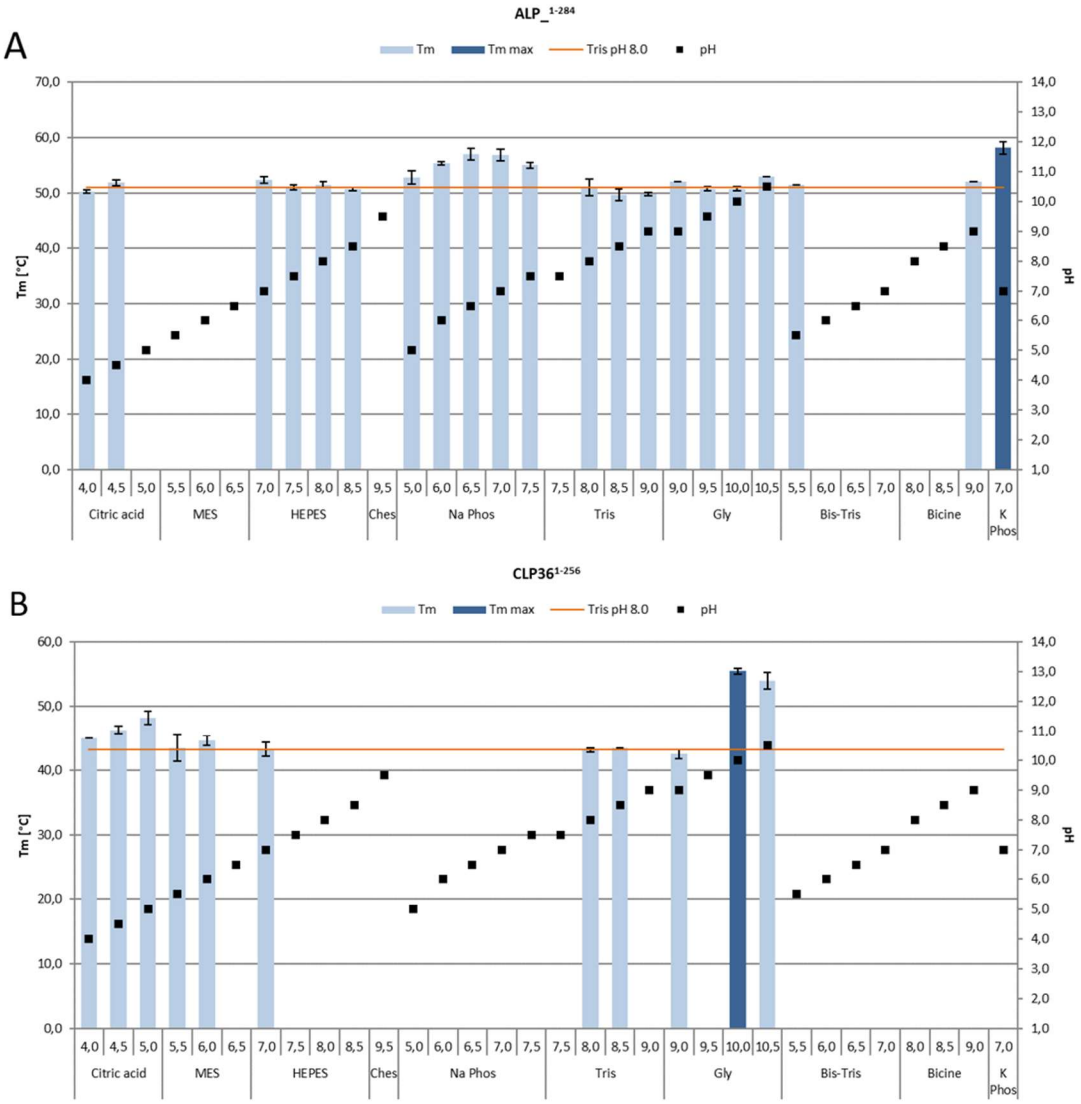

Figure 10 - Thermal Shift Assay Results Obtained for ALP$^{1-284}$ and CLP36$^{1-256}$

Results obtained from a thermal shift assay done on protein constructs ALP$^{1-284}$ and CLP36$^{1-256}$ showing the determined melting temperature (T_m) for varying pH in different buffers, written below the histogram plot. Orange line showing the T_m for Tris buffer pH 8.0 as a reference, the highest T_m in dark blue and others in light blue. Missing histograms show non-usable data which were excluded from the analysis. (A) Thermal shift assay for ALP$^{1-284}$ shows the highest T_m for this construct to be in K phosphate buffer pH 7.0, and for (B) CLP36$^{1-256}$ Glycine buffer pH 10.0.

The concentration of ALP$^{1-284}$ used in the thermal shift assay was 1 mg mL^{-1} whereas for CLP$^{1-256}$ this concentration was too low so 2 mg mL^{-1} was used. Even though the PDZ domain was present in these constructs, the assay resulted in many non-sigmoidal curves suggesting that either, in these conditions the proteins were unstable, or the disordered regions made the measurements not possible. These results were unusable, therefore are also missing from the final analysis. For the final result, the average T_m value from three measurements was used as well as the shown standard deviation (Figure 10). Nevertheless, the highest melting temperature was for ALP$^{1-284}$ observed for the potassium phosphate buffer pH 7.0, whereas CLP36$^{1-256}$ was most stable in Glycine buffer pH 10.0, but for CLP36 most of the data was not

interpretable. Sodium phosphate pH 6.5 – 7.5 was shown to be suitable for ALP, and since other constructs used in this study were previously shown to behave well in sodium phosphate buffer, it was chosen as the main running buffer for further experiments at the pH of 7.5 and shown that CLP36 also behaves well in the buffer even though the thermal shift assay wasn't conclusive for it.

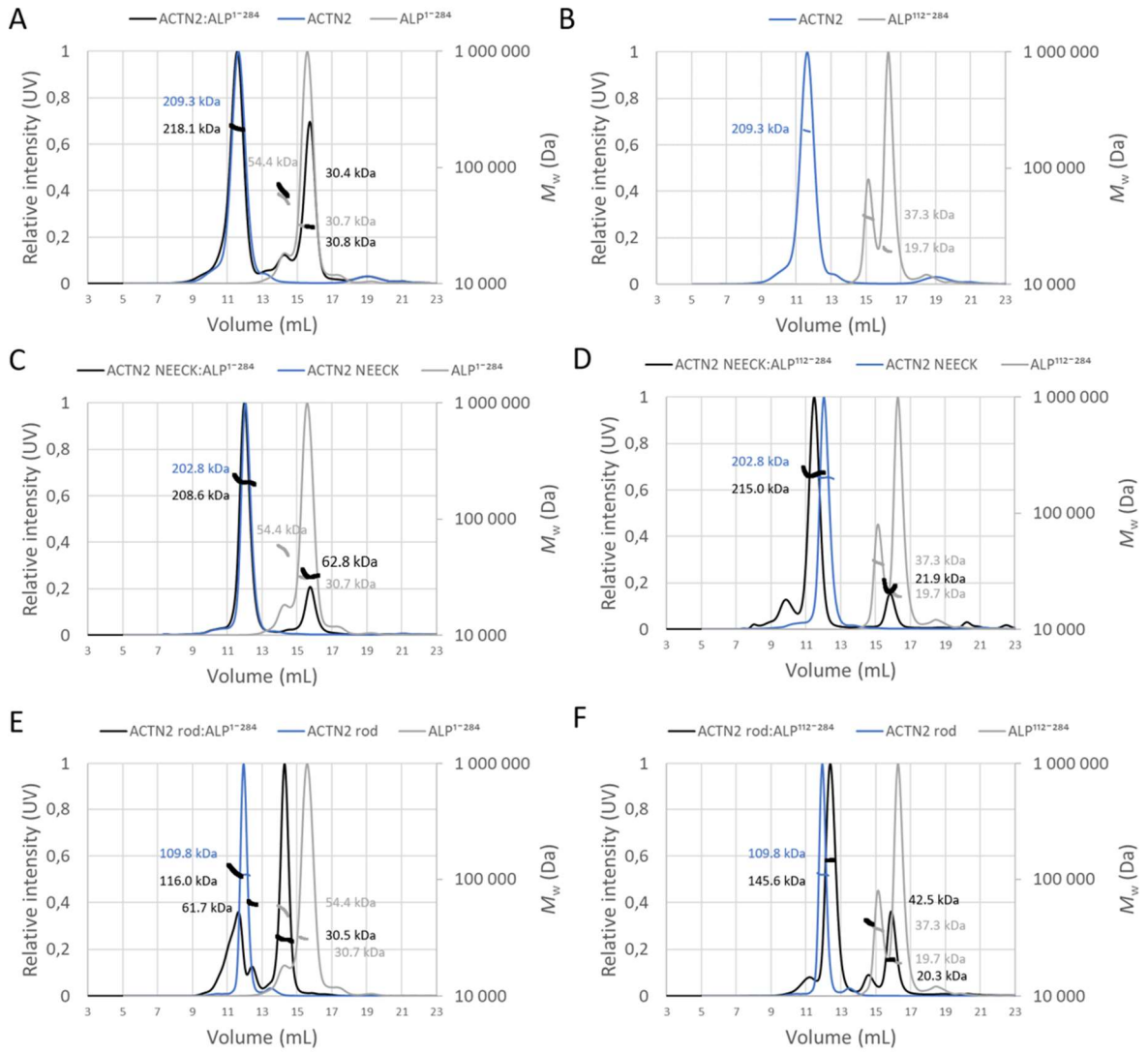

Figure 11 – Characterization of ALP Constructs and Their Complex Formation by SEC-MALLS

ALP^{1-284} and $ALP^{112-284}$ were analyzed on SEC-MALLS as well as investigated for complex formation (Superose 6 Increase 10/300, Superdex Increase 200 10/300) with different α-actinin-2 constructs. No stable complex formation was observed. All obtained weighted molecular weights (M_w) are shown in the figure, the theoretical ones here in parentheses. (A) In blue, α-actinin-2 dimer (206 kDa) with ALP^{1-284} forming a monomer (30 kDa) and a dimer (60 kDa) in grey, the tried complex formation in black. (B) α-actinin-2 dimer (blue) with $ALP^{112-284}$ forming a monomer (18 kDa) and dimer (36 kDa) in grey, complex not tried. (C) α-actinin-2 NEECK mutant dimer (212 kDa) in blue with ALP^{1-284} (grey) and tried complex in black. (D) α-actinin-2 NEECK mutant dimer (blue) with $ALP^{112-284}$ (grey) and tried complex in black. (E) Dimer of the rod domain of α-actinin-2 (112 kDa) in blue with ALP^{1-284} (grey) tried complex (black). (F) Dimer of the rod domain of α-actinin-2 (blue) with $ALP^{112-284}$ (grey) and tested complex (black) with a possible complex formation.

All used protein constructs in this study were subjected to SEC-MALLS to confirm the molecular weight of the construct as well as to check for possible dimer and oligomer

formations, aggregations or other unusual behavior. As expected, all α-actinin-2 constructs including the rod domain form dimers clearly seen on the chromatograms. ALP$^{1-284}$, ALP$^{112-284}$ and CLP36$^{1-256}$ give out a strong signal with molecular weight corresponding to a monomer, but nevertheless for each construct there is a peak with smaller intensity showing molecular weight corresponding to a dimer (Figure 11-12). ZASP ΔC was previously shown to result in one sharp peak corresponding to a monomer and no dimer formation visible. Interestingly, even though CLP36$^{117-256}$ was, without issues, purified on a size exclusion column and showed one clear band on SDS-PAGE (Figure 9D), the protein was not giving out any signal in SEC-MALLS measurements. With different columns tried, and testing the sample after freezing and thawing on DLS as well as running another size exclusion purification, SEC-MALLS signal was continuously missing, suggesting SEC-MALLS specific protein adsorption onto the column or the filter.

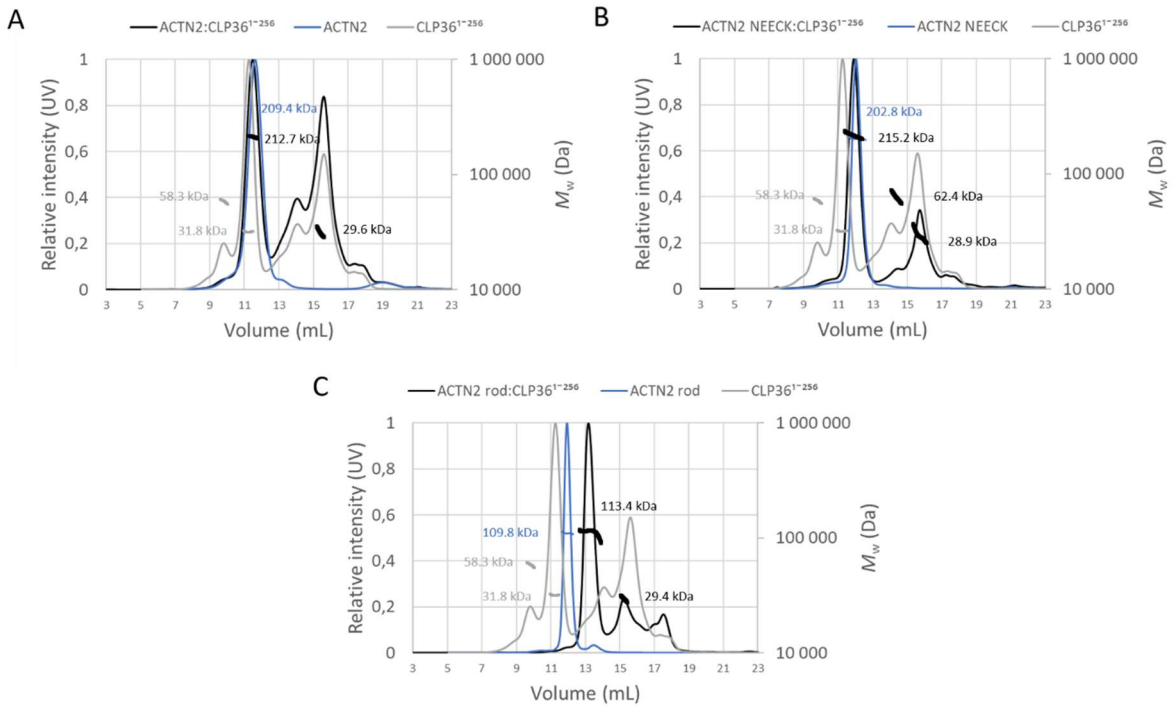

Figure 12 - Characterization of CLP36 and Its Complex Formation by SEC-MALLS

CLP36$^{1-256}$ was analyzed on SEC-MALLS as well as investigated for complex formation (Superose 6 Increase 10/300, Superdex 200 Increase 10/300) with different α-actinin-2 constructs. No stable complex formation was observed. All obtained weighted molecular weights shown in the figure (M_w), the theoretical ones here. (A) In blue, α-actinin-2 dimer (206 kDa) with CLP36$^{1-256}$ forming a monomer (28 kDa) and a dimer (56 kDa) in grey and tried complex formation in black. (B) α-actinin-2 NEECK mutant dimer (212 kDa) in blue with CLP36$^{1-256}$ (grey) and tried complex in black. (C) Dimer of the rod domain of α-actinin-2 (blue) with CLP36$^{1-256}$ (grey) and tested complex (black).

Previous studies on ZASP done by Valeria Stefania showed that ZASP, mixed in solution with different α-actinin-2 constructs in excess, didn't show complex formation when the sample solution was subjected to SEC-MALLS at 22 °C (Stefania and Djinović-Carugo,

unpublished data) suggesting that the formed complex wasn't stable enough to survive size exclusion chromatography. ALP$^{1-256}$, ALP$^{112-284}$ and CLP36$^{1-256}$ were in the same manner tested for complex formation with α-actinin-2 wild-type, NEECK mutant and the rod domain alone. They were mixed in excess with α-actinin-2 constructs, incubated for 30 minutes and ran on SEC-MALLS. As expected, almost all of the combinations didn't show stable complex formation (Figure 11-12), suggesting a needed stabilization of the complex for further analysis. Only in the case of the rod domain and ALP$^{112-284}$ the tested complex formation shows an intense peak corresponding to a M_w of 145 kDa (Figure 11F) which could possibly correspond to a rod domain dimer in a complex with two molecules of ALP$^{112-284}$ where the expected molar mass would be M_w = 150 kDa. These results formed the hypothesis that the affinities of these interactions cannot be in nanomolar range, since the complex would in that case survive SEC-MALLS. The affinities are assumed to be in low micromolar range, not allowing stable complex survival, but opening other possibilities for analysis.

Analysis of the Disulfide-Bridged Complexes Confirms Binding of the α-Actinin-2 to Two Molecules of ALP, CLP36, or ZASP

Due to aforementioned finding that the complex between α-actinin-2 and ALP, CLP36 or ZASP, respectively, isn't stable enough to survive SEC-MALLS, an engineered stabilization of the complexes was needed. The idea for the stabilization came from a naturally occurring disulfide bridge that forms between the PDZ domain of InaD and the C-terminus of NorpA (Kimple et al., 2001). Cysteine mutants of α-actinin-2, ALP, CLP36 and ZASP were engineered to mimic the cysteines involved in the interactions between InaD and NorpA. Therefore, aspartic acid at position 893 in α-actinin-2 was replaced with cysteine, as well as arginine at position 16 for ALP and ZASP and position 17 for CLP36. Cysteine mutants of these proteins were purified in the same manner as their wild-type homologs, resulting in a relative high yield and high concentration capability. All of the constructs were showing one distinct band on SDS-PAGE, as well as expected molecular masses when ran on SEC MALLS (Figure 13) suggesting that the mutation didn't cause any unexpected changes in protein characteristics and behavior.

The analysis of the disulfide-bridged complexes on SDS-PAGE was expected to reveal covalently bound α-actinin-2 with ALP, CLP36 and ZASP, respectively, with expected molecular weights of 134 kDa (α-actinin-2:ALP, α-actinin-2:ZASP) and 133 kDa (α-actinin-2:CLP36), which was exactly the case (Figure 13, right). The idea behind these engineered disulfide-bridged conjugates was to obtain protein complexes stable enough to survive SEC-MALLS, which was confirmed when running the samples (Figure 13, left). In this case,

complexes revealed to form a dimer, something usual for α-actinin-2, with two ALP, CLP36 or ZASP molecules bound to it. Hence, the molecular weights expected here were double of those obtained on SDS-PAGE and confirmed – α-actinin-2:ALP 272 kDa, α-actinin-2:CLP36 266 kDa, α-actinin-2:ZASP 272 kDa – the measured weights deviating from the expected ones not more than 5 kDa.

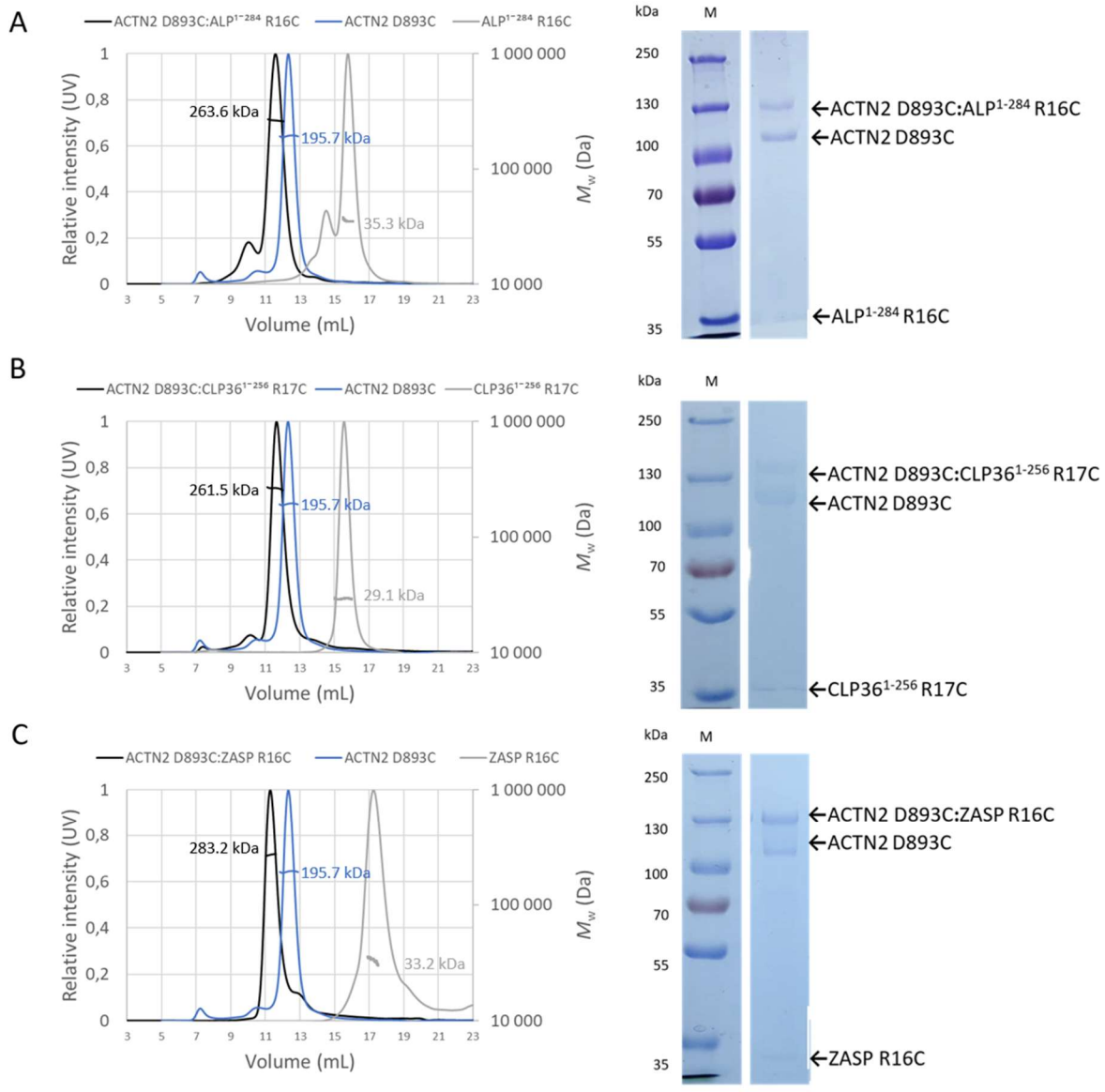

Figure 13 - Disulfide-Bridged Complexes Between α-actinin-2 and ALP, CLP36 and ZASP

SEC-MALLS (left) and SDS-PAGE (right) profiles of individual cysteine mutant protein constructs and the formed disulfide-bridged complex between them. Superose 6 Increase 10/300 GL column was used used except for ACTN2 D893C:ZASP R16C where Superdex 200 Increase 10/300 was used.. Complexes are shown as dimers of the two covalently linked proteins in SEC-MALLS, whereas on the gel they are visible as monomers. Stated molecular weights are the theoretical ones, the experimental ones shown in the figure. (A) On the left side, α-actinin D893C mutant (206 kDa) in blue, ALP1-284 R16C (33 kDa) in grey and the disulfide-bridged complex of them (272 kDa) in black. SDS-PAGE gel shown on left corresponding to the protein constructs SEC-MALLS profiles. (B) On the left side, α-actinin D893C mutant (206 kDa) in blue, CLP1-256 R17C (30 kDa) in grey and the disulfide-bridged complex of them (266 kDa) in black. SDS-PAGE gel shown on left corresponding to the protein constructs SEC-MALLS profiles. (C) On the left side, α-actinin D893C mutant (206 kDa) in blue, ZASP R16C (30 kDa) in grey and the disulfide-bridged complex of them (272 kDa) in black. SDS-PAGE gel shown on left corresponding to the protein constructs SEC-MALLS profiles.

It was observed for every complex that the peak eluting in SEC-MALLS has a small shoulder right before it, suggesting formation of higher-order complexes or minor aggregations, which could be eliminated when doing further analysis such as SEC-SAXS by selecting only the part of the peak that is of interest.

Internal Region of ALP, CLP36 and ZASP is Involved in Binding with α-actinin-2

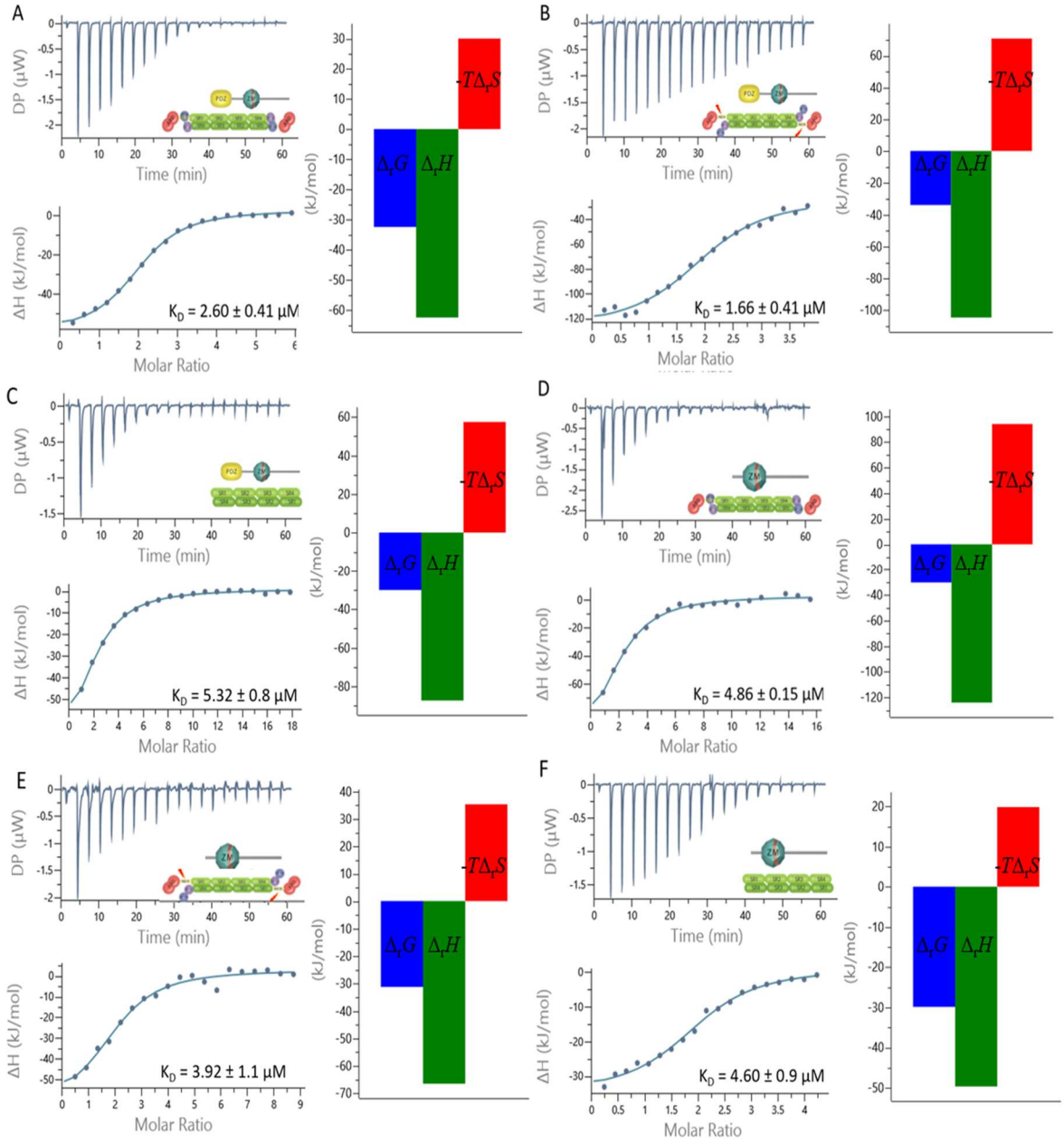

Figure 14 - Interaction Between α-actinin-2 and ALP

Representative ITC raw and interpolated data as well as the energetic diagram (Δ_rG – blue, Δ_rH – green, $-T\Delta_rS$ – red) for the studied interaction between (A) ALP$^{1\text{-}284}$ and α-actinin-2, (B) ALP$^{1\text{-}284}$ and α-actinin-2 NEECK mutant, (C) ALP$^{1\text{-}284}$ and the rod domain of α-actinin-2, (D) ALP$^{112\text{-}284}$ and α-actinin-2, (E) ALP$^{112\text{-}284}$ and α-actinin-2 NEECK mutant and (F) ALP$^{112\text{-}284}$ and the rod domain of α-actinin-2, with the respective average K_D values from three independent measurements in the bottom right corner.

In order to investigate the binding between ALP, CLP36 and ZASP with α-actinin-2, ITC was used. ALP$^{1-284}$, CLP36$^{1-256}$ and ZASP ΔC were used to characterize the binding with the full-length α-actinin-2 where two binding domains are present, whereas constructs lacking the PDZ domain (ALP$^{112-284}$, CLP36$^{117-256}$) or the ZM motif (ZASP PDZ) were used to characterize the binding if only one domain is involved. Furthermore, the rod domain of α-actinin-2 was set to specifically characterize the possible binding between the ZM motif and the spectrin repeats and the NEECK mutant to investigate if the open conformation of the protein affects the binding affinities.

After each ITC run, precipitation of α-actinin-2 constructs was observed, therefore the cell content was collected, spun down and resuspended in 6 M urea to determine the concentration of the precipitated product. It varied from 20%–40%, depending on the construct, where α-actinin-2 precipitated the most. Due to relatively high precipitation of the protein in the cell, during the data analysis, the number of binding sites was fixed to $N = 2$ and the concentration of the protein in the cell was left to vary during the fit, in the end corresponding to the precipitated product being subtracted from the initial concentration. None of the titrants (ALP, CLP36 and ZASP) were precipitating in the cell, which was confirmed when running the resuspended precipitate on SDS-PAGE.

ITC measurements of the interaction between ALP$^{1-284}$ and α-actinin-2 confirmed an interaction with K_D 2.60±0.41 μM (Figure 14A) which decreased when the NEECK mutant was used (1.66±0.41 μM) (Figure 14B) suggesting that the open conformation does indeed affect the binding, in a positive manner. The rod domain of α-actinin-2 binds to ALP$^{1-284}$ with a lower affinity (K_D 5.32±0.8 μM) (Figure 14C) and confirms that the spectrin repeats of α-actinin-2 are involved in the interaction. When using the ALP construct lacking the PDZ domain, binding was again confirmed in all three cases (Figure 14D-F), once more confirming the interaction between an internal region of the protein with the spectrin repeats of α-actinin-2.

Binding assays for CLP36 constructs with α-actinin-2 constructs revealed similar behavior (Figure 15). Binding affinity was again higher for the NEECK mutant of α-actinin-2 (K_D 2.35±0.28 μM) (Figure 15B) then for wild-type α-actinin-2 (Figure 15A). The rod domain was confirmed to interact with the full-length protein (Figure 15C) as well as with the internal region containing the ZM motif (Figure 15F) with K_D in low micromolar range.

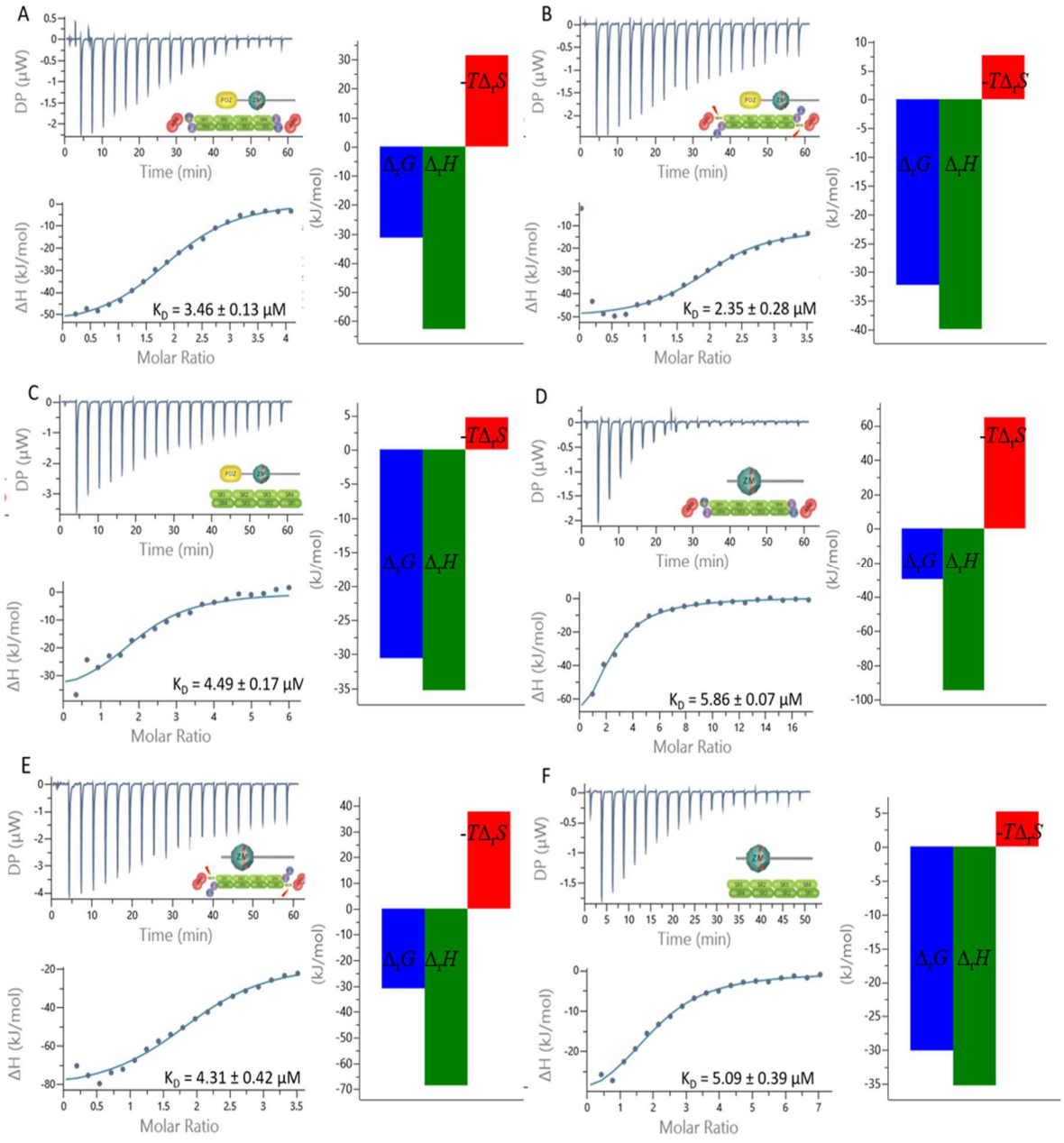

Figure 15 - Interaction Between α-actinin-2 and CLP36

Representative ITC raw and interpolated data alongside the energetic diagram (Δ_rG – blue, Δ_rH – green, $-T\Delta_rS$ – red) for the studied interaction between (A) CLP36$^{1\text{-}256}$ and α-actinin-2, (B) CLP$^{1\text{-}256}$ and α-actinin-2 NEECK mutant, (C) CLP36$^{1\text{-}256}$ and the rod domain of α-actinin-2, (D) CLP36$^{117\text{-}256}$ and α-actinin-2, (E) CLP36$^{117\text{-}256}$ and α-actinin-2 NEECK mutant and (F) CLP36$^{117\text{-}256}$ and the rod domain of α-actinin-2, with the respective average K_D values from three independent measurements in the bottom right corner.

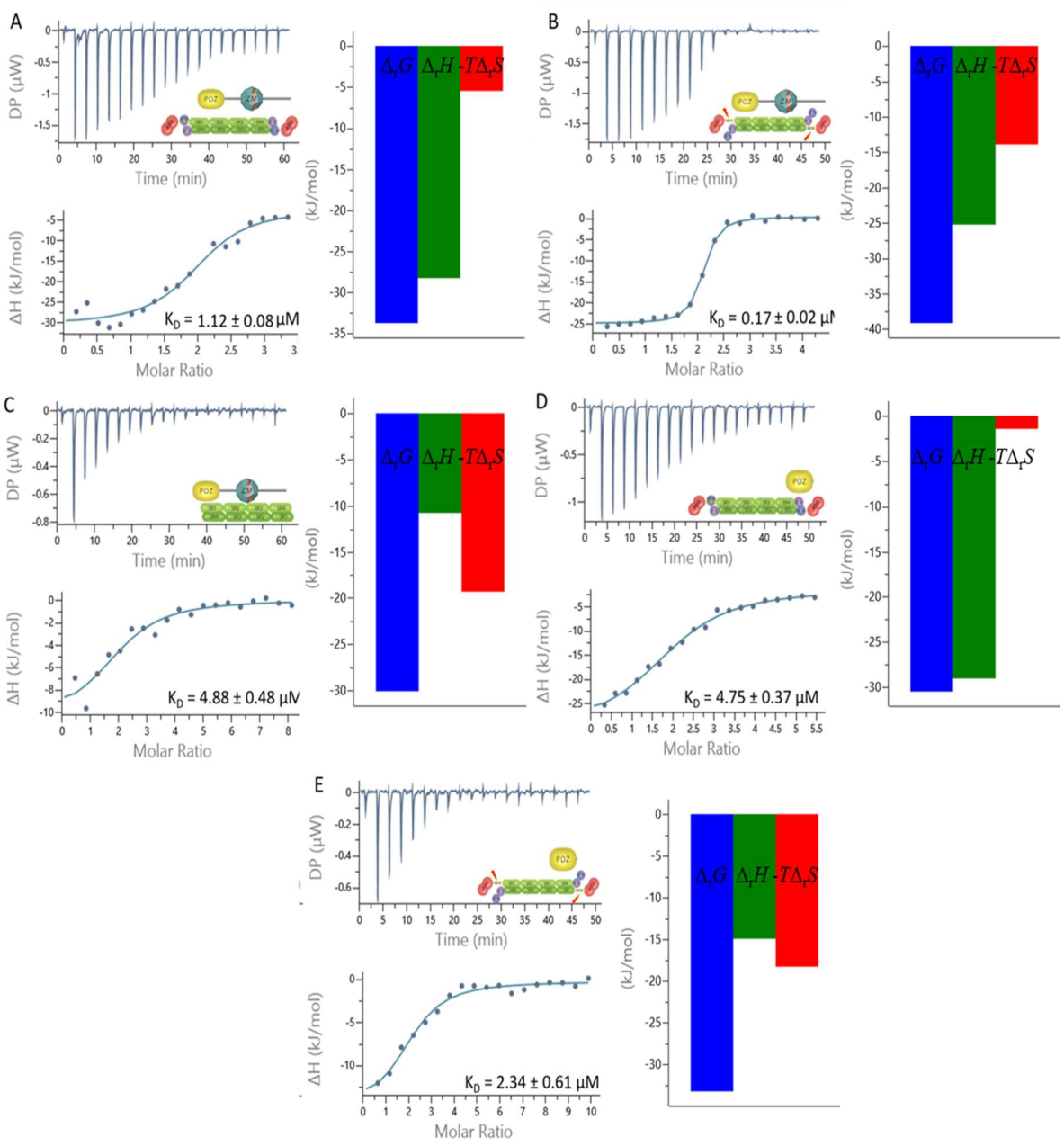

Figure 16 - Interaction Between α-actinin-2 and ZASP

Representative ITC raw and interpolated data alongside the energetic diagram (Δ_rG – blue, Δ_rH – green, $-T\Delta_rS$ – red) for the studied interaction between (A) ZASP ΔC and α-actinin-2, (B) ZASP ΔC and α-actinin-2 NEECK mutant, (C) ZASP ΔC and the rod domain of α-actinin-2, (D) PDZ domain of ZASP and α-actinin-2 and (E) PDZ domain of ZASP and α-actinin-2 NEECK, with the respective average K_D values from three independent measurements in the bottom right corner.

Due to low solubility of numerous ZASP constructs, for binding studies ZASP ΔC was used, lacking the C-terminal part but having the PDZ domain as well as the ZM motif. The PDZ domain of ZASP was purified separately in order to study the interaction when only one domain is present. ZASP ΔC was found out to have the highest affinity for binding to α-actinin-2 (K_D 1.12±0.08 µM) (Figure 16A) when compared to other proteins with the ZM motif. K_D decreased to 0.17±0.02 µM in the interaction with the NEECK mutant of α-actinin-2 (Figure 16B), whereas for the rod domain the binding was confirmed again (Figure 16C). PDZ domain was

interacting with both α-actinin-2 and the NEECK mutant (Figure 16D-E), but with lower affinity when compared to ZASP ΔC which contains the ZM motif, suggesting that the binding occurs not only with the PDZ domain, but also with an internal region containing the ZM motif. Previous studies already showed that the PDZ domain is not binding to the spectrin repeats of the rod domain (Faulkner et al., 1999) , therefore that interaction was not tested. All K_D values as well as the energetic information can be seen in Table 2.

ZASP Interacts with α-actinin-2 with Higher Entropic Contributions

Table 2 - Binding and Energetic Parameters Summarized

Binding affinities, number of binding sites, enthalpic contribution, Gibbs free energy, entropic contribution and the measurements temperature (from left to right) shown alongside with the standard deviation obtained from three measurements.

	K_D [μM]	N	$\Delta_r H$ [kJ/mol]	$\Delta_r G$ [kJ/mol]	$-T\Delta_r S$ [kJ/mol]
α-actinin-2:ALP$^{1-284}$	2.60 ± 0.41	2	–66.43 ± 3.11	–31.94 ± 0.42	34.50 ± 3.52
α-actinin-2 NEECK:ALP$^{1-284}$	1.66 ± 0.41	2	–93.30 ± 3.33	–33.07 ± 0.68	59.97 ± 33.11
α-actinin-2 rod:ALP$^{1-284}$	5.32 ± 0.80	2	–79.43 ± 7.44	–30.17 ± 0.37	49.30 ± 7.22
α-actinin-2:ALP$^{112-284}$	4.86 ± 0.15	2	–109.63 ± 10.40	–30.33 ± 0.09	79.47 ± 10.37
α-actinin-2 NEECK:ALP$^{112-284}$	3.92 ± 1.06	2	–62.87 ± 6.82	–30.97 ± 0.62	31.90 ± 6.20
α-actinin-2 rod:ALP$^{112-284}$	4.60 ± 0.91	2	–39.73 ± 7.15	–30.53 ± 0.49	9.22 ± 0.76
α-actinin-2:CLP36$^{1-256}$	3.45 ± 0.14	2	–54.17 ± 9.34	–31.20 ± 0.08	22.93 ± 9.23
α-actinin-2 NEECK:CLP36$^{1-256}$	2.35 ± 0.28	2	–42.93 ± 2.53	–32.20 ± 0.30	10.75 ± 2.73
α-actinin-2 rod:CLP36$^{1-256}$	4.49 ± 0.17	2	–35.37 ± 2.45	–30.53 ± 0.09	4.83 ± 2.54
α-actinin-2:CLP36$^{117-256}$	5.86 ± 0.07	2	–100.50 ± 8.13	–29.90 ± 0.00	70.57 ± 8.09
α-actinin-2 NEECK:CLP36$^{117-256}$	4.31 ± 0.42	2	–70.20 ± 2.19	–30.67 ± 0.21	39.53 ± 2.18
α-actinin-2 rod:CLP36$^{117-256}$	5.09 ± 0.39	2	–33.63 ± 1.12	–30.27 ± 0.17	3.38 ± 1.30
α-actinin-2:ZASP ΔC	1.12 ± 0.08	2	–23.43 ± 6.81	–34.00 ± 0.16	–10.57 ± 6.81
α-actinin-2 NEECK:ZASP ΔC	0.17 ± 0.02	2	–26.60 ±1.44	–38.77 ± 0.33	–12.17 ± 1.57
α-actinin-2 rod:ZASP ΔC	4.88 ± 0.48	2	–12.47 ± 1.36	–30.37 ± 0.25	–17.87 ± 1.23
α-actinin-2:ZASP PDZ	4.75 ± 0.37	2	–23.3 ± 6.16	–30.40 ± 0.22	–7.05 ± 6.20
α-actinin-2 NEECK:ZASP PDZ	2.34 ± 0.61	2	–14.3 ± 0.85	–32.27 ± 0.74	–18.00 ± 0.80

All interactions studied using isothermal titration calorimetry were characterized with a negative ΔH (Table 2), therefore pointing to all reactions being exothermic and negative ΔG, stating a spontaneous reaction. The entropic contribution ($T\Delta S$) was negative in interactions with ALP and CLP36. Interestingly, ZASP reacts differently with α-actinin-2 compared to other two proteins containing the ZM motif. Enthalpic contribution is still present, but the entropic contribution has a positive effect on the interaction, in some cases even dominating it, which can be possibly explained that the binding doesn't stabilize the ligand as is the case for example,

for ALP (Klaavuniemi et al., 2009). All average energetic contributions as well as the binding affinities can be seen in Table 2 alongside with the standard deviation obtained from three independent measurements.

Statistical Analysis Shows Significant Difference Between Interactions

An independent *t*-test was done to statistically investigate if there is a significant difference between the binding affinities between all ALP, CLP36 and ZASP constructs individually, as well as for ALP and CLP36 constructs in a crossed *t*-test.

Table 3 - t-Test done on K_D values obtained from ITC on ALP interaction with α-actinin-2

	α-actinin-2 rod: $ALP^{112-284}$	α-actinin-2 NEECK: $ALP^{112-284}$	α-actinin-2: $ALP^{112-284}$	α-actinin-2 rod: ALP^{1-284}	α-actinin-2 NEECK: ALP^{1-284}
α-actinin-2:ALP^{1-284}	ns	ns	**	*	ns
α-actinin-2 NEECK:ALP^{1-284}	*	ns	**	*	
α-actinin-2 rod:ALP^{1-284}	ns	ns	ns		
α-actinin-2:$ALP^{112-284}$	ns	ns			
α-actinin-2 NEECK:$ALP^{112-284}$	ns				

Statistical analysis done using *t*-test: ns (not significant), * ($p > 0.05$), ** ($p \leq 0.01$), *** ($p \leq 0.001$).

Statistical analysis shows that there is no significant difference in the K_D values when it comes to $ALP^{1\text{-}284}$ interacting with α-actinin-2 wild-type and the NEECK mutant, even though the average K_D values are lower for the interaction with the NEECK mutant. Nevertheless, there is a statistical significance between the binding of ALP with and without the PDZ domain to α-actinin-2 ($p \leq 0.01$, Table 3). As expected, there is no significant difference in both ALP constructs interacting with the rod domain due to a binding happening only at one binding site, but there is a difference ($p \leq 0.05$, Table 3) when ALP interacts with the rod domain of α-actinin-2 and the full-length construct.

Table 4 - t-Test done on K_D values obtained from ITC on CLP36 interaction with α-actinin-2

	α-actinin-2 rod: $CLP36^{117-256}$	*α-actinin-2 NEECK: $CLP36^{117-256}$*	*α-actinin-2: $CLP36^{117-256}$*	*α-actinin-2 rod: $CLP36^{1-256}$*	*α-actinin-2 NEECK: $CLP36^{1-256}$*
α-actinin-2:$CLP36^{1-256}$	*	*	***	**	*
α-actinin-2 NEECK:$CLP36^{1-256}$	**	**	**	**	
α-actinin-2 rod:$CLP36^{1-256}$	ns	*	**		
α-actinin-2:$CLP36^{117-256}$	ns	*			
α-actinin-2 NEECK:$CLP36^{117-256}$	**				

Statistical analysis done using *t*-test: ns (not significant), * ($p > 0.05$), ** ($p \leq 0.01$), *** ($p \leq 0.001$).

No significant difference was observed between CLP36 constructs interacting with the rod domain of α-actinin-2, again expected as the same binding site is involved in both interactions. The biggest statistical significant difference ($p \leq 0.001$) was observed when $CLP36^{1\text{-}256}$ and $CLP36^{117\text{-}256}$ were interacting with the wild-type α-actinin-2. In general, significant difference was revealed almost between all interactions, with different p values, as seen in Table 4..

Table 5 - T-Test done on KD values obtained from ITC on ZASP interaction with α-actinin-2

	α-actinin-2 NEECK: ZASP PDZ	*α-actinin-2: ZASP PDZ*	*α-actinin-2 rod: ZASP ΔC*	*α-actinin-2 NEECK: ZASP ΔC*
α-actinin-2:ZASP ΔC	ns	**	**	**
α-actinin-2 NEECK:ZASP ΔC	*	**	**	
α-actinin-2 rod:ZASP ΔC	*	ns		
α-actinin-2:ZASP PDZ	*			

Statistical analysis done using t-test: ns (not significant), * ($p > 0.05$), ** ($p \leq 0.01$), *** ($p \leq 0.001$).

ZASP ΔC and the PDZ also bind to α-actinin-2 differently (Table 5), the difference being statistically significant ($p \leq 0.01$), which is explainable with two binding sites when interaction occurs with ZASP ΔC compared to PDZ domain binding alone only to the EF hands

Table 6 - t-Test done on K_D values obtained from ITC on ALP and CLP36 interaction with α-actinin-2

	α-actinin-2 rod: $CLP36^{117-256}$	*α-actinin-2 NEECK: $CLP36^{117-256}$*	*α-actinin-2: $CLP36^{117-256}$*	*α-actinin-2 rod: $CLP36^{1-256}$*	*α-actinin-2 NEECK:$CLP36^{1-256}$*	*α-actinin-2:$CLP36^{1-256}$*
α-actinin-2:ALP^{1-284}	**	*	**	*	ns	ns
α-actinin-2 NEECK:ALP^{1-284}	**	*	**	**	ns	*
α-actinin-2 rod:ALP^{1-284}	ns	*	ns	ns	*	ns
α-actinin-2:$ALP^{112-284}$	ns	*	**	ns	**	***
α-actinin-2 NEECK:$ALP^{112-284}$	ns	*	ns	ns	ns	ns
α-actinin-2 rod:$ALP^{112-284}$	ns	*	ns	ns	ns	ns

Statistical analysis done using *t*-test: ns (not significant), * ($p > 0.05$), ** ($p \leq 0.01$), *** ($p \leq 0.001$).

t-Test was also done between K_D values obtained from ITC measurements of ALP and CLP36 constructs interacting with different α-actinin-2 in order to investigate if ALP and CLP36 interact with α-actinin-2 differently. The longer constructs of ALP and CLP36 interact with α-actinin-2 with no statistical difference, as well as with the NEECK mutant and the rod domain. Constructs lacking the PDZ domain also show no difference when interacting with the rod domain, but with wild-type and NEECK α-actinin-2 a difference was observed ($p \leq 0.01$, p

≤ 0.05, Table 6) . Between different type of constructs of ALP and CLP36 a difference is observed in most cases, as expected since they don't interact with the same binding sites.

ALP Peptide Interacts with the Rod Domain with High Affinity

Following the experiments done in the literature, where 5 peptides were constructed, corresponding to the ZASP-like motif of ALP and the sequence around it, and tested via SPR if they bind to the rod domain (Klaavuniemi et al., 2009), the peptide that bound to the rod domain was obtained and tested for binding via ITC. In the literature, the peptide, when immobilized in SPR, bound to the rod domain with an affinity of K_D = 3.0 µM. Here, the peptide binding to the rod domain of α-actinin-2 was tested in the same manner as other bindings, with the difference of 2% (v/v) DMSO being added to the buffer due to the peptide not being soluble in buffer.

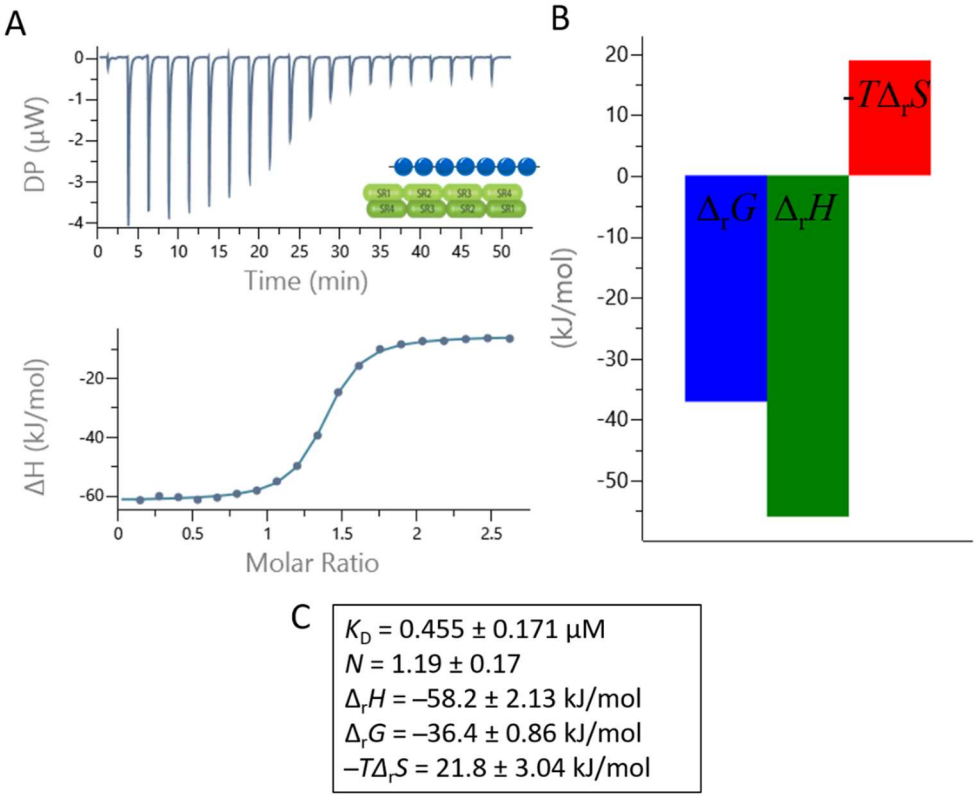

Figure 17 - Binding between ALP Peptide and the Rod Domain of α-actinin-2

(A) Representative ITC raw and interpolated data for the studied interaction between the ALP peptide and the rod domain of α-actinin-2. (B) Obtained binding and energetic parameters from the measurements with the standard deviation of the triplicate.

The ITC measurements revealed a K_D of 0.455 ± 0.171 µM, a much higher affinity than stated in the literature, which could easily be explained with different measuring methods. DMSO didn't cause any issues during the measurements. The higher K_D obtained with the

peptide could suggest a possible inhibiting effect of the surrounding structure when it comes to ALP.

Crosslinking Reveals 2:2 Interactions

After confirming binding between ALP, CLP36, ZASP and α-actinin-2, respectively, crosslinking was carried out in order to confirm the stoichiometry, as well as investigate in more detail how the proteins are interacting. Preliminary crosslinking experiments were done with a constant cross-linker concentration and an increasing concentration of ALP, CLP36 and ZASP, respectively, and a constant concentration of α-actinin-2 constructs. Due to many resulting crosslinking byproducts of α-actinin-2 constructs, western blot was applied to detect which bands correspond to products of cross-linked α-actinin-2 constructs with ALP, CLP36 or ZASP constructs that had a His tag for chromogenic detection. All interactions studied using ITC were subjected to crosslinking, and all of them showed formation of a 2:2 complex confirming the number of binding sites being $N = 2$, as well as other possible ratios (α-actinin-2 construct monomer or dimer interacting either with one or two molecules of ALP, CLP36 and ZASP). Due to all of the experiments being performed in the same manner and yielding the same results, one exemplary SDS-PAGE alongside the western blot (Figure 18) was shown here, whereas the other performed experiments done on other constructs can be found in the appendix (Appendix 1-14).

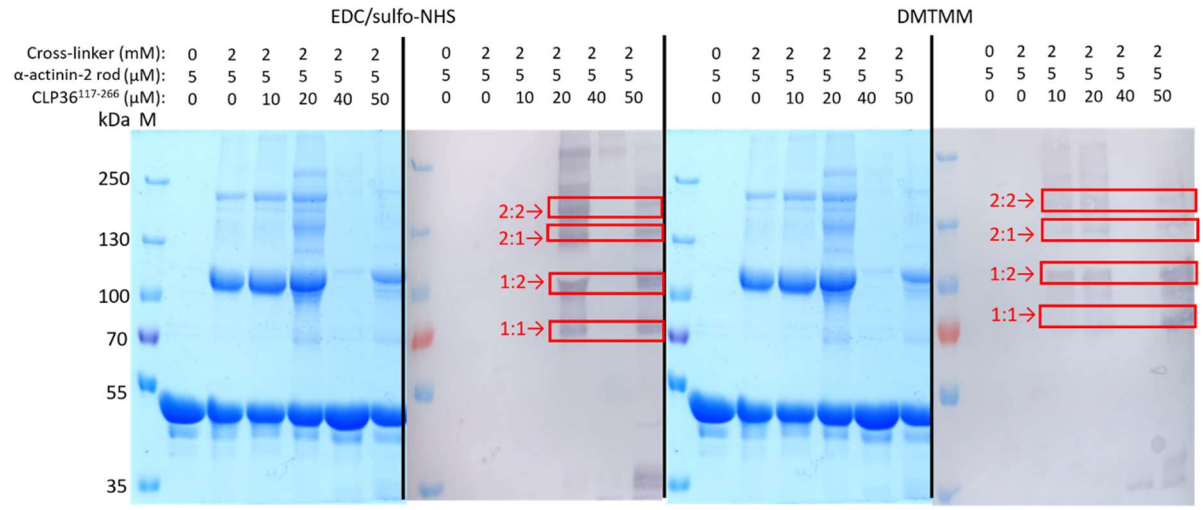

Figure 18 - Exemplary Crosslinking and Western Blot Revealing a 2:2 Interaction

Crosslinking between the rod domain of α-actinin-2 and CLP36$^{117\text{-}256}$ and corresponding western blot using two different cross-linkers. Marked on the figure crosslinking products with different stoichiometries: n(rod):n(CLP$^{117\text{-}256}$) = 2:2 yielding a 148 kDa product, n(rod):n(CLP$^{117\text{-}256}$) = 2:1 yielding a 130 kDa product, n(rod):n(CLP$^{117\text{-}256}$) = 1:2, yielding a 92 kDa product and n(rod):n(CLP$^{117\text{-}256}$) = 1:1, yielding a 74 kDa product.

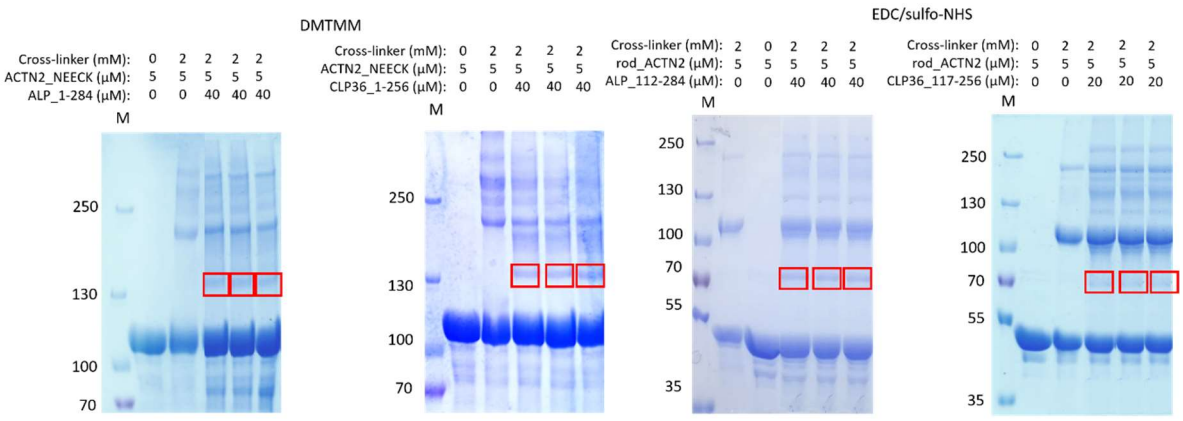

Figure 19 - Crosslinking Repeated with Marked Bands Sent for Analysis

Crosslinking was repeated between α-actinin-2 NEECK mutant and ALP$^{1-284}$ and CLP36$^{1-256}$ in triplicates and the bands corresponding to a product with 1:1 stoichiometry were cut out and sent for analysis. The same was done for the rod domain of α-actinin-2 and ALP$^{112-284}$ and CLP36$^{117-256}$, respectively. Bands that were cut out and sent are marked in red.

The most useful results were expected from analyzing the cross-linked bands between α-actinin-2 NEECK mutant and ALP$^{1-284}$ and CLP36$^{1-256}$ when interacting in a 1:1 ratio due to the open conformation of the protein, as well as between the rod domain and ALP$^{112-284}$ and CLP36$^{117-256}$ due to the interaction happening between the ZM motif and the spectrin repeats. These experiments were repeated in triplicates in the most optimal conditions and the corresponding bands (Figure 19) were cut out and sent for MS analysis which is ongoing.

Crosslinking of the Disulfide-Bridged Complexes

Preparation of the disulfide-bridged conjugates between α-actinin-2 and ALP, CLP36 and ZASP, respectively, revealed a monomeric covalent complex formation on SDS-PAGE and dimeric complex formation on SEC-MALLS. It is known that the disulfide bridge stabilizes the interaction and allows complex analysis using size exclusion chromatography, and potentially other methods such as SEC-SAXS and cryo-EM. In order to investigate which amino-acid residues from the two protein partners in the complex are in close proximity, the complexes were subjected to crosslinking, where one portion of the cross-linked complexes was subjected to a reducing agent which would reduce the disulfide bridge and, potentially still reveal a cross-linked complex, even without the stabilizing disulfide bond.

All three disulfide-bridged complexes were subjected to crosslinking with DMTMM and EDC:sulfo-NHS and both cross-linkers showed the same results. Gels showing stronger bands were shown as examples (Figure 20). For all three complexes, in non-reduced conditions a clear band at around 130 kDa can be seen, as well as α-actinin-2, but only very vaguely. When adding the reducing agent, the band corresponding to the complex fades away, but not completely, showing that the disulfide-bridged product is still present as a crosslinking product,

only in lower concentrations. Due to the breakage of the disulfide bond, in reduced conditions α-actinin-2 is present with much higher band intensity, as well as ALP (Figure 20A), CLP36 (Figure 20B) and ZASP (Figure 20C). Possible improvement of crosslinking conditions is needed in order to send the bands for further analysis.

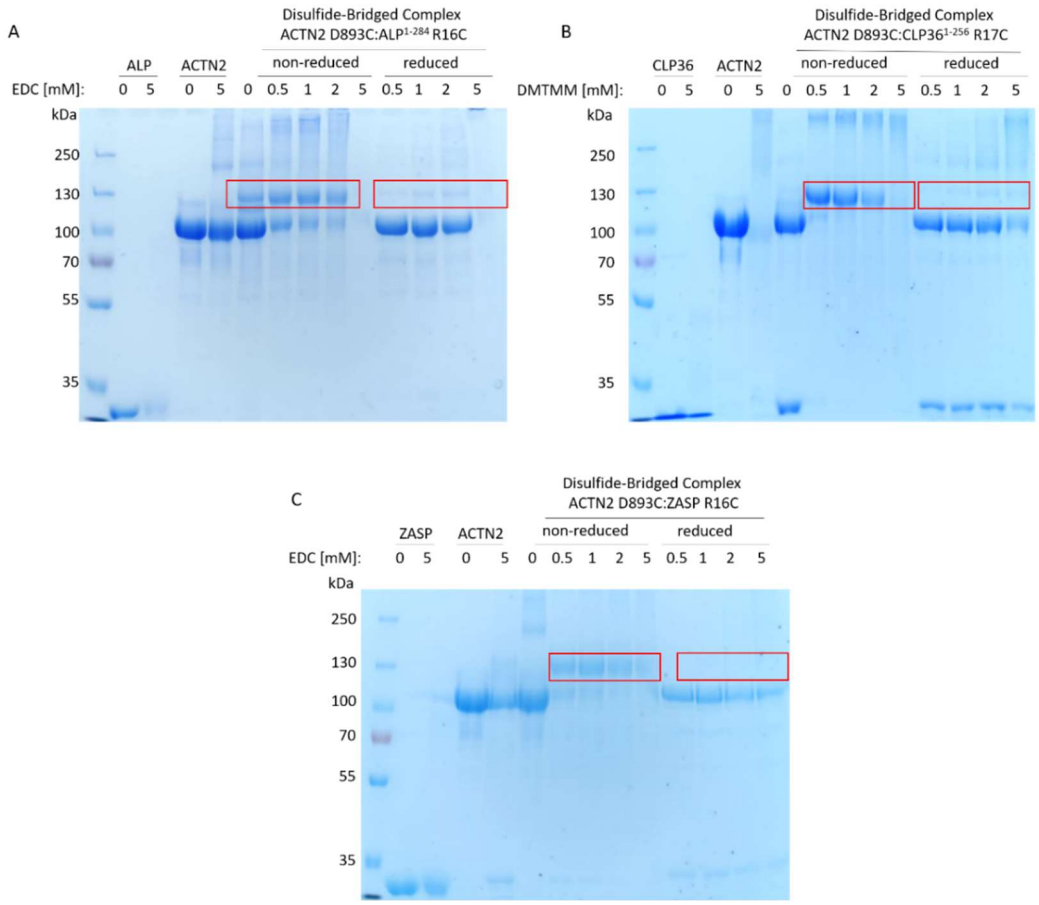

Figure 20 - Crosslinking of Disulfide-Bridged Complexes Revealed Complex Formation in Reduced Conditions

Crosslinking of disulfide-bridged complexes revealed complex formation in reduced conditions. (A) α-actinin-2 D893C and ALP$^{1-284}$ R16C complex in reduced conditions shows a cross-linking product (137 kDa) in reduced conditions, like (B) α-actinin-2 D893C and CLP36$^{1-256}$ R17C (134 kDa) and (C) α-actinin-2 D893C and ZASP R16C (137 kDa) showing weaker bands, presumably due to lower concentrations.

Crystallization Screening Resulted in Numerous Positive Hits

Initial crystallization screening for the rod domain of α-actinin-2 with ALP$^{112-284}$ and CLP36$^{117-256}$, respectively was set up with the idea that, due to the relatively loose crystal packing of the rod domain and the binding affinity in low micromolar range, crystals containing the formed complex will be formed. It is known that the rod domain of α-actinin-2 forms crystals in high salt conditions (Ylänne et al., 2001). The initial screening resulted in crystal formation in 12 different conditions in the screens containing the mixture of the rod domain and ALP$^{112-284}$ and in 47 different conditions in the screens with the rod domain and CLP36^{117-}

^{256}, everything at 22 ºC degrees. The initial screening at 4 ºC didn't result in any positive hits. The majority of the conditions were characterized by various polymer presence, mostly PEG, but some of the conditions also had relatively high salt conditions suggesting possible crystals of the rod domain alone.

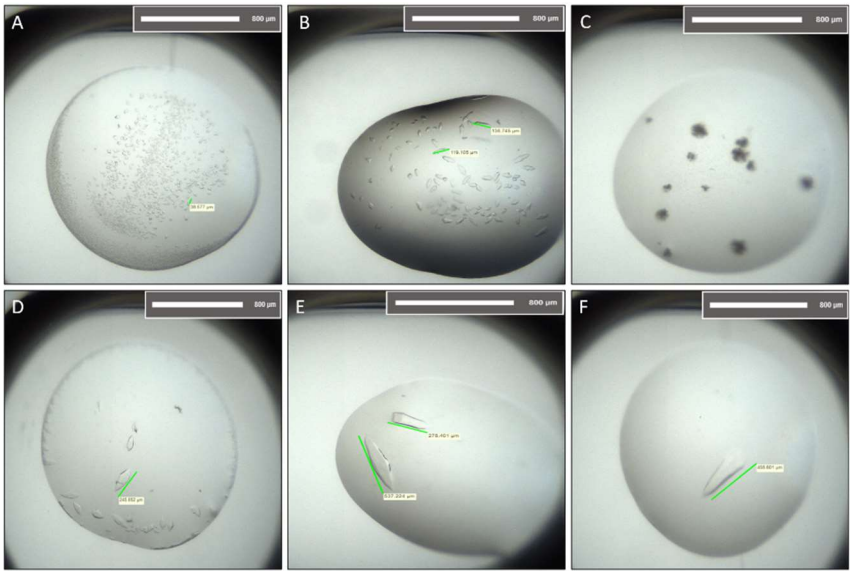

Figure 21 - Examples of the Results from the Initial Crystallization Screening

The initial screening of the rod domain and ALP$^{112-284}$ resulted in many microcrystals, bigger crystals of about (A) 30 µm and (B) 136 µm. Microcrystals dominated the initial screening of the rod domain and CLP36$^{117-256}$, but there were examples of (C) sea-urchin-like formations and crystals from (D) 50 µm and (E) and (F) bigger than 200 µm. Scale bar: 800 µm.

ALP$^{112-284}$ and the rod domain screens resulted mainly in formation of microcrystals, but some bigger crystals of about 30 µm in 20% w/v PEG 1K, 0.1 M Tris pH 8.5 (Figure 21A) and 136 µm in 10% w/v PEG 8K, 0.1 M imidazole pH 8.0 (Figure 21B) were also observed. CLP36$^{117-256}$ screens were also dominating with microcrystals, but sea-urchin-like crystals were also observed in 15% v/v ethanol, 40% v/v PE5/4 (Figure 21C), as well as bigger crystals from 50–200 µm (Figure 21D-F) (in order: 0.1 M HEPES pH 7.0, 0.3 M ammonium formate, 20% v/v SOK-CP5; 20% w/v PEG 3350 0.2 M NaI; 12% Tascimate pH 7.0, 12% w/v PEG 3350). Crystals that could be harvested from different conditions were harvested and if necessary, put into a cryo-protectant to be sent for diffraction. After carefully examining all the conditions where crystals formed, for both ALP$^{112-284}$ and CLP36$^{117-256}$, multiple optimization screens were designed (Figure 22) in order to obtain better crystals which would better diffract and be bigger for examining the crystal on SDS-PAGE.

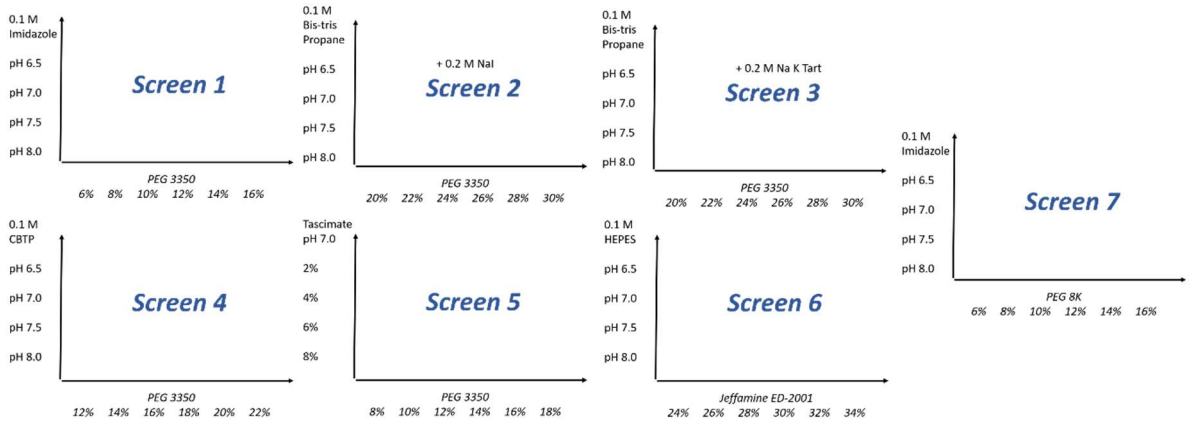

Figure 22 - Crystallization Optimization Screen Design

Optimization screening resulted as well in numerous positive hits, especially for the screening of the rod domain of α-actinin-2 and CLP36$^{117-256}$, whereas the screening of the rod domain with ALP$^{118-284}$ resulted again in numerous microcrystals and a few bigger formations. CLP36$^{117-256}$ optimization screen revealed numerous bigger crystals all ranging from 50 µm – 250 µm, some of the examples showed in Figure 23) (in order: 0.1 M imidazole pH 6.5, 14% PEG 3350; 0.1 M imidazole pH 6.5, 16% PEG 3350; 0.1 M imidazole pH 7.0, 6% PEG 3350; 6% Tascimate pH 7.0, 16% PEG 3350; 6% Tascimate pH 7.0, 8% PEG 3350; 6% Tascimate pH 7.0, 12% PEG 3350). Some of these crystals were as well harvested and frozen for diffraction analysis.

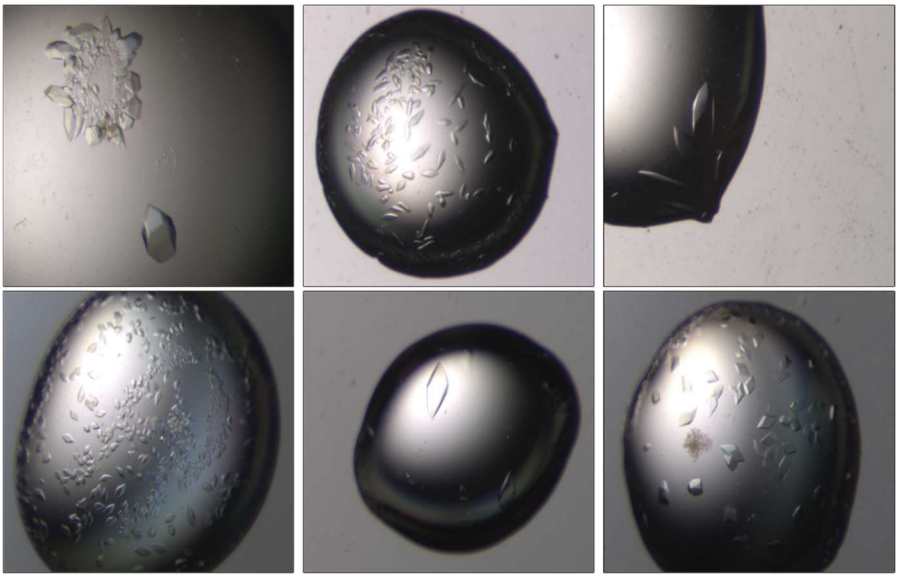

Figure 14 – Optimization Screening Resulted in Bigger Crystals

Optimization co-crystallization of the rod domain of α-actinin-2 and ALP$^{112-284}$ and CLP36$^{117-256}$ resulted in many positive hits, the crystals obtained this time, much bigger, whereas the shape showed no difference.

Co-crystallization of the ALP peptide with the rod domain of α-actinin-2 was done in the optimization screens (Figure 22), and resulted in numerous microcrystals which were not suitable for harvesting. Co-crystallization of the peptide is in the need of an initial crystallization screening and more optimization in order to obtain viable crystals.

Crystals from the initial and optimization screens were also harvested and prepared for running on SDS-PAGE in order to try and confirm the presence of a complex or the rod domain alone. Unfortunately, when running the crystals as well as the positive control for $ALP^{112-284}$ and $CLP36^{117-256}$ it was observed that both constructs do not stain with silver staining, but only with standard Commassie Brilliant Blue staining, therefore the small concentrations possibly present in the crystals are not detectable and the presence of a complex cannot be detected.

Structure Determination did't Reveal Any Additional Electron Density that Can Be Attributed to ALP or CLP36

The harvested crystals were used in the synchrotron X-ray diffraction analysis. Most of them showed no or very poor diffraction. The other analyzed samples showed diffraction patterns with the highest resolution 3.5 Å for one sample from the co-crystallization with $ALP^{112-284}$ and in a range 2.8–4.2 Å for 11 different samples from the co-crystallization with $CLP36^{117-256}$. Solving each structure revealed electron density for the rod domain of α-actinin-2, but no additional electron density which could be assigned to a fragment of either $ALP^{112-284}$ or $CLP36^{117-256}$.

Discussion

α-actinin-2 has always played a crucial role in the formation and stabilization of the Z-disk. It has a central place in the protein network of the Z-disk and due to a high number of binding partners it has been a protein of great interest in research for many years. On the other hand, the proteins of the ALP and Enigma subfamilies haven't been studied in that much detail, their binding partners and functions remaining unclear to this day. The most interesting characteristic in these two subfamilies is shared between three proteins: ALP, CLP36 and ZASP, that being the 26 amino acid long motif called the ZM motif which has been on some occasions proved to be a key binding site, but on the other been disputed in the literature. All three proteins are known to interact with α-actinin-2, but details on this interaction and especially the role of the ZM motif in it, are vaguely known. Due to rising evidence that the mutations in exons encoding this motif are the main disease cause in this protein family, it is of great importance to deepen the knowledge on the function of it. This study confirmed that the interaction between α-actinin-2 and ALP, CLP36 and ZASP, respectively, is not only mediated by the binding of the EF hands with the PDZ domain. There is indeed another binding site in the internal region, the ZM motif with the rod domain of α-actinin-2. Additionally, it is proved that this interaction is a 2:2 interaction, confirmed via crosslinking and disulfide-bridge formation stabilizing the complex. There is a clear difference between the interaction of α-actinin-2 with ALP or CLP36 and with ZASP, ZASP binding to α-actinin-2 with significantly higher entropic contributions. Finally, a solid base has been made on the structural characterization of these interactions, needing further improvement in order to solve the structure of the interaction between the spectrin repeats of α-actinin-2 and the ZM motif.

On the Complex Formation between α-actinin-2 and ZM Motif Containing Proteins

In this study, it was revealed that α-actinin-2 doesn't form a complex with ALP, CLP36 or ZASP which is stable enough to survive SEC-MALLS (Figure 11-12). In order to tackle that problem, cysteine mutants were engineered that would form a disulfide bond between EF hands of α-actinin-2 and the PDZ domain of the binding proteins. The idea was taken from a naturally occurring disulfide bond between the PDZ domain of InaD and the C-terminus of NorpA (Kimple et al., 2001). The disulfide-bridged complexes revealed a chimera formation on SDS-PAGE and confirmed that the binding occurs between a α-actinin-2 dimer and two molecules of ALP, CLP36 or ZASP, respectively (Figure 13). Furthermore, it has been shown by using crosslinking that similar complexes form in the absence of the disulfide bond (Appendix). MS

analysis of these crosslinked bands is ongoing and will hopefully reveal interesting results. These disulfide-bridged complexes, if optimized further, can be subjected to SAXS and/or cryo-EM which could pose a problem due to highly flexible internal region of ALP, CLP36, ZASP. One solution might be an engineered complex with different constructs, which would reduce the flexible region and open up more possibilities for analysis (Djinović-Carugo, unpublished data).

On the Binding α-actinin-2 and the ZM Motif Containing Proteins

ITC was employed here to characterize the binding between α-actinin-2 and ALP, CLP36 and ZASP, respectively. Different constructs were used in order to investigate the interaction between the full-length proteins, as well as proteins lacking either one of two possible binding sites. ALP^{1-284} was shown to interact with α-actinin-2 (K_D = 2.60 ± 0.41 µM) as well as with the NEECK mutant (K_D = 1.61 ± 0.41 µM), but with no statistically significant difference (Table 3) suggesting that the open conformation of α-actinin-2 doesn't affect the binding. Binding between the rod domain and ALP was as well proven, even with $ALP^{112-284}$ lacking the PDZ domain, confirming an interaction with K_D 4.60 ± 0.91 µM between the spectrin repeats of α-actinin-2 and the internal region of ALP (Figure 14). Similar binding behavior was observed for CLP36 as well. It interacts with α-actinin-2 (K_D = 3.44 ± 0.14 µM) and the rod domain (K_D = 4.49 ± 0.17 µM), even when lacking the PDZ domain (Figure 15). Even though ALP appears to bind with a higher affinity to α-actinin-2 when compared to CLP36, the difference between the affinities has proven to be not significant (Table 6). ZASP was shown to interact with α-actinin-2 with higher affinity compared to ALP and CLP36, whereas the PDZ domain alone revealed a binding affinity to α-actinin-2 of K_D = 4.75 ± 0.37 µM (Figure 16), disapproving of a much weaker affinity stated in the literature (Au et al., 2004).

The binding between α-actinin-2 and ALP, CLP36 and ZASP, respectively, was further investigated using crosslinking, which confirmed the 2:2 interaction (Figure 18, Appendix 1-14), where a α-actinin-2 or rod dimer interacts with two molecules of ALP, CLP36 and ZASP, respectively, with the possibility of one ligand binding to the dimer as well . Further MS analysis of the cross-linked monomeric products of α-actinin-2 NEECK with ALP^{1-284} and $CLP36^{1-256}$ as well as the monomeric products of the rod domain with $ALP^{112-284}$ and $CLP36^{117-256}$ (Figure 19) are expected to give more insight on the binding with α-actinin-2 in an open conformation, and on binding of the internal region of the spectrin repeats and the ZM motif.

ITC experiments with ALP peptide (Klaavuniemi et al., 2009) and the rod domain of α-actinin-2 revealed a high affinity of the peptide for the rod domain (K_D = 0.455 ± 0.171 μM) (Figure 17). When comparing the obtained affinities for ALP constructs, one can see that the peptide clearly binds with a higher affinity than ALP$^{117-284}$ which includes the whole ZASP-like motif. It is possible that the surrounding residues have some sort of an inhibitory effect on the binding, or the conformation of the formed complex has an effect on the affinity, which is naturally not the case if only the peptide is used.

The Nature of the Interaction Varies in Entropic Contributions

Both ALP and CLP36 interaction with α-actinin-2 was shown to be governed by enthalpic contributions (Table 2) which would suggest that, given a high disorder tendency (Figure 4-5) of ALP and CLP36, when binding to α-actinin-2, the binding is governed by formation of stabilizing polar interactions. Concerning ZASP, which itself has a higher disorder tendency then ALP and CLP36 (Figure 6) and its interaction with α-actinin-2, there is a much higher entropic contribution suggesting possibly a highly flexible region existing even after complex formation or hydrophobic interactions between the proteins causing a positive entropy change. The same case can be observed in the binding of the PDZ domain with α-actinin-2, which itself is ordered. If the binding is resulting in hiding of the water-accessible surface area and the release of interfacial water molecules, that could explain the positive entropy change which is usually a strong indication that water molecules have been released from the surface of the complex.

Structural Characterization Needs More Improvement

Initial crystallization screening of the rod domain with ALP$^{112-284}$ and CLP36$^{117-256}$ resulted in numerous positive hits which unfortunately diffracted very weakly or not at all. Only one crystal diffracted significantly better (the highest resolution 3.7 Å) and the structure didn't show any additional electron density which would correspond to CLP36$^{117-256}$. Due to low resolution, it cannot be clear if the complex is present, or CLP36$^{117-256}$ is just not seen. Optimization screening as well resulted in many positive hits, the crystals were bigger, but again, only the rod domain could be seen when resolving the structure. Still, the majority of the crystals didn't diffract, or did very badly.

Major problem was the inability to detect the presence of ALP$^{112-284}$ or CLP36$^{117-256}$ in the crystals, since both proteins cannot be stained by silver staining, most probably because the silver ion-protein interaction is too strong and doesn't allow posterior reduction. One possible improvement here would be fluorescently tagging the proteins so that it can be right away

visible if they are present in the crystal. Still, further improvement and optimization is needed in order to obtain viable crystals that would diffract better and finally, allow to solve the structure, if the complex is present in the crystal.

Future Steps on Structural Characterization of the ZM Motif

This study was able to characterize the binding of α-actinin-2 with proteins containing the ZM motif and point to the importance of it in the binding with the spectrin repeats of the rod domain. It provides a ground to understand how the interaction is happening and what are the governing parameters in the binding. It would be interesting to investigate the possible competition between ALP/Enigma proteins when they bind to α-actinin-2, and to find out how other proteins of the Z-disk are involved in modulating the interaction. More improvement is needed in optimizing the behavior and stability of the disulfide-bridged complexes in order to allow high resolution structural characterization. When it comes to the ZM motif itself, as it is not sure if co-crystallization with the rod domain is resulting in a complex present in the crystal, a recommendable step would be to continue co-crystallization and/or soaking with the peptide, that showed a high affinity for the rod domain. That would be a step forward structural characterization of the ZM motif, which alongside the structure determination of disulfide-bridged complexes could potentially reveal the full structure of the interaction between α-actinin-2 and ALP, CLP36 and ZASP.

Appendix

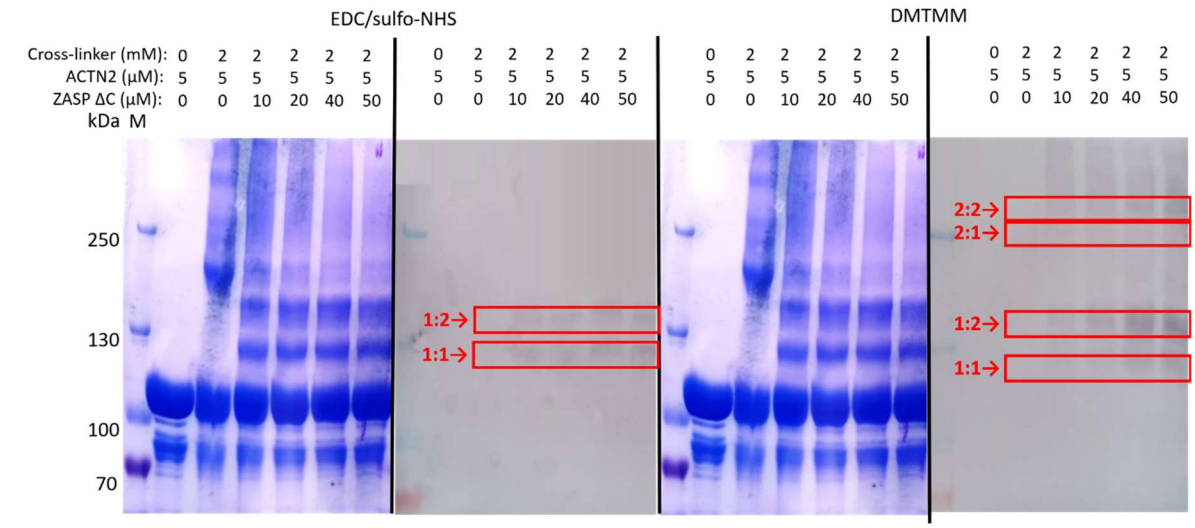

Appendix 1 – Crosslinking and Western Blot of α-actinin-2 and ZASP ΔC

Crosslinking between of α-actinin-2 and ZASP ΔC and corresponding western blot using two different cross-linkers. Marked on the figure crosslinking products with different stoichiometries: *n*(ACTN2):*n*(ZASP) = 2:2 yielding a 248 kDa product, *n*(ACTN2):*n*(ZASP) = 2:1 yielding a 227 kDa product, *n*(ACTN2):*n*(ZASP) = 1:2, yielding a 145 kDa product and *n*(ACTN2):*n*(ZASP) = 1:1, yielding a 124 kDa product.

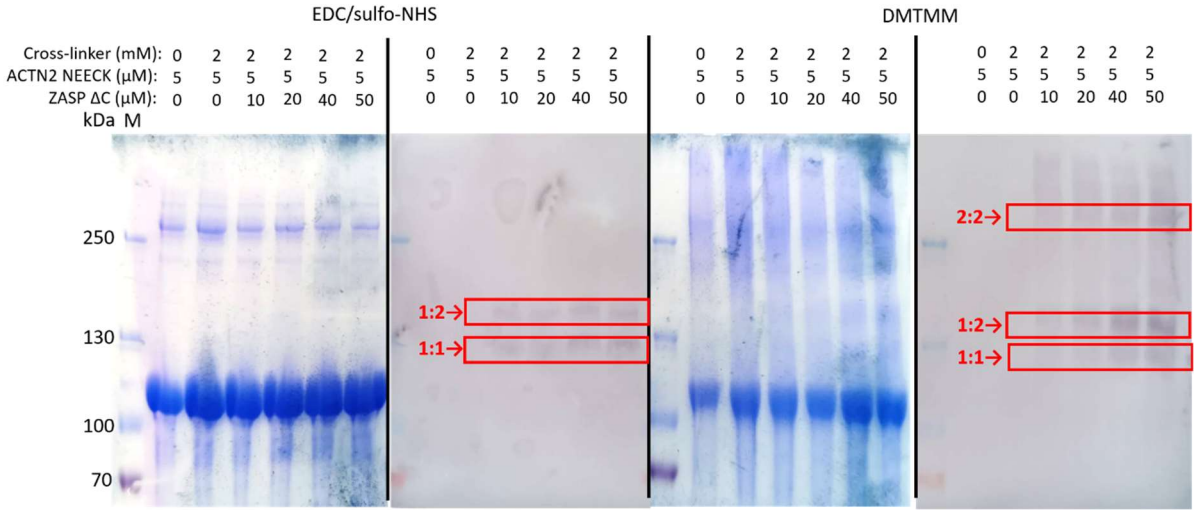

Appendix 2 - Crosslinking and Western Blot of α-actinin-2 NEECK and ZASP ΔC

Crosslinking between of α-actinin-2 NEECK and ZASP ΔC and corresponding western blot using two different cross-linkers. Marked on the figure crosslinking products with different stoichiometries: *n*(NEECK):*n*(ZASP) = 2:2 yielding a 248 kDa product, *n*(NEECK):*n*(ZASP) = 1:2, yielding a 145 kDa product and *n*(NEECK):*n*(ZASP) = 1:1, yielding a 124 kDa product.

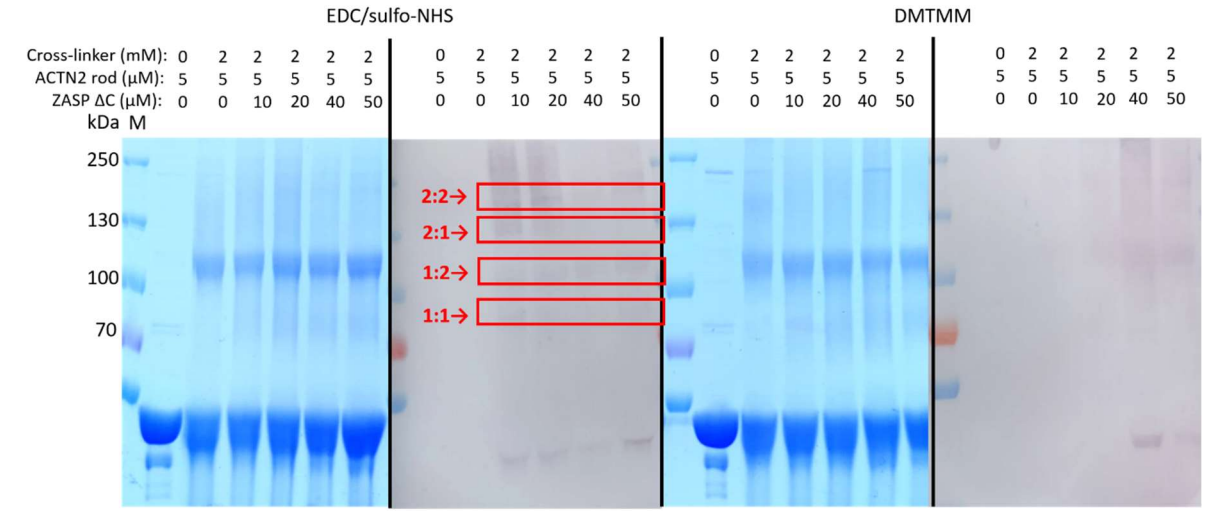

Appendix 3 - Crosslinking and Western Blot of the rod domain of α-actinin-2 and ZASP ΔC

Crosslinking between of the rod domain of α-actinin-2 and ZASP ΔC and corresponding western blot using two different cross-linkers. Marked on the figure crosslinking products with different stoichiometries: *n*(rod):*n*(ZASP) = 2:2 yielding a 154 kDa product, *n*(rod):*n*(ZASP) = 2:1 yielding a 133 kDa product, *n*(rod):*n*(ZASP) = 1:2, yielding a 98 kDa product and *n*(rod):*n*(ZASP) = 1:1, yielding a 77 kDa product.

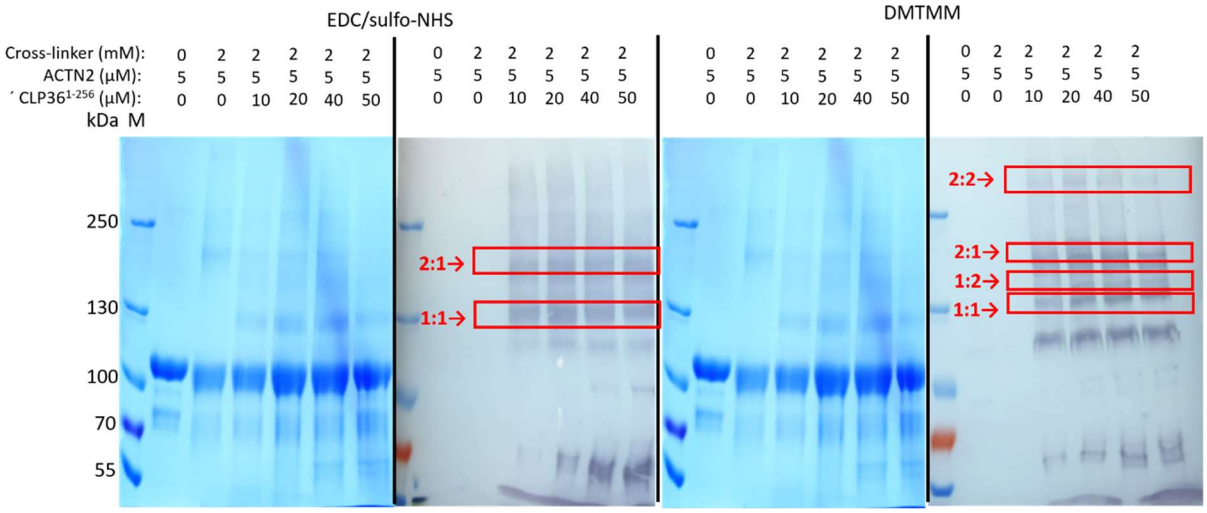

Appendix 4 – Crosslinking and Western Blot of α-actinin-2 and CLP36[1-256]

Crosslinking between α-actinin-2 and CLP36[1-256] and corresponding western blot using two different cross-linkers. Marked on the figure crosslinking products with different stoichiometries: *n*(ACTN2):*n*(CLP[1-256]) = 2:2 yielding a 268 kDa product, *n*(ACTN2):*n*(CLP[1-256]) = 2:1 yielding a 237 kDa product, *n*(ACTN2):*n*(CLP[1-256]) = 1:2, yielding a 165 kDa product and *n*(ACTN2):*n*(CLP[1-256]) = 1:1, yielding a 134 kDa product.

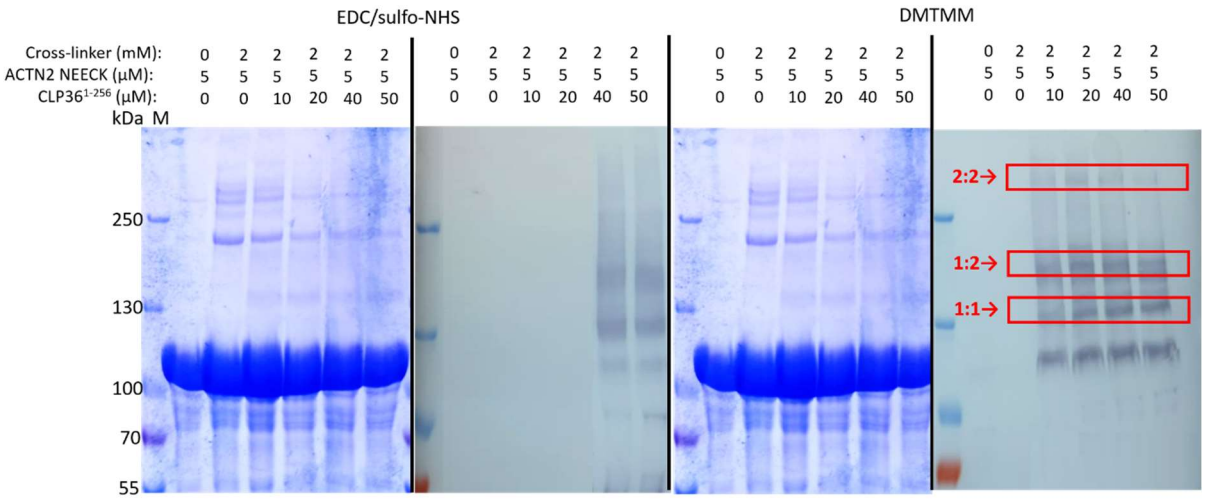

Appendix 5 - Crosslinking and Western Blot of α-actinin-2 NEECK and CLP36[1-256]

Crosslinking between α-actinin-2 NEECK and CLP36[1-256] and corresponding western blot using two different cross-linkers. Marked on the figure crosslinking products with different stoichiometries: *n*(NEECK):*n*(CLP[1-256]) = 2:2 yielding a 268 kDa product, *n*(NEECK):*n*(CLP[1-256]) = 2:1 yielding a 237 kDa product, *n*(NEECK):*n*(CLP[1-256]) = 1:2, yielding a 165 kDa product and *n*(NEECK):*n*(CLP[1-256]) = 1:1, yielding a 134 kDa product.

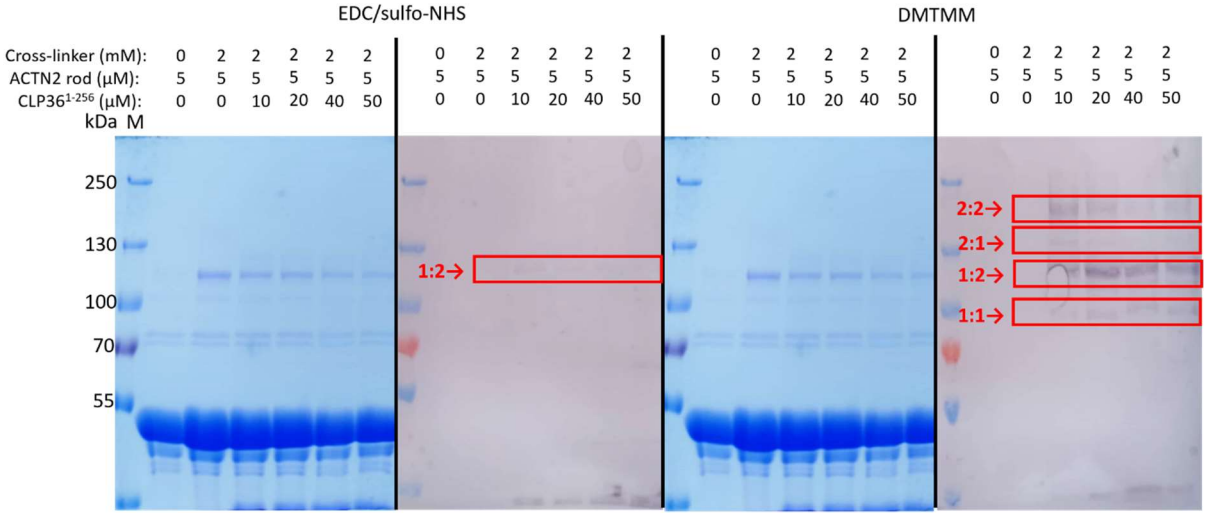

Appendix 6 - Crosslinking and Western Blot of the rod domain of α-actinin-2 and CLP36[1-256]

Crosslinking between the rod domain of α-actinin-2 and CLP36[1-256] and corresponding western blot using two different cross-linkers. Marked on the figure crosslinking products with different stoichiometries: *n*(rod):*n*(CLP[1-256]) = 2:2 yielding a 174 kDa product, *n*(rod):*n*(CLP[1-256]) = 2:1 yielding a 143 kDa product, *n*(rod):*n*(CLP[1-256]) = 1:2, yielding a 118 kDa product and *n*(rod):*n*(CLP[1-256]) = 1:1, yielding a 87 kDa product.

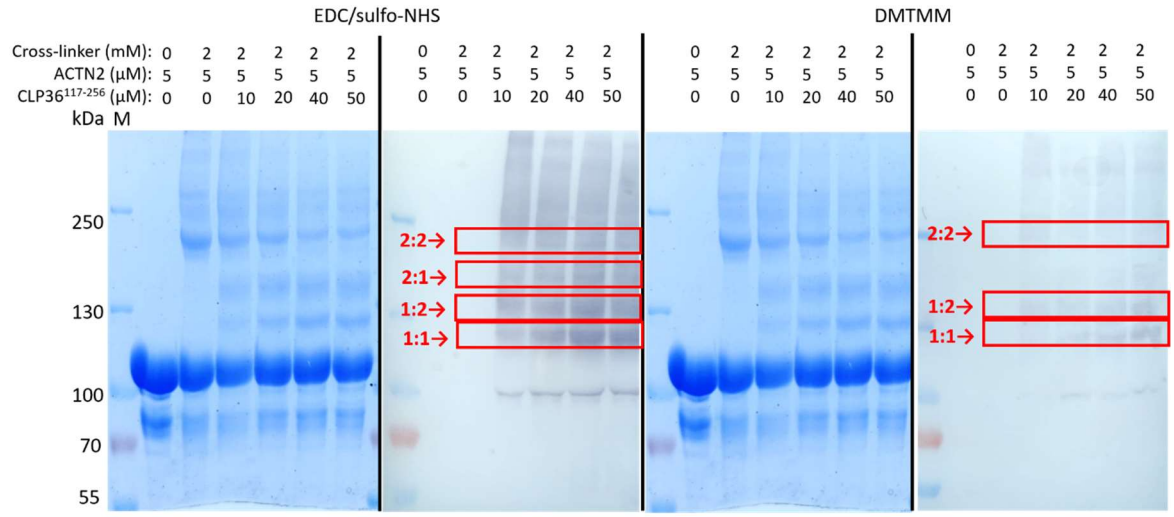

Appendix 7 - Crosslinking and Western Blot of α-actinin-2 and CLP36$^{117-256}$

Crosslinking between the α-actinin-2 and CLP36$^{117-256}$ and corresponding western blot using two different cross-linkers. Marked on the figure crosslinking products with different stoichiometries: n(ACTN2):n(CLP$^{117-256}$) = 2:2 yielding a 242 kDa product, n(ACTN2):n(CLP$^{117-256}$) = 2:1 yielding a 224 kDa product, n(ACTN2):n(CLP$^{117-256}$) = 1:2, yielding a 139 kDa product and n(ACTN2):n(CLP$^{117-256}$) = 1:1, yielding a 121 kDa product.

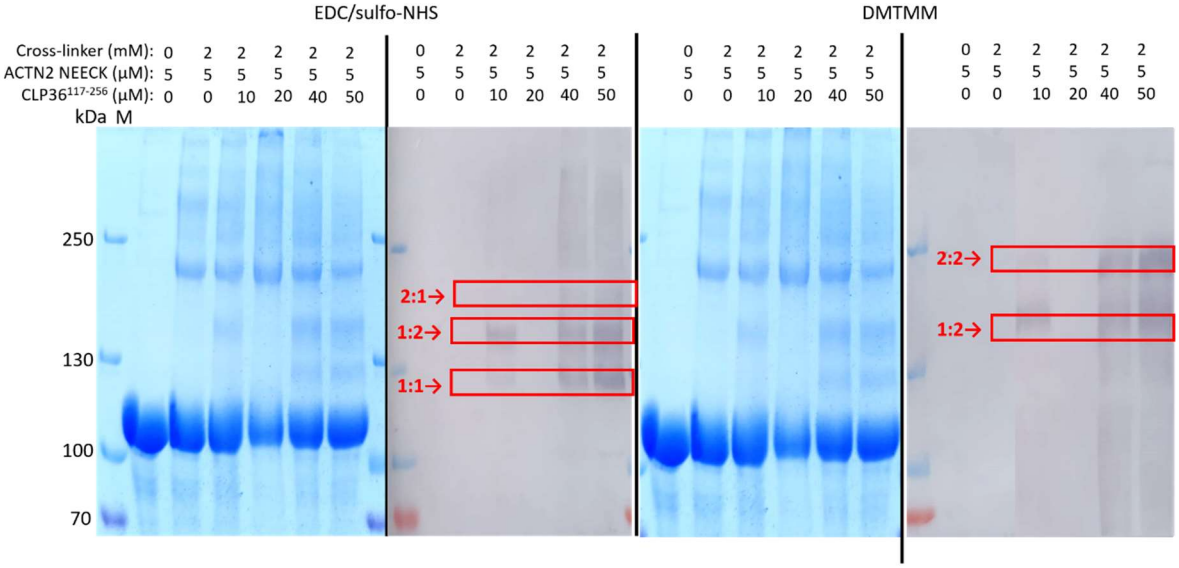

Appendix 8 - Crosslinking and Western Blot of α-actinin-2 NEECK and CLP36$^{117-256}$

Crosslinking between the α-actinin-2 NEECK and CLP36$^{117-256}$ and corresponding western blot using two different cross-linkers. Marked on the figure crosslinking products with different stoichiometries: n(NEECK):n(CLP$^{117-256}$) = 2:2 yielding a 242 kDa product, n(NEECK):n(CLP$^{117-256}$) = 2:1 yielding a 224 kDa product, n(NEECK):n(CLP$^{117-256}$) = 1:2, yielding a 139 kDa product and n(NEECK):n(CLP$^{117-256}$) = 1:1, yielding a 121 kDa product.

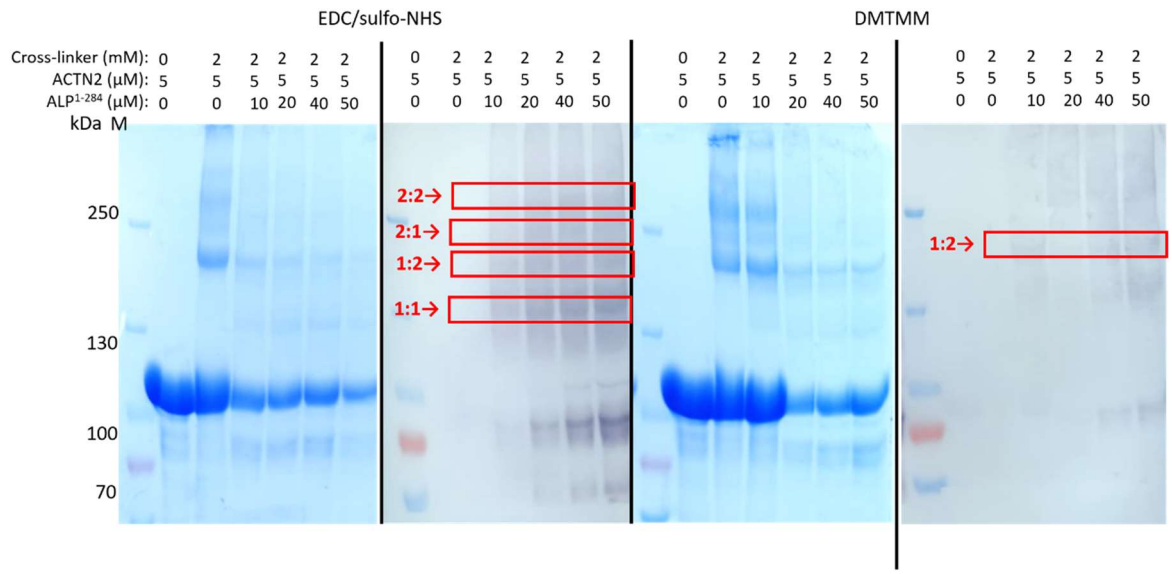

Appendix 9 - Crosslinking and Western Blot of α-actinin-2 and ALP$^{1-284}$

Crosslinking between the α-actinin-2 and ALP$^{1-284}$ and corresponding western blot using two different cross-linkers. Marked on the figure crosslinking products with different stoichiometries: n(ACTN2):n(ALP$^{1-284}$) = 2:2 yielding a 272 kDa product, n(ACTN2):n(ALP$^{1-284}$) = 2:1 yielding a 239 kDa product, n(ACTN2):n(ALP$^{1-284}$) = 1:2, yielding a 169 kDa product and n(ACTN2):n(ALP$^{1-284}$) = 1:1, yielding a 136 kDa product.

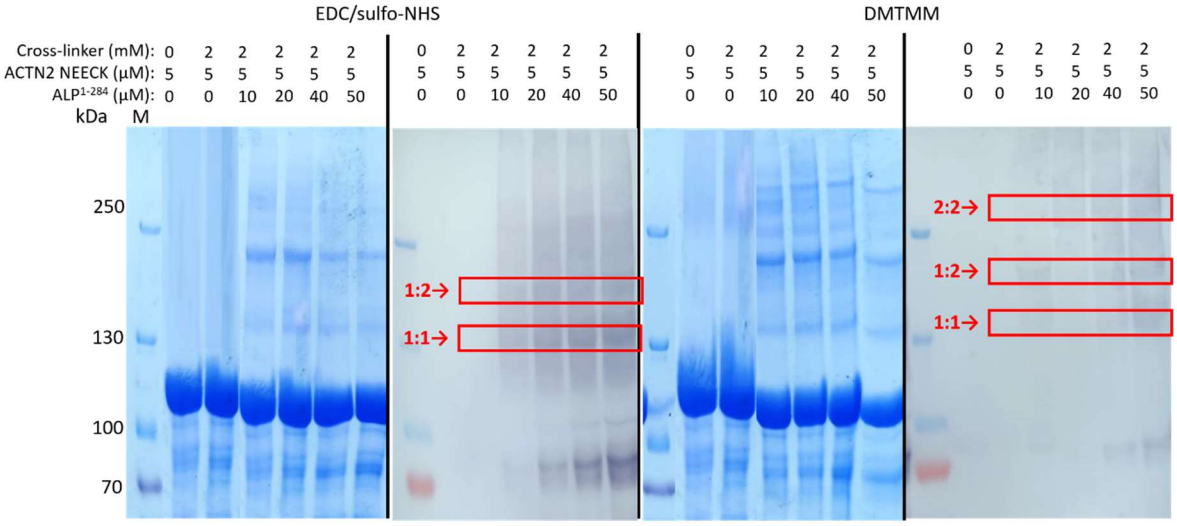

Appendix 10 - Crosslinking and Western Blot of α-actinin-2 NEECK and ALP$^{1-284}$

Crosslinking between the α-actinin-2 NEECK and ALP$^{1-284}$ and corresponding western blot using two different cross-linkers. Marked on the figure crosslinking products with different stoichiometries: n(NEECK):n(ALP$^{1-284}$) = 2:2 yielding a 272 kDa product, n(NEECK):n(ALP$^{1-284}$) = 1:2, yielding a 169 kDa product and n(NEECK):n(ALP$^{1-284}$) = 1:1, yielding a 136 kDa product.

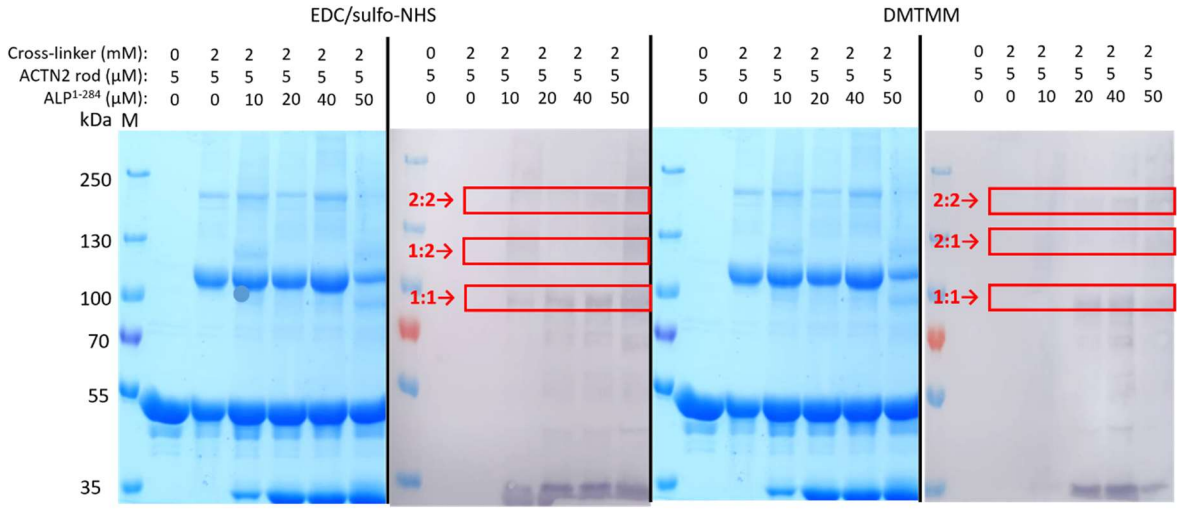

Appendix 11 - Crosslinking and Western Blot of the rod domain of α-actinin-2 and ALP$^{1-284}$

Crosslinking between the rod domain of α-actinin-2 and ALP$^{1-284}$ and corresponding western blot using two different cross-linkers. Marked on the figure crosslinking products with different stoichiometries: n(rod):n(ALP$^{1-284}$) = 2:2 yielding a 178 kDa product, n(rod):n(ALP$^{1-284}$) = 2:1 yielding a 145 kDa product, n(rod):n(ALP$^{1-284}$) = 1:2, yielding a 122 kDa product and n(rod):n(ALP$^{1-284}$) = 1:1, yielding a 89 kDa product.

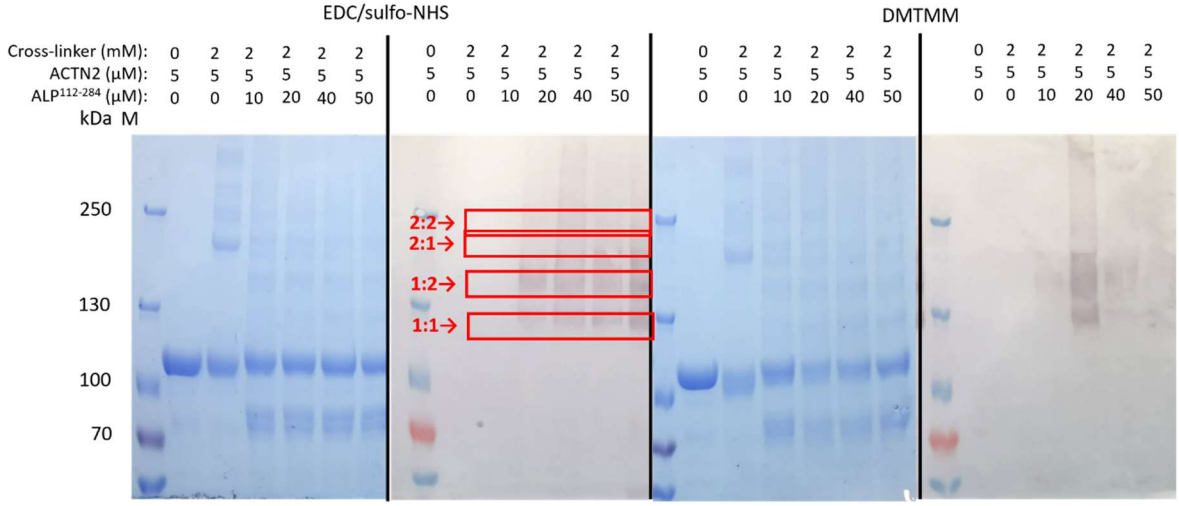

Appendix 12 - Crosslinking and Western Blot of α-actinin-2 and ALP$^{112-284}$

Crosslinking between the α-actinin-2 and ALP$^{112-284}$ and corresponding western blot using two different cross-linkers. Marked on the figure crosslinking products with different stoichiometries: n(ACTN2):n(ALP$^{112-284}$) = 2:2 yielding a 248 kDa product, n(ACTN2):n(ALP$^{112-284}$) = 2:1 yielding a 227 kDa product, n(ACTN2):n(ALP$^{112-284}$) = 1:2, yielding a 145 kDa product and n(ACTN2):n(ALP$^{112-284}$) = 1:1, yielding a 124 kDa product.

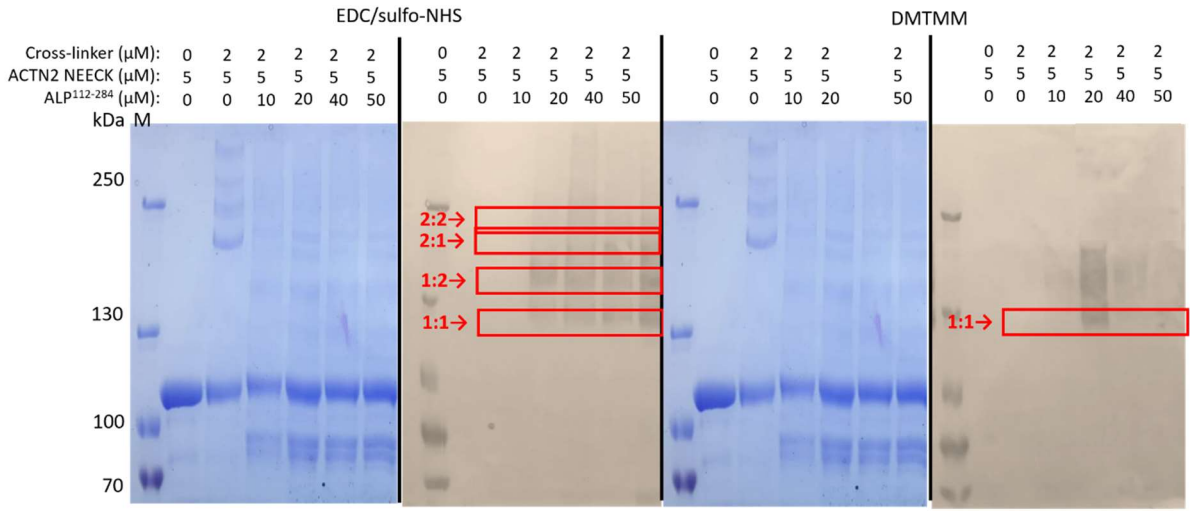

Appendix 13 - Crosslinking and Western Blot of α-actinin-2 NEECK and ALP$^{112-284}$

Crosslinking between the α-actinin-2 NEECK and ALP$^{112-284}$ and corresponding western blot using two different cross-linkers. Marked on the figure crosslinking products with different stoichiometries: *n*(NEECK):*n*(ALP$^{112-284}$) = 2:2 yielding a 248 kDa product, *n*(NEECK):*n*(ALP$^{112-284}$) = 2:1 yielding a 227 kDa product, *n*(NEECK):*n*(ALP$^{112-284}$) = 1:2, yielding a 145 kDa product and *n*(NEECK):*n*(ALP$^{112-284}$) = 1:1, yielding a 124 kDa product.

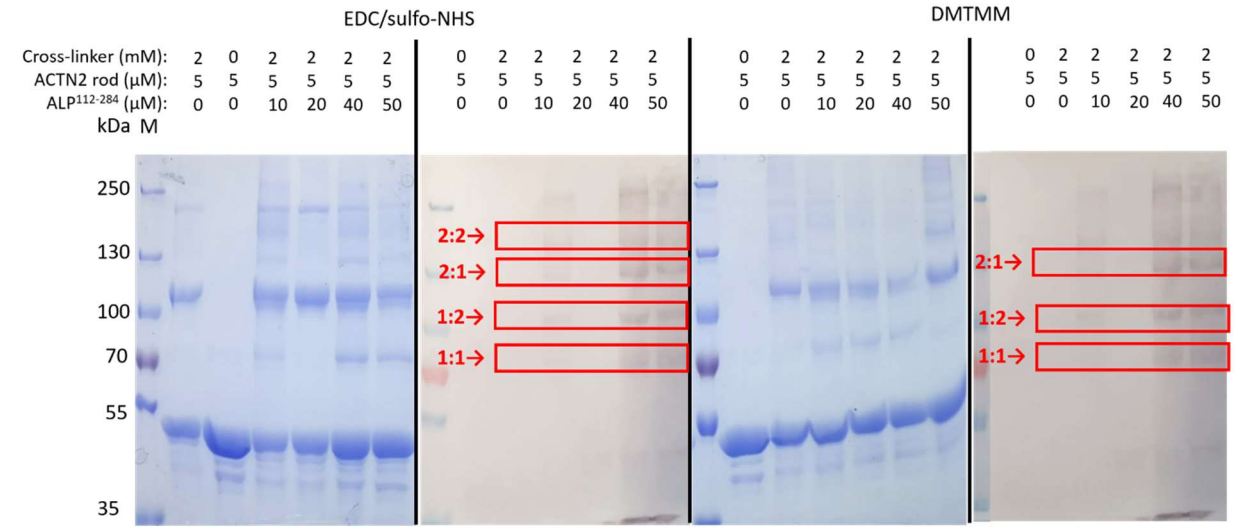

Appendix 14 - Crosslinking and Western Blot of the rod domain of α-actinin-2 and ALP$^{112-284}$

Crosslinking between the rod domain of α-actinin-2 and ALP$^{112-284}$ and corresponding western blot using two different cross-linkers. Marked on the figure crosslinking products with different stoichiometries: *n*(rod):*n*(ALP$^{112-284}$) = 2:2 yielding a 154 kDa product, *n*(rod):*n*(ALP$^{112-284}$) = 2:1 yielding a 133 kDa product, *n*(rod):*n*(ALP$^{112-284}$) = 1:2, yielding a 98 kDa product and *n*(rod):*n*(ALP$^{112-284}$) = 1:1, yielding a 77 kDa product.

Abbreviations

ABD	actin-binding-domain
ALP	Actinin-associated LIM protein
ALPM	ALP-like motif
CAMD	Calmodulin-like domain
CH	calponin homology
CLP36	36 kDa C-Terminal LIM Domain Protein
DMTMM	4-(4,6-dimethoxy-1,3,5-triazin-2-yl)-4-methyl-morpholinium chloride
DTT	dithiothreitol
EDC	1-ethyl-3-(3-dimethylaminopropyl)carbodiimide hydrochloride
EDTA	ethylenediaminetetraacetic acid
ENH	actin-associated protein enigma homolog
FATZ	gamma-filamin/ABP-L, alpha-actinin and telethonin binding protein
InaD	Inactivation-no-after-potential D protein
IPTG	isopropyl β- d-1-thiogalactopyranoside
LB	lysogeny broth
NorpA	1-phosphatidylinositol 4,5-bisphosphate phosphodiesterase
PBS	Phosphate-Buffered Saline
PKC	Protein-Kinase C
PMSF	phenylmethylsulfonyl fluoride
SR	spectrin repeats
TBS	Tris-buffered saline
TBST	Tris-buffered saline, polysorbate 20
TCEP	tris(2-carboxyethyl)phosphine
TEV	Tobacco Etch Virus nuclear-inclusion-a endopeptidase
ZASP	Z-Disk-Associated, Alternatively Spliced, PDZ Motif-Containing Protein
ZM	ZASP-like motif

References

Arimura, T., Hayashi, T., Terada, H., Lee, S.-Y., Zhou, Q., Takahashi, M., Ueda, K., Nouchi, T., Hohda, S., Shibutani, M., Hirose, M., Chen, J., Park, J.-E., Yasunami, M., Hayashi, H., Kimura, A., 2004. A Cypher/ZASP Mutation Associated with Dilated Cardiomyopathy Alters the Binding Affinity to Protein Kinase C. J. Biol. Chem. 279, 6746–6752. https://doi.org/10.1074/jbc.M311849200

Arimura, T., Inagaki, N., Hayashi, T., Shichi, D., Sato, A., Hinohara, K., Vatta, M., Towbin, J.A., Chikamori, T., Yamashina, A., Kimura, A., 2009. Impaired binding of ZASP/Cypher with phosphoglucomutase 1 is associated with dilated cardiomyopathy. Cardiovasc Res 83, 80–88. https://doi.org/10.1093/cvr/cvp119

Au, Y., Atkinson, R.A., Guerrini, R., Kelly, G., Joseph, C., Martin, S.R., Muskett, F.W., Pallavicini, A., Faulkner, G., Pastore, A., 2004. Solution Structure of ZASP PDZ Domain: Implications for Sarcomere Ultrastructure and Enigma Family Redundancy. Structure 12, 611–622. https://doi.org/10.1016/j.str.2004.02.019

Bang, M.-L., Mudry, R.E., McElhinny, A.S., Trombitás, K., Geach, A.J., Yamasaki, R., Sorimachi, H., Granzier, H., Gregorio, C.C., Labeit, S., 2001. Myopalladin, a Novel 145-Kilodalton Sarcomeric Protein with Multiple Roles in Z-Disc and I-Band Protein Assemblies. Journal of Cell Biology 153, 413–428. https://doi.org/10.1083/jcb.153.2.413

Barrès, R., Grémeaux, T., Gual, P., Gonzalez, T., Gugenheim, J., Tran, A., Le Marchand-Brustel, Y., Tanti, J.-F., 2006. Enigma interacts with adaptor protein with PH and SH2 domains to control insulin-induced actin cytoskeleton remodeling and glucose transporter 4 translocation. Mol Endocrinol 20, 2864–2875. https://doi.org/10.1210/me.2005-0455

Bauer, K., Kratzer, M., Otte, M., de Quintana, K.L., Hagmann, J., Arnold, G.J., Eckerskorn, C., Lottspeich, F., Siess, W., 2000. Human CLP36, a PDZ-domain and LIM-domain protein, binds to α-actinin-1 and associates with actin filaments and stress fibers in activated platelets and endothelial cells. Blood 96, 4236–4245. https://doi.org/10.1182/blood.V96.13.4236

Britson, K.A., Yang, S.Y., Lloyd, T.E., 2018. New developments in the genetics of Inclusion Body Myositis. Curr Rheumatol Rep 20, 26. https://doi.org/10.1007/s11926-018-0738-0

Casella, J.F., Craig, S.W., Maack, D.J., Brown, A.E., 1987. Cap Z(36/32), a barbed end actin-capping protein, is a component of the Z-line of skeletal muscle. J Cell Biol 105, 371–379. https://doi.org/10.1083/jcb.105.1.371

Chiu Christine, Bagnall Richard D., Ingles Jodie, Yeates Laura, Kennerson Marina, Donald Jennifer A., Jormakka Mika, Lind Joanne M., Semsarian Christopher, 2010. Mutations in Alpha-Actinin-2 Cause Hypertrophic Cardiomyopathy. Journal of the American College of Cardiology 55, 1127–1135. https://doi.org/10.1016/j.jacc.2009.11.016

Chu, M., Gregorio, C.C., Pappas, C.T., 2016. Nebulin, a multi-functional giant. Journal of Experimental Biology 219, 146–152. https://doi.org/10.1242/jeb.126383

Cooper, J.A., Schafer, D.A., 2000. Control of actin assembly and disassembly at filament ends. Curr Opin Cell Biol 12, 97–103. https://doi.org/10.1016/s0955-0674(99)00062-9

Durick, K., Gill, G.N., Taylor, S.S., 1998. Shc and Enigma Are Both Required for Mitogenic Signaling by Ret/ptc2. Mol Cell Biol 18, 2298–2308.

Emsley, P., Lohkamp, B., Scott, W.G., Cowtan, K., 2010. Features and development of Coot. Acta Crystallogr D Biol Crystallogr 66, 486–501. https://doi.org/10.1107/S0907444910007493

Faulkner, G., Pallavicini, A., Comelli, A., Salamon, M., Bortoletto, G., Ievolella, C., Trevisan, S., Kojic', S., Dalla Vecchia, F., Laveder, P., Valle, G., Lanfranchi, G., 2000. FATZ, a filamin-, actinin-, and telethonin-binding protein of the Z-disc of skeletal muscle. J Biol Chem 275, 41234–41242. https://doi.org/10.1074/jbc.M007493200

Faulkner, G., Pallavicini, A., Formentin, E., Comelli, A., Ievolella, C., Trevisan, S., Bortoletto, G., Scannapieco, P., Salamon, M., Mouly, V., Valle, G., Lanfranchi, G., 1999. ZASP: A New Z-band Alternatively Spliced PDZ-motif Protein. J Cell Biol 146, 465–475. https://doi.org/10.1083/jcb.146.2.465

Foley, K.S., Young, P.W., 2014. The non-muscle functions of actinins: an update. Biochem J 459, 1–13. https://doi.org/10.1042/BJ20131511

Franzot, G., Sjöblom, B., Gautel, M., Carugo, K.D., 2005. The Crystal Structure of the Actin Binding Domain from α-Actinin in its Closed Conformation: Structural Insight into Phospholipid Regulation of α-Actinin. Journal of Molecular Biology 348, 151–165. https://doi.org/10.1016/j.jmb.2005.01.002

Frontera, W.R., Ochala, J., 2015. Skeletal Muscle: A Brief Review of Structure and Function. Calcif Tissue Int 96, 183–195. https://doi.org/10.1007/s00223-014-9915-y

Galkin, V.E., Orlova, A., Salmazo, A., Djinovic-Carugo, K., Egelman, E.H., 2010. Opening of tandem calponin homology domains regulates their affinity for F-actin. Nat Struct Mol Biol 17, 614–616. https://doi.org/10.1038/nsmb.1789

Gautel, M., Djinović-Carugo, K., 2016. The sarcomeric cytoskeleton: from molecules to motion. Journal of Experimental Biology 219, 135–145. https://doi.org/10.1242/jeb.124941

Gill, G.N., 1995. The enigma of LIM domains. Structure 3, 1285–1289. https://doi.org/10.1016/s0969-2126(01)00265-9

Goldstein, M.A., Schoeter, J.P., Sass, R.L., 1990. Two structural states of the vertebrate Z band. Electron Microscopy Reviews 3, 227–248. https://doi.org/10.1016/0892-0354(90)90003-B

González-Morales, N., Xiao, Y.S., Schilling, M.A., Marescal, O., Liao, K.A., Schöck, F., 2019. Myofibril diameter is set by a finely tuned mechanism of protein oligomerization in Drosophila. eLife 8, e50496. https://doi.org/10.7554/eLife.50496

Griggs, R., Vihola, A., Hackman, P., Talvinen, K., Haravuori, H., Faulkner, G., Eymard, B., Richard, I., Selcen, D., Engel, A., Carpen, O., Udd, B., 2007. Zaspopathy in a large classic late-onset distal myopathy family. Brain 130, 1477–1484. https://doi.org/10.1093/brain/awm006

Harris, B.Z., Lim, W.A., 2001. Mechanism and role of PDZ domains in signaling complex assembly. J Cell Sci 114, 3219–3231.

Hasegawa, T., Ohno, K., Funahashi, S., Miyazaki, K., Nagano, A., Sato, K., 2010. CLP36 interacts with palladin in dorsal root ganglion neurons. Neuroscience Letters 476, 53–57. https://doi.org/10.1016/j.neulet.2010.03.081

Holmes, W.B., Moncman, C.L., 2008. Nebulette interacts with filamin C. Cell Motil Cytoskeleton 65, 130–142. https://doi.org/10.1002/cm.20249

Jani, K., Schöck, F., 2007. Zasp is required for the assembly of functional integrin adhesion sites. J Cell Biol 179, 1583–1597. https://doi.org/10.1083/jcb.200707045

Jin, J.-P., Wang, K., 1991. Nebulin as a giant actin-binding template protein in skeletal muscle sarcomere Interaction of actin and cloned human nebulin fragments. FEBS Letters 281, 93–96. https://doi.org/10.1016/0014-5793(91)80366-B

Jo, K., Rutten, B., Bunn, R.C., Bredt, D.S., 2001. Actinin-Associated LIM Protein-Deficient Mice Maintain Normal Development and Structure of Skeletal Muscle. Molecular and Cellular Biology 21, 1682–1687. https://doi.org/10.1128/MCB.21.5.1682-1687.2001

Jokl, E.J., Blanco, G., 2016. Disrupted autophagy undermines skeletal muscle adaptation and integrity. Mamm Genome 27, 525–537. https://doi.org/10.1007/s00335-016-9659-2

Kabsch, W., 2010. XDS. Acta Cryst D 66, 125–132. https://doi.org/10.1107/S0907444909047337

Kadrmas, J.L., Beckerle, M.C., 2004. The LIM domain: from the cytoskeleton to the nucleus. Nature Reviews Molecular Cell Biology 5, 920–931. https://doi.org/10.1038/nrm1499

Kimple, M.E., Siderovski, D.P., Sondek, J., 2001. Functional relevance of the disulfide-linked complex of the N-terminal PDZ domain of InaD with NorpA. EMBO J 20, 4414–4422. https://doi.org/10.1093/emboj/20.16.4414

Klaavuniemi, T., Alho, N., Hotulainen, P., Kelloniemi, A., Havukainen, H., Permi, P., Mattila, S., Ylänne, J., 2009. Characterization of the interaction between Actinin-Associated LIM Protein (ALP) and the rod domain of α-actinin. BMC Cell Biology 10, 22. https://doi.org/10.1186/1471-2121-10-22

Klaavuniemi, T., Kelloniemi, A., Ylänne, J., 2004. The ZASP-like Motif in Actinin-associated LIM Protein Is Required for Interaction with the α-Actinin Rod and for Targeting to the Muscle Z-line. J. Biol. Chem. 279, 26402–26410. https://doi.org/10.1074/jbc.M401871200

Klaavuniemi, T., Ylänne, J., 2006. Zasp/Cypher internal ZM-motif containing fragments are sufficient to co-localize with α-actinin—Analysis of patient mutations. Experimental Cell Research 312, 1299–1311. https://doi.org/10.1016/j.yexcr.2005.12.036

Kotaka, M., Ngai, S.-M., Garcia-Barcelo, M., Tsui, S.K.W., Fung, K.-P., Lee, C.-Y., Waye, M.M.Y., 1999. Characterization of the human 36-kDa carboxyl terminal LIM domain protein (hCLIM1). Journal of Cellular Biochemistry 72, 279–285. https://doi.org/10.1002/(SICI)1097-4644(19990201)72:2<279::AID-JCB12>3.0.CO;2-7

Kuroda, S., Tokunaga, C., Kiyohara, Y., Higuchi, O., Konishi, H., Mizuno, K., Gill, G.N., Kikkawa, U., 1996. Protein-Protein Interaction of Zinc Finger LIM Domains with Protein Kinase C*. Journal of Biological Chemistry 271, 31029–31032. https://doi.org/10.1074/jbc.271.49.31029

Lee, H.-J., Zheng, J.J., 2010. PDZ domains and their binding partners: structure, specificity, and modification. Cell Communication and Signaling 8, 8. https://doi.org/10.1186/1478-811X-8-8

Liao, K.A., González-Morales, N., Schöck, F., 2020. Characterizing the actin-binding ability of Zasp52 and its contribution to myofibril assembly. PLOS ONE 15, e0232137. https://doi.org/10.1371/journal.pone.0232137

Liao, K.A., González-Morales, N., Schöck, F., 2016. Zasp52, a Core Z-disc Protein in Drosophila Indirect Flight Muscles, Interacts with α-Actinin via an Extended PDZ Domain. PLOS Genetics 12, e1006400. https://doi.org/10.1371/journal.pgen.1006400

Lornage, X., Romero, N.B., Grosgogeat, C.A., Malfatti, E., Donkervoort, S., Marchetti, M.M., Neuhaus, S.B., Foley, A.R., Labasse, C., Schneider, R., Carlier, R.Y., Chao, K.R., Medne, L., Deleuze, J.-F., Orlikowski, D., Bönnemann, C.G., Gupta, V.A., Fardeau, M., Böhm, J., Laporte, J., 2019. ACTN2 mutations cause “Multiple structured Core Disease” (MsCD). Acta Neuropathol 137, 501–519. https://doi.org/10.1007/s00401-019-01963-8

Loughran, G., Healy, N.C., Kiely, P.A., Huigsloot, M., Kedersha, N.L., O’Connor, R., 2005. Mystique Is a New Insulin-like Growth Factor-I-regulated PDZ-LIM Domain Protein That Promotes Cell Attachment and Migration and Suppresses Anchorage-independent Growth. MBoC 16, 1811–1822. https://doi.org/10.1091/mbc.e04-12-1052

Luther, P.K., 2009. The vertebrate muscle Z-disc: sarcomere anchor for structure and signalling. J Muscle Res Cell Motil 15.

Luther, P.K., Barry, J.S., Squire, J.M., 2002. The three-dimensional structure of a vertebrate wide (slow muscle) Z-band: lessons on Z-band assembly. J Mol Biol 315, 9–20. https://doi.org/10.1006/jmbi.2001.5217

M, K., B, S., A, A., A, H., R, K., I, S.-W., R, S., 1995. Expression of ril, a novel LIM domain gene, is down-regulated in Hras-transformed cells and restored in phenotypic revertants. Oncogene 10, 61–68.

Maday, S., Anderson, E., Chang, H.C., Shorter, J., Satoh, A., Sfakianos, J., Fölsch, H., Anderson, J.M., Walther, Z., Mellman, I., 2008. A PDZ-Binding Motif Controls Basolateral Targeting of Syndecan-1 Along the Biosynthetic Pathway in Polarized Epithelial Cells. Traffic 9, 1915–1924. https://doi.org/10.1111/j.1600-0854.2008.00805.x

Maeda, M., Asano, E., Ito, D., Ito, S., Hasegawa, Y., Hamaguchi, M., Senga, T., 2009. Characterization of interaction between CLP36 and palladin. The FEBS Journal 276, 2775–2785. https://doi.org/10.1111/j.1742-4658.2009.07001.x

Maisonneuve, P., Caillet-Saguy, C., Raynal, B., Gilquin, B., Chaffotte, A., Pérez, J., Zinn-Justin, S., Delepierre, M., Buc, H., Cordier, F., Wolff, N., 2014. Regulation of the catalytic activity of the human phosphatase PTPN4 by its PDZ domain. The FEBS Journal 281, 4852–4865. https://doi.org/10.1111/febs.13024

Martinelli, V.C., Kyle, W.B., Kojic, S., Vitulo, N., Li, Z., Belgrano, A., Maiuri, P., Banks, L., Vatta, M., Valle, G., Faulkner, G., 2014. ZASP Interacts with the Mechanosensing Protein Ankrd2 and p53 in the Signalling Network of Striated Muscle. PLOS ONE 9, e92259. https://doi.org/10.1371/journal.pone.0092259

Masaki, T., Endo, M., Ebashi, S., 1967. Localization of 6S component of a alpha-actinin at Z-band. J Biochem 62, 630–632. https://doi.org/10.1093/oxfordjournals.jbchem.a128717

McCoy, A.J., Grosse-Kunstleve, R.W., Adams, P.D., Winn, M.D., Storoni, L.C., Read, R.J., 2007. Phaser crystallographic software. J Appl Cryst 40, 658–674. https://doi.org/10.1107/S0021889807021206

Mészáros, B., Erdős, G., Dosztányi, Z., 2018. IUPred2A: context-dependent prediction of protein disorder as a function of redox state and protein binding. Nucleic Acids Research 46, W329–W337. https://doi.org/10.1093/nar/gky384

Mills, M., Yang, N., Weinberger, R., Vander Woude, D.L., Beggs, A.H., Easteal, S., North, K., 2001. Differential expression of the actin-binding proteins, α-actinin-2 and -3, in different species: implications for the evolution of functional redundancy. Human Molecular Genetics 10, 1335–1346. https://doi.org/10.1093/hmg/10.13.1335

Miyazaki, K., Ohno, K., Tamura, N., Sasaki, T., Sato, K., 2012. CLP36 and RIL recruit α-actinin-1 to stress fibers and differentially regulate stress fiber dynamics in F2408 fibroblasts. Experimental Cell Research 318, 1716–1725. https://doi.org/10.1016/j.yexcr.2012.05.006

Mlynek, G., Kostan, J., Leeb, S., Djinović-Carugo, K., 2020. Tailored Suits Fit Better: Customized Protein Crystallization Screens. Crystal Growth & Design 20, 984–994. https://doi.org/10.1021/acs.cgd.9b01328

Mohapatra, B., Jimenez, S., Lin, J.H., Bowles, K.R., Coveler, K.J., Marx, J.G., Chrisco, M.A., Murphy, R.T., Lurie, P.R., Schwartz, R.J., Elliott, P.M., Vatta, M., McKenna, W., Towbin, J.A., Bowles, N.E., 2003. Mutations in the muscle LIM protein and α-actinin-2 genes in dilated cardiomyopathy and endocardial fibroelastosis. Molecular Genetics and Metabolism 80, 207–215. https://doi.org/10.1016/S1096-7192(03)00142-2

Murshudov, G.N., Skubák, P., Lebedev, A.A., Pannu, N.S., Steiner, R.A., Nicholls, R.A., Winn, M.D., Long, F., Vagin, A.A., 2011. REFMAC5 for the refinement of macromolecular

crystal structures. Acta Cryst D 67, 355–367. https://doi.org/10.1107/S0907444911001314
Nakagawa, N., Hoshijima, M., Oyasu, M., Saito, N., Tanizawa, K., Kuroda, S., 2000. ENH, containing PDZ and LIM domains, heart/skeletal muscle-specific protein, associates with cytoskeletal proteins through the PDZ domain. Biochem Biophys Res Commun 272, 505–512. https://doi.org/10.1006/bbrc.2000.2787
Nave, R., Fürst, D.O., Weber, K., 1990. Interaction of alpha-actinin and nebulin in vitro. Support for the existence of a fourth filament system in skeletal muscle. FEBS Lett 269, 163–166. https://doi.org/10.1016/0014-5793(90)81144-d
North, K.N., Beggs, A.H., 1996. Deficiency of a skeletal muscle isoform of alpha-actinin (alpha-actinin-3) in merosin-positive congenital muscular dystrophy. Neuromuscul Disord 6, 229–235. https://doi.org/10.1016/0960-8966(96)00361-6
Nowak, K.J., Wattanasirichaigoon, D., Goebel, H.H., Wilce, M., Pelin, K., Donner, K., Jacob, R.L., Hübner, C., Oexle, K., Anderson, J.R., Verity, C.M., North, K.N., Iannaccone, S.T., Müller, C.R., Nürnberg, P., Muntoni, F., Sewry, C., Hughes, I., Sutphen, R., Lacson, A.G., Swoboda, K.J., Vigneron, J., Wallgren-Pettersson, C., Beggs, A.H., Laing, N.G., 1999. Mutations in the skeletal muscle alpha-actin gene in patients with actin myopathy and nemaline myopathy. Nat Genet 23, 208–212. https://doi.org/10.1038/13837
Oikonomou, K.G., Zachou, K., Dalekos, G.N., 2011. Alpha-actinin: A multidisciplinary protein with important role in B-cell driven autoimmunity. Autoimmunity Reviews 10, 389–396. https://doi.org/10.1016/j.autrev.2010.12.009
Okagawa, H., Kimura, K., Okuno, M., Hattori, M., Nakagawa, M., 1993. Case of Williams elfin facies syndrome with pulmonary artery sling. Int J Cardiol 42, 295–297. https://doi.org/10.1016/0167-5273(93)90064-n
Ottenheijm, C.A.C., van Hees, H.W.H., Heunks, L.M.A., Granzier, H., 2010. Titin-based mechanosensing and signaling: role in diaphragm atrophy during unloading? American Journal of Physiology-Lung Cellular and Molecular Physiology 300, L161–L166. https://doi.org/10.1152/ajplung.00288.2010
Parast, M.M., Otey, C.A., 2000. Characterization of Palladin, a Novel Protein Localized to Stress Fibers and Cell Adhesions. Journal of Cell Biology 150, 643–656. https://doi.org/10.1083/jcb.150.3.643
Pashmforoush, M., Pomiès, P., Peterson, K.L., Kubalak, S., Ross, J., Hefti, A., Aebi, U., Beckerle, M.C., Chien, K.R., 2001. Adult mice deficient in actinin–associated LIM-domain protein reveal a developmental pathway for right ventricular cardiomyopathy. Nature Medicine 7, 591–597. https://doi.org/10.1038/87920
Perz-Edwards, R.J., Reedy, M.K., 2011. Electron Microscopy and X-Ray Diffraction Evidence for Two Z-Band Structural States. Biophys J 101, 709–717. https://doi.org/10.1016/j.bpj.2011.06.024
Pomiès, P., Macalma, T., Beckerle, M.C., 1999. Purification and Characterization of an α-Actinin-binding PDZ-LIM Protein That Is Up-regulated during Muscle Differentiation. J. Biol. Chem. 274, 29242–29250. https://doi.org/10.1074/jbc.274.41.29242
Ponting, C.P., Phillips, C., 1995. DHR domains in syntrophins, neuronal NO synthases and other intracellular proteins. Trends Biochem Sci 20, 102–103. https://doi.org/10.1016/s0968-0004(00)88973-2
Powers, J.D., Malingen, S.A., Regnier, M., Daniel, T.L., 2021. The Sliding Filament Theory Since Andrew Huxley: Multiscale and Multidisciplinary Muscle Research. Annual Review of Biophysics 50, null. https://doi.org/10.1146/annurev-biophys-110320-062613

Pyle, W.G., Solaro, R.J., 2004. At the crossroads of myocardial signaling: the role of Z-discs in intracellular signaling and cardiac function. Circ Res 94, 296–305. https://doi.org/10.1161/01.RES.0000116143.74830.A9

Ribeiro, E. de A., Pinotsis, N., Ghisleni, A., Salmazo, A., Konarev, P.V., Kostan, J., Sjöblom, B., Schreiner, C., Polyansky, A.A., Gkougkoulia, E.A., Holt, M.R., Aachmann, F.L., Žagrović, B., Bordignon, E., Pirker, K.F., Svergun, D.I., Gautel, M., Djinović-Carugo, K., 2014. The Structure and Regulation of Human Muscle α-Actinin. Cell 159, 1447–1460. https://doi.org/10.1016/j.cell.2014.10.056

Salmikangas, P., Mykkänen, O.-M., Grönholm, M., Heiska, L., Kere, J., Carpén, O., 1999. Myotilin, a Novel Sarcomeric Protein with Two Ig-like Domains, is Encoded by a Candidate Gene for Limb-Girdle Muscular Dystrophy. Human Molecular Genetics 8, 1329–1336. https://doi.org/10.1093/hmg/8.7.1329

Schaffar, G., Taniguchi, J., Brodbeck, T., Meyer, A.H., Schmidt, M., Yamashita, T., Mueller, B.K., 2008. LIM-only protein 4 interacts directly with the repulsive guidance molecule A receptor Neogenin. Journal of Neurochemistry 107, 418–431. https://doi.org/10.1111/j.1471-4159.2008.05621.x

Selcen, D., Engel, A.G., 2005. Mutations in ZASP define a novel form of muscular dystrophy in humans. Annals of Neurology 57, 269–276. https://doi.org/10.1002/ana.20376

Shadrin, I.Y., Khodabukus, A., Bursac, N., 2016. Striated Muscle Function, Regeneration, and Repair. Cell Mol Life Sci 73, 4175–4202. https://doi.org/10.1007/s00018-016-2285-z

Sjöblom, B., Salmazo, A., Djinović-Carugo, K., 2008. α-Actinin structure and regulation. Cell. Mol. Life Sci. 65, 2688–2701. https://doi.org/10.1007/s00018-008-8080-8

Squire, J.M., 1997. Architecture and function in the muscle sarcomere. Current Opinion in Structural Biology 7, 247–257. https://doi.org/10.1016/S0959-440X(97)80033-4

Takahashi, K., Hattori, A., 1989. α-Actinin Is a Component of the Z-Filament, a Structural Backbone of Skeletal Muscle Z-Disks. The Journal of Biochemistry 105, 529–536.

Tamura, N., Ohno, K., Katayama, T., Kanayama, N., Sato, K., 2007. The PDZ–LIM protein CLP36 is required for actin stress fiber formation and focal adhesion assembly in BeWo cells. Biochemical and Biophysical Research Communications 364, 589–594. https://doi.org/10.1016/j.bbrc.2007.10.064

Theis, J., Bos, J., Bartleson, V., Will, M., Binder, J., Vatta, M., Towbin, J., Gersh, B., Ommen, S., Ackerman, M., 2007. Echocardiographic-determined septal morphology in Z-disc hypertrophic cardiomyopathy. Biochemical and biophysical research communications 351, 896–902. https://doi.org/10.1016/j.bbrc.2006.10.119

Torrado, M., Senatorov, V.V., Trivedi, R., Fariss, R.N., Tomarev, S.I., 2004. Pdlim2, a Novel PDZ–LIM Domain Protein, Interacts with α-Actinins and Filamin A. Invest. Ophthalmol. Vis. Sci. 45, 3955–3963. https://doi.org/10.1167/iovs.04-0721

Vallenius, T., Luukko, K., Mäkelä, T.P., 2000. CLP-36 PDZ-LIM Protein Associates with Nonmuscle α-Actinin-1 and α-Actinin-4. J. Biol. Chem. 275, 11100–11105. https://doi.org/10.1074/jbc.275.15.11100

Vallenius, T., Scharm, B., Vesikansa, A., Luukko, K., Schäfer, R., Mäkelä, T., 2004. The PDZ-LIM protein RIL modulates actin stress fiber turnover and enhances the association of α-actinin with F-actin. Experimental cell research 293, 117–28. https://doi.org/10.1016/j.yexcr.2003.09.004

van den Berk, L.C.J., Landi, E., Walma, T., Vuister, G.W., Dente, L., Hendriks, W.J.A.J., 2007. An Allosteric Intramolecular PDZ−PDZ Interaction Modulates PTP-BL PDZ2 Binding Specificity. Biochemistry 46, 13629–13637. https://doi.org/10.1021/bi700954e

van der Meer, D.L.M., Marques, I.J., Leito, J.T.D., Besser, J., Bakkers, J., Schoonheere, E., Bagowski, C.P., 2006. Zebrafish cypher is important for somite formation and heart development. Developmental Biology 299, 356–372. https://doi.org/10.1016/j.ydbio.2006.07.032

Vatta Matteo, Mohapatra Bhagyalaxmi, Jimenez Shinawe, Sanchez Ximena, Faulkner Georgine, Perles Zeev, Sinagra Gianfranco, Lin Jiuann-Huey, Vu Thuy M, Zhou Qiang, Bowles Karla R, Di Lenarda Andrea, Schimmenti Lisa, Fox Michelle, Chrisco Michelle A, Murphy Ross T, McKenna William, Elliott Perry, Bowles Neil E, Chen Ju, Valle Giorgio, Towbin Jeffrey A, 2003. Mutations in Cypher/ZASPin patients with dilated cardiomyopathy and left ventricular non-compaction. Journal of the American College of Cardiology 42, 2014–2027. https://doi.org/10.1016/j.jacc.2003.10.021

Velthuis, A.J.W. te, Isogai, T., Gerrits, L., Bagowski, C.P., 2007. Insights into the Molecular Evolution of the PDZ/LIM Family and Identification of a Novel Conserved Protein Motif. PLOS ONE 2, e189. https://doi.org/10.1371/journal.pone.0000189

von Nandelstadh, P., Ismail, M., Gardin, C., Suila, H., Zara, I., Belgrano, A., Valle, G., Carpen, O., Faulkner, G., 2009. A Class III PDZ Binding Motif in the Myotilin and FATZ Families Binds Enigma Family Proteins: a Common Link for Z-Disc Myopathies. Mol Cell Biol 29, 822–834. https://doi.org/10.1128/MCB.01454-08

Wang, H., Harrison-Shostak, D.C., Lemasters, J.J., Herman, B., 1995. Cloning of a rat cDNA encoding a novel LIM domain protein with high homology to rat RIL. Gene 165, 267–271. https://doi.org/10.1016/0378-1119(95)00542-E

Wang, K., Ash, J.F., Singer, S.J., 1975. Filamin, a new high-molecular-weight protein found in smooth muscle and non-muscle cells. PNAS 72, 4483–4486. https://doi.org/10.1073/pnas.72.11.4483

Wang, K., McClure, J., Tu, A., 1979. Titin: major myofibrillar components of striated muscle. Proceedings of the National Academy of Science 76, 3698–3702. https://doi.org/10.1073/pnas.76.8.3698

Watts, N.R., Zhuang, X., Kaufman, J.D., Palmer, I.W., Dearborn, A.D., Coscia, S., Blech-Hermoni, Y., Alfano, C., Pastore, A., Mankodi, A., Wingfield, P.T., 2017. Expression and Purification of ZASP Subdomains and Clinically Important Isoforms: High-Affinity Binding to G-Actin. Biochemistry 56, 2061–2070. https://doi.org/10.1021/acs.biochem.7b00067

Winder, S.J., Ayscough, K.R., 2005. Actin-binding proteins. Journal of Cell Science 118, 651–654. https://doi.org/10.1242/jcs.01670

Winn, M.D., Ballard, C.C., Cowtan, K.D., Dodson, E.J., Emsley, P., Evans, P.R., Keegan, R.M., Krissinel, E.B., Leslie, A.G.W., McCoy, A., McNicholas, S.J., Murshudov, G.N., Pannu, N.S., Potterton, E.A., Powell, H.R., Read, R.J., Vagin, A., Wilson, K.S., 2011. Overview of the CCP4 suite and current developments. Acta Crystallogr D Biol Crystallogr 67, 235–242. https://doi.org/10.1107/S0907444910045749

Wu, R.Y., Gill, G.N., 1994. LIM domain recognition of a tyrosine-containing tight turn. Journal of Biological Chemistry 269, 25085–25090. https://doi.org/10.1016/S0021-9258(17)31502-8

Xi, Y., Ai, T., De Lange, E., Li, Z., Wu, G., Brunelli, L., Kyle, W.B., Turker, I., Cheng, J., Ackerman, M.J., Kimura, A., Weiss, J.N., Qu, Z., Kim, J.J., Faulkner, G., Vatta, M., 2012. Loss of function of hNav1.5 by a ZASP1 mutation associated with intraventricular conduction disturbances in left ventricular noncompaction. Circ Arrhythm Electrophysiol 5, 1017–1026. https://doi.org/10.1161/CIRCEP.111.969220

Xia, H., Winokur, S.T., Kuo, W.-L., Altherr, M.R., Bredt, D.S., 1997. Actinin-associated LIM Protein: Identification of a Domain Interaction between PDZ and Spectrin-like Repeat Motifs. J Cell Biol 139, 507–515. https://doi.org/10.1083/jcb.139.2.507

Yamashiro, S., Yamakita, Y., Ono, S., Matsumura, F., 1998. Fascin, an actin-bundling protein, induces membrane protrusions and increases cell motility of epithelial cells. Mol Biol Cell 9, 993–1006. https://doi.org/10.1091/mbc.9.5.993

Yamashita, Y., Matsuura, T., Kurosaki, T., Amakusa, Y., Kinoshita, M., Ibi, T., Sahashi, K., Ohno, K., 2014. LDB3 splicing abnormalities are specific to skeletal muscles of patients

with myotonic dystrophy type 1 and alter its PKC binding affinity. Neurobiology of Disease 69, 200–205. https://doi.org/10.1016/j.nbd.2014.05.026

Ylänne, J., Scheffzek, K., Young, P., Saraste, M., 2001. Crystal Structure of the α-Actinin Rod Reveals an Extensive Torsional Twist. Structure 9, 597–604. https://doi.org/10.1016/S0969-2126(01)00619-0

Young, P., Ferguson, C., Bañuelos, S., Gautel, M., 1998. Molecular structure of the sarcomeric Z-disk: two types of titin interactions lead to an asymmetrical sorting of α-actinin. The EMBO Journal 17, 1614–1624. https://doi.org/10.1093/emboj/17.6.1614

Young, P., Gautel, M., 2000. The interaction of titin and α-actinin is controlled by a phospholipid-regulated intramolecular pseudoligand mechanism. EMBO J 19, 6331–6340. https://doi.org/10.1093/emboj/19.23.6331

Zheng, M., Cheng, H., Banerjee, I., Chen, J., 2010. ALP/Enigma PDZ–LIM Domain Proteins in the Heart. J Mol Cell Biol 2, 96–102. https://doi.org/10.1093/jmcb/mjp038

Zheng, M., Cheng, H., Li, X., Zhang, J., Cui, L., Ouyang, K., Han, L., Zhao, T., Gu, Y., Dalton, N.D., Bang, M.-L., Peterson, K.L., Chen, J., 2009. Cardiac-specific ablation of Cypher leads to a severe form of dilated cardiomyopathy with premature death. Hum Mol Genet 18, 701–713. https://doi.org/10.1093/hmg/ddn400

Zhou, Q., Ruiz-Lozano, P., Martone, M.E., Chen, J., 1999. Cypher, a striated muscle-restricted PDZ and LIM domain-containing protein, binds to alpha-actinin-2 and protein kinase C. J Biol Chem 274, 19807–19813. https://doi.org/10.1074/jbc.274.28.19807